1-31-2013

Biofilm formation by Shewanella oneidensis MR-1 towards fundamental understanding of anode respiring communities

Jared Roy

Jared Neal Roy
Candidate

Nanoscience & Microsystems
Department

This dissertation is approved, and it is acceptable in quality and form for publication:

Approved by the Dissertation Committee:

Plamen Atanassov, PhD, Chairperson

Glenn Johnson, PhD

Andrew Schuler, PhD

Linnea Ista, PhD

Biofilm formation by *Shewanella oneidensis* MR-1 towards fundamental understanding of anode respiring communities

by

Jared Neal Roy

B.S. Civil Engineering, University of New Mexico, 2007

DISSERTATION

Submitted in Partial Fulfillment of the
Requirements for the Degree of

Doctor of Philosophy
Nanoscience & Microsystems

The University of New Mexico
Albuquerque, New Mexico

December 2012

ACKNOWLEDGEMENTS

This study was in part funded by the Material Science Directorate of the U.S. Air Force Research Laboratory and the Air Force Office of Scientific Research. Jared Roy was supported through a pre-doctoral fellowship from Oak Ridge Institute for Science and Education.

I would like to acknowledge everyone that has helped me through this process, professionally and personally. Dr. Heather Luckarift and Dr. Carolin Lau, both of whom have mentored me in microbiology and electrochemistry, respectively. The people of the Air Force Research Lab in Panama City, FL have generously given their time over 3 summers of internship at that facility. Of course everyone at the Keck Lab at UNM. Other mentors: Yuri Gorby, Kenneth Nealson, Orianna Bretschger, Kerry Howe, and Mohammed Al-Naggar. My brothers Aaron Roy and Gregory Roy White, my cousins John James Freeman and Jamie Freeman and my departed family; mother Rebecca Freeman Roy and grandparents Dennis and Doris Gonzales. A debt of gratitude to Susan Valdez, Jackie and Jim Muth, and Judith Rinehart for their lifetime of encouragement and support.. My great friends over the years in Albuquerque: Jennifer Gordon, Bayo Falase, Erin Canfield (the whole Canfield Clan), Aaron Reinhardt, Julie Bryant, Rosalba Rincon, Brittany Branch, Kasey Thomas, Jason Skarsgard, Derek Feldhahn, Melissa Baca, Amalia Lucero, and Stanley Finkelstein. My committee of studies: Plamen Atanassov (advisor), Glenn Johnson, Andrew Schuler and Linnea Ista. Finally, the woman that makes everything happen in the office of Nanoscience & Microsystems, Heather Armstrong. Thank you.

Biofilm formation by *Shewanella oneidensis* MR-1 towards fundamental understanding of anode respiring communities

by

Jared Neal Roy

B.S. Civil Engineering, University of New Mexico, 2007

Ph.D. Nanoscience & Microsystems, University of New Mexico, 2012

ABSTRACT

Microbial fuel cells are bioelectrochemical devices where, on the anode, microorganisms oxidize complex carbon sources and reduce the electrode via complex mechanisms of extra-cellular electron transfer (EET). To date, *Geobacter sulfurreducens* has been identified as producing not only the largest current density but also large population density biofilms, of the known model organisms commonly used within the field. Another common model organism associated with microbial fuel cells is *Shewanella oneidensis*, containing multiple EET mechanisms and an apparent inability to form multi-layered biofilms in anaerobic culturing, i.e. microbial fuel cell operating conditions. In contrast to *G. sulfurreducens*, *S. oneidensis* biofilm formation appears to coincide with

oxygen metabolism, with removal of such, prompting biomass detachment. In this study, to overcome obstacles in biofilm formation a method was employed to encapsulate biomass onto the surface of an electrode. This method used the chemical vapor deposition (CVD) of the silica precursor, tetramethyl orthosilicate (TMOS), causing SiO_2 to form a porous thin film effectively binding the culture to the electrode surface and acting as an artificial exopolysaccharide (EPS) biofilm binder. As a demonstration of proof, this methodology was applied to novel biocompatible electrode materials (PHBV-CF) and combined with a laccase catalyzed oxygen reduction cathode in a hybrid biological fuel cell. In comparison to the encapsulated anodes, additional experiments were performed to optimize the growth conditions at which *S. oneidensis* will naturally form biofilms on PHBV-CF. Observations indicated initial biofilm formation occurred at the onset of stationary phase growth in mirco-aerobic and anaerobic cultures, indicating a biofilm response to carbon substrate limitation. This observation was explored further and led to results indicating the importance of intra-cellular carbon fluxes and the subsequent metabolic response of riboflavin production by *S. oneidensis.* It was also observed that riboflavin production occurred in micro-aerobic and anaerobic environments at the onset of carbon limitation but no riboflavin was detectable in anaerobic cultures. As riboflavin has been indicated in many studies as one primary mechanism employed in EET via mediated electron transfer (MET; results herein contradict the idea of riboflavin MET due to the lack of carbon required to produce riboflavin, with carbon being essential to drive metabolic reduction of the electrode. Therefore, the hypotheses within this study explores the idea of riboflavin acting as an electrochemical signal, leading *S. oneidensis* cells to populate and form a biofilm on the surface of an electrode as the culture transitions from

aerobic to anaerobic metabolism. To test this, *S. oneidensis* cells in anaerobic media were exposed to electrodes with externally applied potentials (-0.4 , -0.3, +0.1 and open circuit vs Ag/AgCl). Results indicated only the electrode with an applied potential of -0.3 V (corresponding to accumulation of oxidized riboflavin on the surface) retained biomass in the form of a biofilm. Furthermore, this biofilm exhibited a nonreversible oxidation species centered at +0.2 V vs Ag/AgCl, which was identified as outer membrane cytochromes. This novel culturing method provides for the first time, anaerobically formed biofilms of *S. oneidensis* engaged in direct electron transfer (DET) of the anode. Based on this methodology, *S. oneidensis* based anodes were made with current densities comparable to those reported within the literature for *G. sulfurreducens*. While providing novel *S. oneidensis* based anodes, a methodology is also described herein for statistical quantification of essential electrochemical characteristics for comparison between these electrodes, a first such description for microbial fuel cells

Table of Contents

List of Figures

Chapter 1 – Introduction

With the promise of alternative forms of energy, every aspect of our infrastructure is being scrutinized for the possibility of energy neutrality or greater efficiency. This includes harvesting energy from biomass, which currently requires energy input to expel from the effluent wastewater. Microbial fuel cells (MFCs) offer an exciting new technology to harness this energy from biomass by bridging the biological components together with electrochemical devices. With the incorportion of dissimilatory metal reducing bacteria, microorganisms capable of incorporating their metabolic pathways for the reduction of insoluble electron acceptors, mediator-less microbial fuel cells are taking a leap forward. With any new generation of technology, however, fundamental aspects of the system must be elucidated before microbial-based biological fuel cells be industrial relevant. This includes the catalyst, moreover, an understanding of how these microbial populations incorporate within the device itself. While this is predominant, it is not limited to the biofilm being a key component in the functionality of the microbial fuel cell. Of the two model organisms widely studied, *S. oneidensis* and *Geobacter sulfurreducens*, the former is known to exhibit biofilm formation on the order of tens of microns thick on electrode surfaces;[1] whereas, *S. oneidensis* is not known to form large biofilms anaerobically on an insoluble electron acceptors.[2] This observation may be the key in the consensus of the literature that *S. oneidensis* populated microbial fuel cell devices do not produce the large current densities as those based on *G. sulfurreducens*.[3,4]

1.1 Bioelectrochemical Systems

Bioelectrochemical systems (BES) are devices that transform chemical energy to electrical energy catalyzed by microbial or enzymatic constituents.[5] These devices have an array of applications, from enzymatic based glucose sensors to microbial fuel cells. In terms of microbial fuel cells, the technology is in the development phase with targeted application in biological wastewater treatment or other biologically based remediation systems. Apart from direct engineering application, BES may also be utilized to probe charge transport phenomena between electrodes (acting as terminal electron acceptors) and biological catalysts. This method of interrogation may provide insight into the understanding of complex metabolic processes of microorganisms, singularly or within a biofilm community. Therefore, the study of microbial metabolism, in part characterized by BES, could help to evolve microbial fuel cell technology beyond the lab bench top.

1.1.1 Microbial Fuel Cells

At the beginning of the 20th century, Potter first described how microbial conversions could create reducing power and electrical current.[6,7] By the 1960's this "reducing" power of bacteria was combined with fuel cells to create the first microbial fuel cells. However, these first MFCs relied heavily on the addition of chemical mediators to function, and the power density was extremely low. A breakthrough in this technology occured when Kim et al. first published reports of *Shewanella putrefaciens* functioning in mediator-less (such as ferricyanide, exogenously added to mediated electron transfer from the organisms' to the electrode) microbial fuel cells in 1999[8]. Since then, mediator-less microbial fuel cells have dominated the literature in this field[9-11]. MFCs are designed

in a range of configurations, from batch (bio-batteries) to seafloor sediment type fuel cells, depending on intended application.[12,13]

The basic concept of a MFC incorporates anodes and cathodes connected by a current collector, separated by a membrane or distance (Figure 1.1). On the anode, complex fuels such as acetate or lactate are oxidized by a monoculture biofilms or a consortia of microorganisms. In terms of aerobic respiration, oxidation of organic growth constituents ends with the reduction of oxygen as the terminal electron acceptor. In MFCs the anode acts as that terminal electron acceptor, replacing oxygen, for organisms associated with MFCs (or other relevant environments). Therefor, it is essential that oxygen not be present near the anode surface, as the electrode will function as the terminal electron acceptor. In order for respiration to work in these systems, an electrochemical reaction occurs at the surface, catalyzed by the microorganisms. At the cathode, another electrochemical reaction (biological or not) occurs causing the reduction of oxygen or some other compound. Molecules commonly associated with wastewater remediation process, such as nitrates, for example would be biologically reduced at the cathode end[14].

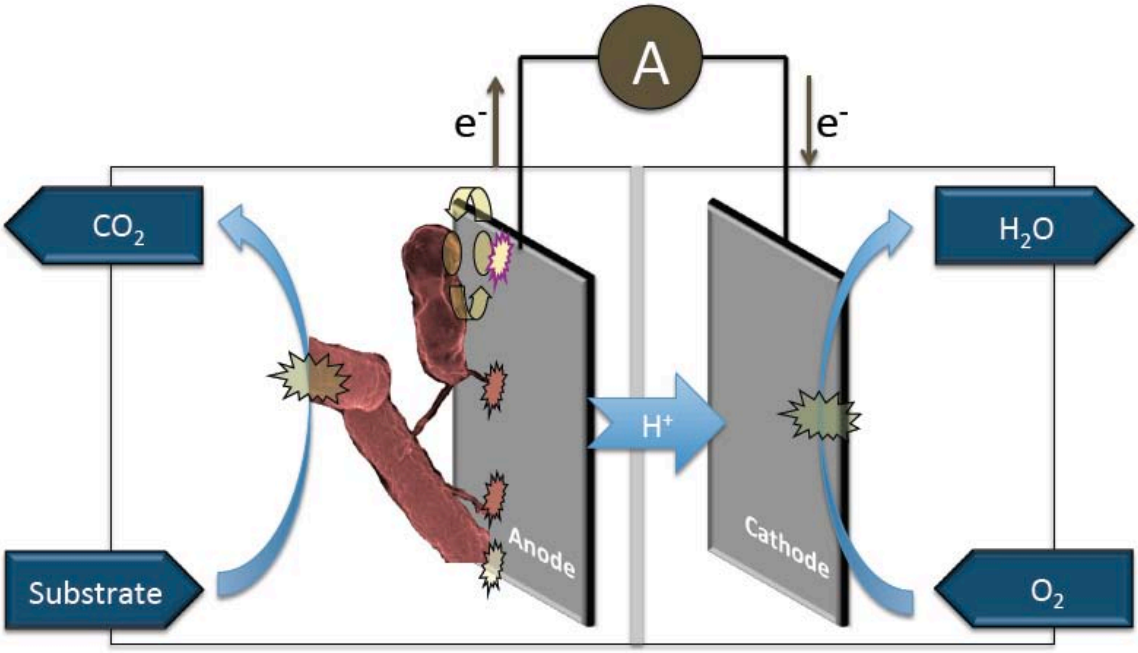

Figure 1.1: Schematic of an idealized microbial fuel cell

1.1.1.2 Application

The most industrial relevant application for developing microbial fuel cell technology is currently wastewater treatment or other types of biologically based water remediation processes. Commercial, industrial and municipal wastewater treatment schemes often center on a biological oxidation processes for remediation deemed "activated sludge".[15] This biological oxidation of dissolved organic constituents is an aerobic process consisting of a vast and complex microbial consortia, with many different organisms playing various roles.[12] By nature of the process, energy (and money) is invested into developing the required microbial biomass through aeration of vast bioreactors with additional energy required to remove the biomass at the end of the process. Due to this, wastewater treatment infrastructure requires massive capitol investment and operational costs and is therefore primarily a luxury of more developed regions of the world and

widespread access to this infrastructure is a hallmark of a developed country. For this reason, microbial fuel cells are an attractive alternative to activated sludge (AS) where this technology can replace or supplement AS and reduce energy requirements. While microbial fuel cells may never yield energy density to make wastewater treatment a cost beneficial process, incorporating MFC technology into wastewater treatment processes may reduce operating costs of this essential public utility.

1.2 Dissimilatory Metal Reducing Bacteria

Essential to the understanding of how microbial fuel cells operate is the idea of dissimilatory metal reducing bacteria (DMRB). DMRBs are capable of using insoluble metals as terminal electron acceptors for respiration during metabolic oxidation of a carbon source.[16] In nature, these insoluble electron acceptors are metal oxides of various composition and this process drives natural metal cycling throughout the world[17]. Biological reduction of metal oxides can parallel microbial fuel cell operation, as the anode becomes an inexhaustible terminal electron source.

1.2.1 Model Organisms

The most common model organism for the study of microbial fuel cells is the organism *G. sulfurreducens sulfurreducens*. In 2010 there were approximately 150 publications that refered to *G. sulfurreducens.* In 2009 there were over 4500 articles published referencing this model organism. *G. sulffrurreducens* is an obligate anaerobe producing large biofilms on the electrode, oxidizing acetate, and reducing a range of insoluble electron acceptors.[4,18,19] This organism tends to be the preferred laboratory tool in the study of EET, this is due to the larger observed current densities.

Another common model organism is *Shewanella oneidensis* MR-1. First reported as *Alteromonas putrefaciens* MR-1 in 1988 by Ken Nealson, this organism was isolated from anaerobic sediments of Lake Oneida in upstate New York. Lake Oneida experiences extensive Mn(IV) reduction during the summer months, prompting the investigators to isolate MR-1 in an effort to understand the biological oxidation event.[17] In this study, MR-1 was shown to reduce Mn(IV) within a range of pH and temperature variation while the presence of molecular oxygen hindered the process. It was also determined in this study that the organism was incapable of fermentation, thus requiring Mn(IV) respiration to anaerobic growth of MR-1. Unlike *G. sulfurreducens,* however, *S. oneidensis* is a facultative anaerobe which has contributed to its popularity among MFC research groups due to ease of culturing.

1.2.2 Metabolic Profile of *S. oneidensis*

S. oneidensis is a Gram-negative ϒ-Proteobacteria facultative anaerobe, with the ability to oxidize fermentation end products such as: lactate, formate, certain amino acids and hydrogen, making this a niche organism living in rich environments throughout the world[17,20]. Furthermore, Nealson speculates that *Shewanellae* are syntropic partners of fermentative communities, consuming fermentation end products and driving fermentation metabolism forward in anaerobic environments.[20] In aerobic metabolism, *S. oneidensis* is known to utilize the tricarboxylic acid cycle (TCA) in carbon metabolism. However, under anaerobiosis, the TCA cycle becomes truncated and acetate accumulates as a metabolic end product providing the foundation for symbiosis with fermentative communities.[21] In terms of terminal electron acceptors, *S. oneidensis* is known to reduce a broad range of substrates: nitrate, nitrite, ferric iron, thiosulfate, sulfite, tetrathionate,

glycine, fumarate, mandanese dioxide, and trimethylamine N-oxide.[17] Of particular interest is the organisms' utilization of insoluble forms of electron acceptors during anaerobic metabolism.

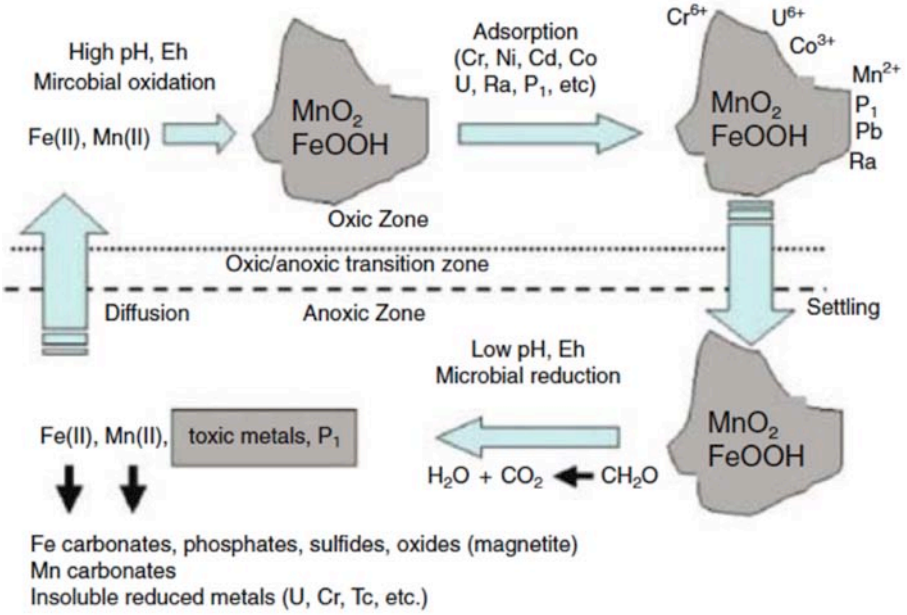

Figure 1.2: The biogeochemical cycling processes of iron and manganese oxides across oxygen boundaries in natural water sources as described in Nealson et al. (2006).

Biological metal cycling has been a controversial topic within the literature; the fact that biological reduction of metal oxides was even occurring was debated for many years, as most of the metal oxides found in nature are solids. It was not believable by many within the community that solid metal oxides could be reduced biologically. Therefor, the first task was to provide a direct metabolic link in microorganisms to the coupling of carbon substrate oxidation and metal oxide reduction. This was accomplished in the late 1980's by Lovley and Nealson with the first descriptions of DMRB.[17,22] The hypothesis for biological metal cycling was then established by Nealson: In stratified water bodies

(water bodies with anoxic/oxygen boundaries such as lakes and fjords) the oxidized solids sink, in effect creating an "oxidation pump" delivering oxidative constituents to deep waters.[20] Kenneth Nealson describes this in *The Prokaryotes* as a "gravity-driven redox cycle" (Figure 1.2).

1.2.3 Extra-Cellular Electron transfer

Electron flows are essential to the life cycle of microorganisms and play are the focal point of primary metabolism. Microorganisms transfer electrons from an electron donor (low potential) to a higher potential terminal electron acceptor. In aerobic bacteria this terminal electron is oxygen, while anaerobic bacteria can use a variety of soluble terminal electron acceptors[7]. Certain bacteria deemed dissimilatory metal reducing bacteria (DMRB) are able to use insoluble terminal electron acceptors such as iron oxide. These bacteria are of specific interest to researchers in the field of microbial fuel cells as they have been implicated in cultures capable of reducing anodes in mediator-free microbial fuel cells.

S. oneidensis MR-1 and other species are known to transfer electrons to electrodes in MFCs and use these electrodes as either terminal electron acceptors or electron donors. The specific mechanism the electron transfer occurs remains controversial; with a number of mechanisms being proposed in numerous studies, including: direct electron transfer (DET) via outer membrane-bound cytochromes[23], mediated electron transfer (MET) by soluble redox compounds[24-27], and electrically conductive biological filaments

or nanowires[28,29]. Collectively these pathways provide a means for extra-cellular electron transfer (EET).

1.2.4 Direct Electron Transfer via Cytochromes

Direct electron transfer via outer membrane *c*-type cytochromes has been implicated for *S. oneidensis*. Studies have shown the ability, under anaerobic metabolism, that

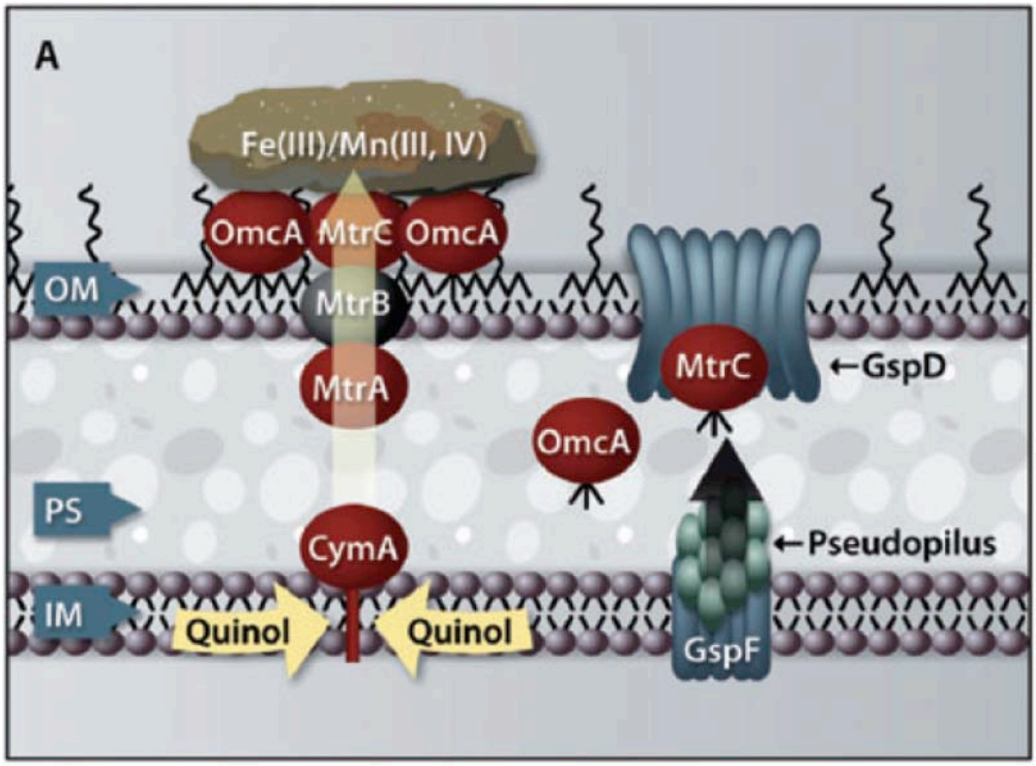

Figure 1.3: Proposed Mtr pathway consisting of various c-type cytochromes through the inner and outer membrane of *S. oneidensis* (Shi et al., 2007)

S. oneidensis will express cytochrome production in the outer membrane; where it is postulated that they may come in direct contact with metal oxides.[30,31] Specifically, genetic knockout studies have implicated MtrA, MtrB, MtrC, and OmcA in the dissimilatory reduction of insoluble metal oxides[31]. These proteins comprise the "Mtr

pathway", a series of proteins delivering electrons from the metabolic core of the cell to the outer membrane (Figure 1.3).

CymA is thought to serve as the introductory electron transfer protein in the Mtr pathway; this protein serves as an intermediate between the quinol pool of the inner membrane space to the Mtr pathway and the fumarate reductases[32]. Next, MtrA is a soluble *c*-type cytochrome with 10 hemes that is located in the periplasm.[33] In studies utilizing mutants lacking MtrA, iron oxide reduction was compromised in *S. oneidensis*; however, fumarate reduction was still apparent.[34] This suggests that MtrA provides a pivotal link through the periplasm to the outer membrane cytochromes. Following MtrA, MtrB is not a *c*-type, but is nonetheless essential for oxide reduction.[35] According to one publication, this protein may provide an essential role in localization and insertion of the MtrC/OmcA outer membrane complex.[36] Terminal proteins in this pathway consist of MtrC and OmcA. Both proteins contain 10 haems, and are bound to the extracellular side of the outer membrane.[37]

1.2.5 Biological Nanowires

Biological production of electrically conductive nanowires has been observed in *G. sulfurreducens* and *S. oneidensis*. In *S. oneidensis*, Gorby et al (2006) published the seminal paper linking nanowire production to cultures experiencing electron acceptor limitation. Namely, a 5% dissolved oxygen tension prepared the culture to express nanowires.[38] Using scanning tunneling microscopy (STM), the authors observed that nanowire diameters were approximately 50 to 150 nm and consists of "ridges" of 3-5 nm diameters. These ridges are speculated to be individually conductive filaments,

comprising the nanowire structure as a whole.[38] Aside from STM, scanning electron microscopy (SEM) was to characterize nanowires from *S. oneidensis* on conductive substrates (Figure 1.4).

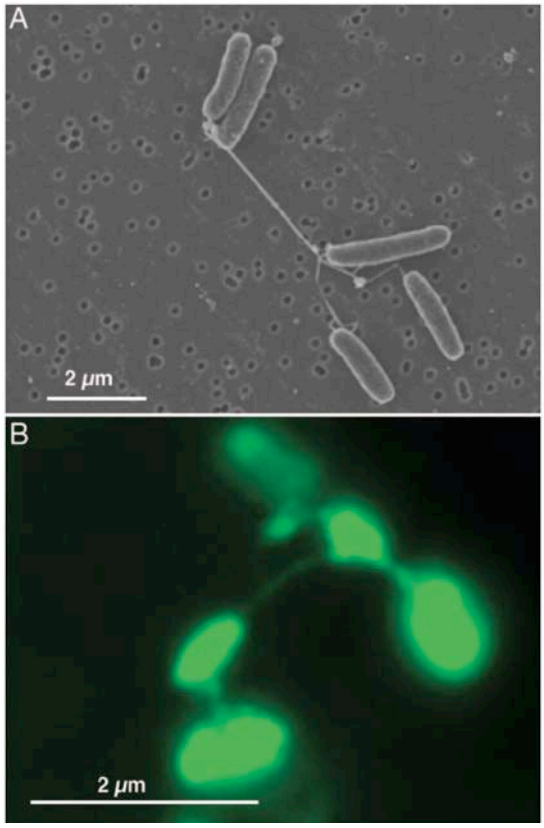

Figure 1.4: (A) SEM image of *S. oneidensis* MR-1 from electron acceptor limited culture and (B) epifluorescence micrograph of *S. oneidensis* stained with NanoOrange (Gorby et al. 2006)

Furthermore, in 2006 Gorby et al. used atomic force microscopy, (AFM) showing the conductivity of the nanowire of the native strain through the plane perpendicular to the substrate. Using mutants, subsequent authors have observed the essential role of nanowires in reduction of electron acceptors such as hydrous ferric oxide (HFO), with mutants lacking the *PilD* anchoring mechanism for nanowires unable to reduce significant concentrations of HFO.[39] Additional studies have indicated the essential role

of nanowires in maintaining current density in BES.[40] For other organisms, namely *G. sulfurreducens*, studies have concluded that their nanowires exhibit "metallic like conductivity".[41] However, these conclusions have yet to be accepted by the community at-large with other groups preferring the "hopping" behavior of electrons across cytochromes within the nanowire.[42]

1.2.6 Mediated Electron transfer via Endogenous Metabolites

Within the last few years the idea of endogenously secreted electrochemically active metabolites mediating electron transfer to insoluble electron acceptors has gained widespread attention for *S. oneidensis*. Riboflavin, specifically, is known to be an electrochemically active molecule andhas been implicated as one such metabolite thought to reduce iron oxides or chelate ferric iron for cellular uptake.[26] Although many microorganisms are known to produce extracellular riboflavin, *S. oneidensis* has been observed to utilize this metabolite in conjunction with producing current density in BES.[43,44] In Marsili et al., nominal current density was established for an existing biofilm of *S. oneidensis* MR-1 when the media was replaced the current density appeared to drop; only returning once the original medium had been returned to the system (Figure 1.5). The authors speculated upon the vital role of riboflavin in this system, stating that riboflavin was responsible for the normalized current density, removing the diffusible mediator severely affected the current density.[26] Mediated electron transfer is one speculated mechanism of extra-cellular electron transfer in *S. oneidensis*, with the roles and relationships of other EET mechanisms still undefined.

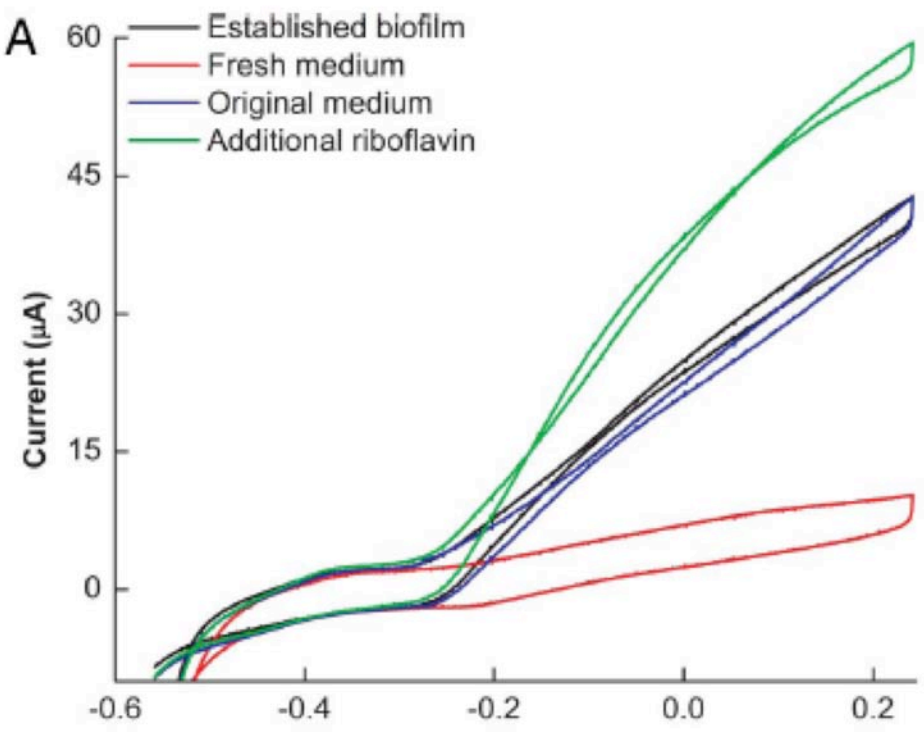

Figure 1.5: Voltammogram from Marsili et al (2008) describing catalytic activity ascribed to the presence of riboflavin before and after media replacement and with the addition of riboflavin

1.2.7 Biofilm Formation

In nature, most microorganisms live in communities called a biofilm. These communities sometimes consist of multiple strains while some biofilms may be dominated by one particular strain that can out compete others. In terms of structure, biologically synthesized extracellular polymeric substance or EPS is essential for biofilm formation and stability.[45] For microbial fuel cells, biofilms are essential in substrate oxidation and current production, as large biofilms effectively increase the kinetics of substrate oxidation in MFCs. For of *G. sulfurreducens sulfureducens,* it was shown that an increase of biofilm thickness leads to an increase of current production on the anode, with

these large biofilm formations occurring anaerobically for *G. sulfurreducens.*[46] This study, among others, shows the importance of large anode respiring biofilms. *S. oneidensis onediensis* is a facultative anaerobe unlike the strict anaerobe *G. sulfurreducens*. It has been shown that *S. oneidensis* strains form relatively large biofilms in the presence of oxygen, with the removal of oxygen from the environment stimulating biomass detachment.[47-49] This puts into question the ability of *S. oneidensis* to form large biofilms on anaerobic anodes, which could account for smaller reported current densities in comparison to pure cultures of *G. sulfurreducens.*[50-52]

Chapter 2 – Problem Statement & Objectives

Microbial fuel cells represent an exciting advancement in the fields of engineering (in terms of biological remediation) and towards fundamental understanding of microbial physiology. *S. oneidensis* has been targeted as a model organism as an anode respiring organism. The role of this facultative anaerobe in natural ecology is centered on biogeochemical processes of metal cycling. Another isolated organism with a similar role is *G. sulfurreducens sulfurreducens*, which of the two most common model organisms has been identified as having the largest current density associated with biofilms of tens of microns thick.[1] Of interest for researchers engaged in *S. oneidensis* is the ability of this organism to form effective anode respiring biofilms on the surface of the electrode. While studies have implicated *S. oneidensis* in metal oxide and electrode reduction via several EET mechanisms, the ability for biofilm formation on the electrode itself remains vague, especially in anaerobic operating conditions.[2,53-56] To elucidate the mechanisms of biofilm formation, particularly under anaerobic conditions for *S. oneidensis*, this study will be consistent with the following objectives, beginning with an engineering aim:

Objective 1:

To establish the formation of an artificially bound biofilm by extending the methodology of biological encapsulation onto substrates by the chemical vapor deposition of tetramethyl orthosilicate (TMOS)

Objective 2:

Provide a methodology to construct a scalable, hierarchically structured electrode compatible for biological systems. Then integrate *S. oneidensis* artificially bound biofilms within the electrode.

The first two objectives will culminate with demonstration of proof of a viable biofilm capable of the oxidation of lactate and production of current density. Then these electrodes will be incorporated into previously funded biological cathodes as a demonstration of a bridge technology to the next generation of research:

Objective 3:

Incorporate encapsulated and non-encapsulated *S. oneidensis* biofilms onto the hierarchically structured porous carbon electrode as the anode, connected to a laccase oxygen reduction cathode for a fully biological fuel cell

The first 3 engineering objectives are centered on the fabrication of electrodes with well-established and bound biofilms, irrespective of aerobic or anaerobic operating conditions. The final part of this study, although contradictory to traditional research aims, will begin with the fundamental aspects of biofilm formation and electron transfer in anaerobic cultures of *S. oneidensis*. The first objective will be to address the ability of the culture to engage electrochemically active metabolites as mediators:

Objective 4:

Elucidate the role of riboflavin, as it has been implicated in many studies, as an essential molecule, or electrochemical bystander, in mediated electron transfer in catalytic systems of planktonic or biofilms of *S. oneidensis*.

Objective 5:

Establish if anaerobic cultures of *S. oneidensis* can form biofilms engaged in anode respiration in anaerobic culturing conditions. Furthermore, if these cultures are engaged in metabolic electrode reduction, identify electrochemical redox couples responsible for catalytic behavior.

The last engineering objective will bring this research study full circle by employing the methodology ascribed to the first 5 objectives:

Objective 6:

Create a high density populated biofilm on an electrode surface, anaerobically, and standardize this system using electrode characteristics with uncertainty calculations elucidating regions of electrochemical and operating significance.

Chapter 3 – Experimental Methodology

3.1 Electrochemical Techniques

According to the Electrochemical Society (ECS), electrochemistry is the branch of chemistry that deals with solid-state reactions. Mostly, this particular discipline concerns itself with the study of chemical changes caused by passing electric current and the production of electrical energy.[57] In terms of biological systems (enzymatic/microbial biofuel cells or biosensors), analytical electrochemical measurements are essential to characterize the system. In particular, this field can be useful to probe the metabolic states of microorganisms with increasing interest in cultures capable of dissimilatory metal reduction. This section will, in brief, explain the fundamental concepts of electrochemical characterization as relevant for this study.

3.1.1 Electrode Reactions

For the purposes of this study, all experiments are conducted in a 3-electrode electrochemical cell containing a working electrode (usually populated by *S. oneidensis* MR-1), a counter electrode (platinum), reference electrode (3 M KCl, Ag/AgCl), and all electrodes are within an electrolyte of 50 mM concentration. The reference electrode enables the user to define an interrogation potential with a known point of reference. The working electrode is the electrode of interrogation usually populated with a biofilm. Finally the counter electrode is the electrode of opposite reaction. As previously discussed, the working electrode populated with a DMRB biofilm has been observed to transfer electrons: i) directly via outer membrane cytochromes, ii) via conductive

microbial pili aka "nanowires", and iii) via endogenously secreted electrochemically active metabolites.[58] One or a combination of these mechanisms are involved with transporting electrons from the microorganisms to the electrode at the electrode surface. A simple example of this pathway of oxidation or reduction processes is as follows: ($O + ne^- \leftrightarrow R$), where R is the reduced species and O is the corresponding oxidized species (Figure 3.1).[59] How the charged species are distributed affects the electrode processes which differs at the electrode surface and bulk solution:[57]

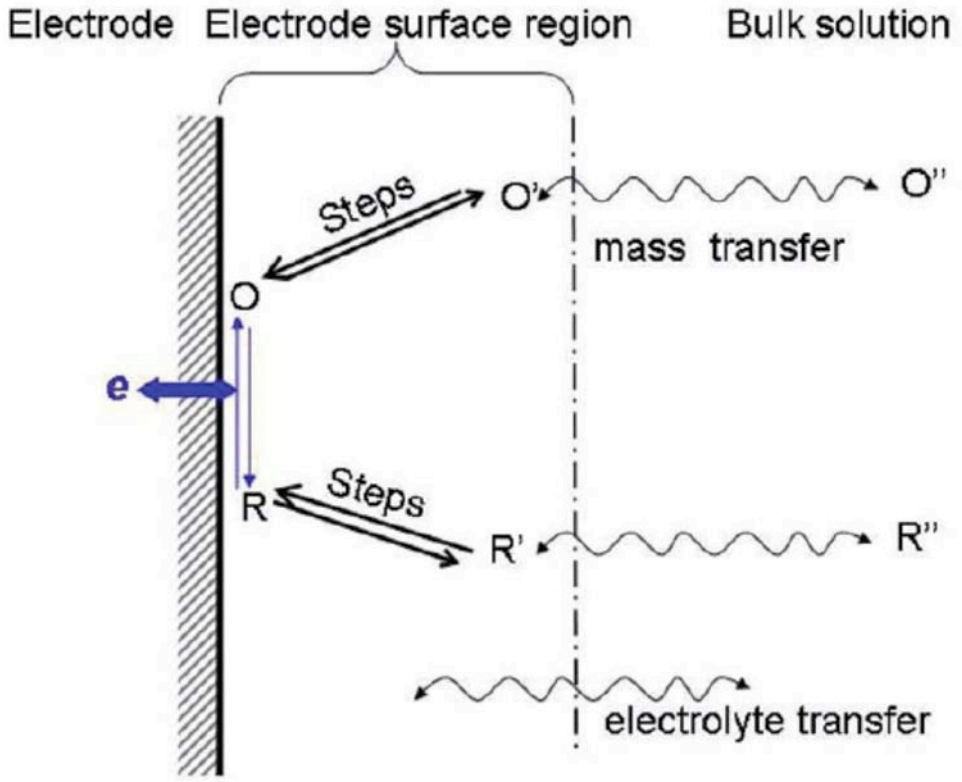

Figure 3.1: Illustration of conventional solution bound electrochemical reactions on a working electrode in an electrochemical cell (Zhao et al. 2009)

1. Mass transport of the *O''* species from the bulk solution to the electrode surface where the reaction occurs;
2. On the surface of the electrode, competing electrochemical reactions may occur (adsorption, desorption, protonation and decomposition steps (*O''* $\leftrightarrow$ *O'* and *R''* $\leftrightarrow$ *R'*);
3. Electron transfer at the electrode surface ($O + ne^- \leftrightarrow R$);
4. Transport of the reduction by product *R'* from the electrode surface to the bulk solution;
5. Transport of the electrolyte (migration)

Considerations of mass transfer will include: i) diffusion from concentration gradients, ii) migration due to an electric field, iii) convection due to the presence of mechanical agitation. In traditional electrochemical experimental designs, these mass transfer issues are usually mitigated by incorporating a buffered solution (usually > 100 mM, although this is not practical for biological systems) and preventing stirring or agitation.[40] When one considers the presence of the biofilm on the working electrode, several considerations must be addressed for EET (Figure 3.2):

1. Transport of the carbon source from the bulk solution region to the biofilm surface;
2. Transport of the carbon source through the biofilm;
3. Different metabolic states of the microorganisms within the biofilm community;
4. Direct electron transfer between the biofilm community and the electrode surface (orientation of the outer membrane proteins);

5. Transport of the metabolites for mediated electron transfer;

6. Transport of the electrolyte to and from the electrode surface.

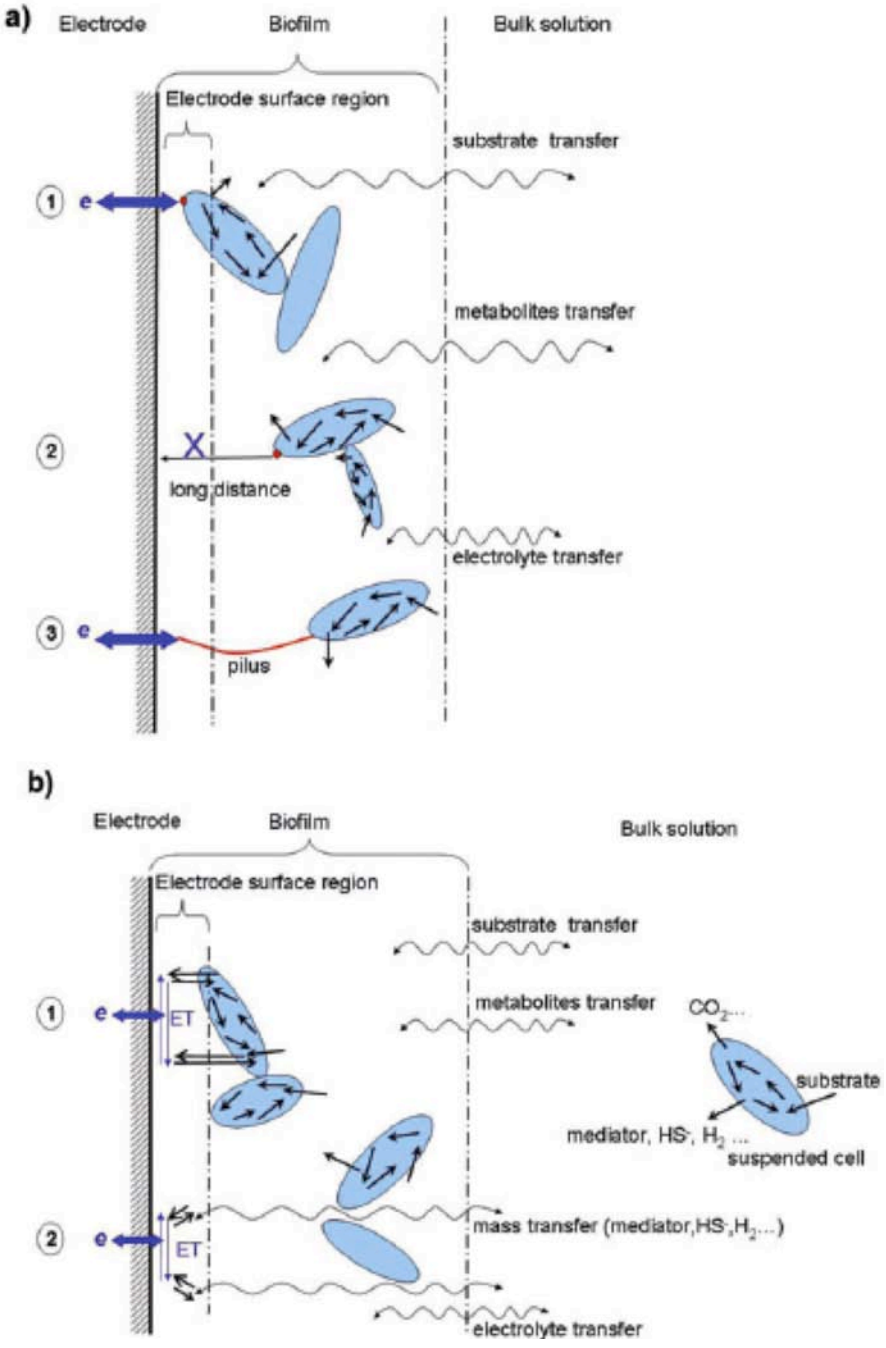

Figure 3.2: Proposed pathways of electron transfer from microorganisms to the surface of the electrode (a) direct electron transfer and (b) mediated (Zhao et al. 2009)

All considerations for anode respiring communities must include regeneration of the biofilm itself, including non-participating cells.[59]

3.1.2 Cyclic Voltammetry

One of the basic tools for electrochemists is cyclic voltammetry (CV); when used correctly CV can probe the underlying reduction and oxidation phenomena of the working electrode at the surface. Particularly, CV can determine if redox reactions at the surface are reversible redox couples or irreversible.[57] For a reversible redox couple, the ratio of peak anodic and cathodic currents is 1, with peak potential separations of 59.2 mV/n, where n is the number of electrons involved in the reaction. This would be the case for a mediator dominated electrochemical reactions on the electrode surface. In comparison, quasi-reversible and irreversible reactions will show large separations between the peak potentials with either the reduction or oxidation peak being of different size (Figure 3.3).[57,60] In MFCs, CVs can be utilized to:

1. Prove the mechanism of electrode interactions between the biomass and the electrode surface;
2. Identify the potential of dominating electrochemical reactions involved with EET, usually the standard potential is reported, the average between the peak potentials;
3. Evaluate the performance of the catalysts being used.[59] (Figure 3.3)

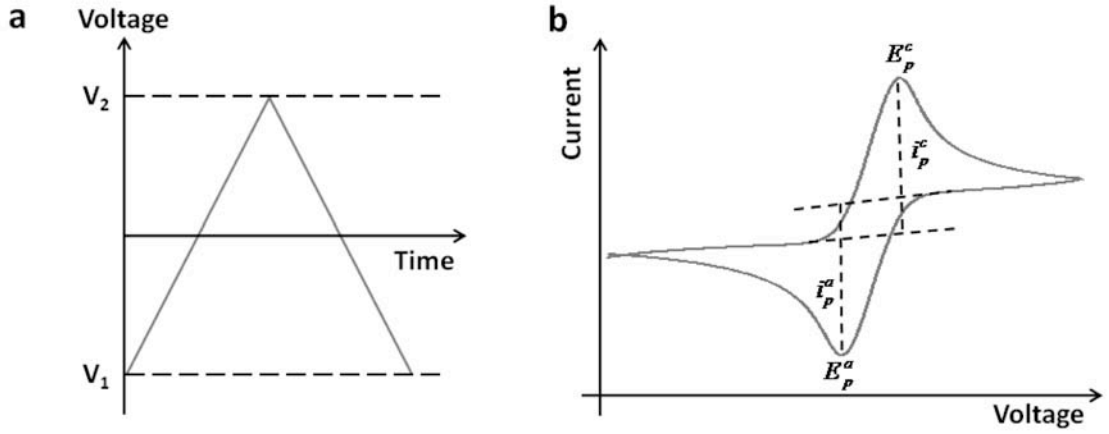

Figure 3.3: (a) voltage sweep, forward (oxidation of the catalyst) and back scan (reduction of the catalyst) (b) subsequent cyclic voltammogram identifying a reversible redox reaction with peak currents and peak potentials (Andrade et al. 2011)

3.1.3 Polarization

Electrode polarization refers to the change in potential from its equilibrium (open circuit potential) due to a flow of current.[59] Subsequent polarization curves are plotted with electrode potential on one axis and current or current density on the other. These type of plots can yield valuable information for your system and can be obtained with whole fuel cells or in half cells (with interest on the working electrode). Of the information that is particularly relevant for the system, one may obtain open circuit potentials, and losses due to: activation (charge transfer) [η_{act}], Ohmic resistance (inert to the material properties [η_{ohm}], electrolyte, membrane resistance and resistance due to the biofilm), and concentration (prevalent at high current densities due to the fact that products and reactants cannot diffuse to and from the electrode surface and the bulk electrolyte) [η_{conc}].[59,61] Again, these measurements can be obtained individually for the anode and

cathode or in a full fuel cell to observe the performance of the total system and total losses (Figure 3.4).

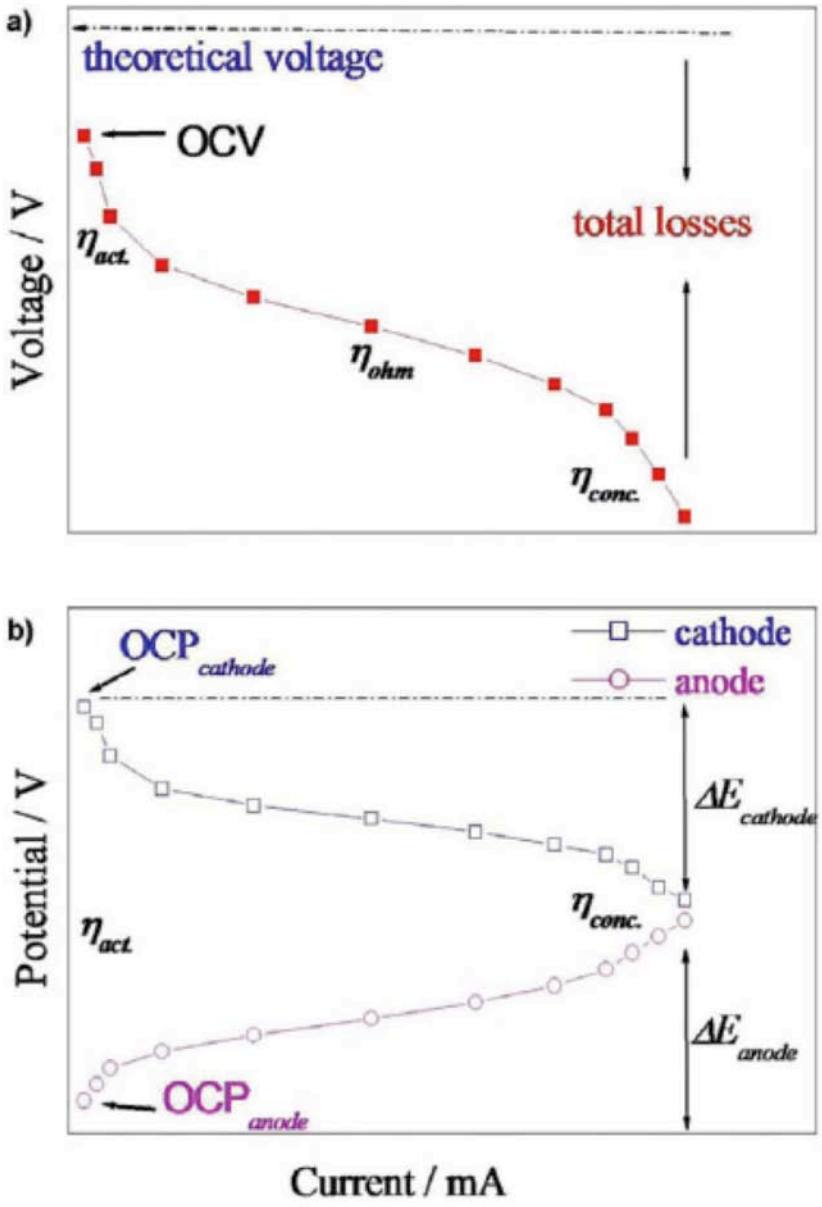

Figure 3.4: (a) polarization curve of a biological fuel cell showing losses (overpotentials) and (b) individual polarization curves from the anode and cathode identifying contributing overpotentials from each electrode and each open circuit potential leading toward the full cell polarization (Zhao et al. 2009)

3.1.3.1 Chronoamperometry

Chronoamperometry (CA) measurements are, for the purposes of this study and most biological systems, the first polarization technique employed. This measurement starts from the open circuit potential (OCP), and in the case of the anode, is a negative potential with the potentiostat applying a potential from the OCP towards zero and more positive potentials. The applied potential is stepped and then held constant, with current being measured and recorded. The step can be anything from 10 to 50 mV at times required for stabilization of the electrode. The appropriate time steps for these measurements is still being debated within the literature; however, as described in Zhao et al. it is difficult to record appropriate steady state polarization curves with MFCs for these reasons: i) microbial communities continually evolve with time and the communication with the electrode is a dynamic relationship; ii) the concentration of electrochemically active metabolites is constantly changing within the biofilm; iii) the mechanisms, as previously described, of EET are constantly changing with each biofilm and electrode assembly. Therefore, it is difficult to achieve a stabilized current measurement from electrode polarization and in this study short polarization steps are employed, approximately 5 minute steps. Once CA measurements are finished, a polarization curve can be built and a range of current densities is known.

3.1.3.2 Chronopotentiometry

Chronopotentiometries (CP) is usually the second polarization technique employed in characterizing a system. Once the current range is obtained for a biological system, those currents (starting at zero current) are applied to the working electrode and stepped up to

the maximum current from the CA. Again, this time step is approximately 5 minutes, but can vary between evaluators. Ideally, polarization curves based on chronoamperometries and chronopotentiometries should be similar but can differ as the biofilm changes quickly.[57]

3.1.4 Calculation of Electrochemical Accessible Surface Area

In order to standardize some of the previously described measurements, the working electrode was evaluated to determine the electrochemically accessible surface area. This is a measurement relating similar electrode based on surface area "seeing" the electrolyte in the electrochemical cell. This method first required the user to obtain a CV of the abiotic electrode. Observing a flat region within the CV (capacitive current), oxidation and reduction currents were obtained from the same potential. The equation used is as follows:

$$EASA = \frac{i_{ox} - i_{red}}{2\nu} C \quad \textbf{Equation 3.1}$$

where i_{ox} and i_{red} are the oxidation and reduction currents at v (scan rate) and C is the specific capacitance of the electrode material. For the carbon-based materials used within this study, a C value of 35μF/cm^2 was used.

3.2 Biological Methods

Basic cultivation of the microorganisms techniques are described in detail within each chapter, all sterile protocols were followed to ensure purity and continuity of the samples.

Chapter 4 – Standardized Microbial Fuel Cell Anodes of Silica-Immobilized *S. oneidensis*

Co-authors: Heather R. Luckarift, Susan R. Sizemore, Carolin Lau, Gautum Gupta, Plamen Atanassov & Glenn R. Johnson

4.1 Introduction

Microbial fuel cells (MFC) convert chemical energy to electrical energy by capitalising on the metabolism and respiration of certain microbial species.[62,63] Dissimilatory metal-reducing bacteria such as *S. oneidensis* can transfer electrons from reduced electron donors (e.g. lactate) to insoluble electron acceptors (e.g. iron and manganese oxides).[64] In MFC, graphite fiber (GF) electrodes can act as a respiratory sink for the available electrons and when combined with a suitable cathode will generate electricity.[65] The association between bacteria and electrodes, however, is inconsistent due to inherent variations in bacterial growth in response to changes in physiological conditions, (i.e. electron donor concentrations, diffusion limitations and pH) that are difficult to control in the MFC reactor.[66,67] In addition, in order to most effectively use insoluble electron acceptors, the metal-reducing bacteria form a complex biofilm.[68,69] Biofilms generally benefit MFC power output as the bacterial cells become tightly associated with the electron acceptor (electrode). Biofilms, however, require significant time to become established and as such, can lead to irreproducible power density.[65]

In order to address the design optimization of MFC, specific variables and limitations of the system must be defined. In order to evaluate modifications at the cathode, for

example, MFC require a standardized anode in which the number, activity and status of the bacterial population is known and controlled. Here, we demonstrate a method to associate bacterial cells in a silica matrix by using *S. oneidensis* as a model system to produce standardized anodes with defined bacterial physiology and electrochemical activity. Silica sol-gel materials have served well for diverse applications in electrochemistry but the process can often lead to cellular lysis.[70-73]

A one-step vapor deposition of silica provides an alternative to aqueous sol-gel formations that retains the activity of biomolecules and preserves integrity of whole cells.[74,75] (Figure 4.1) *S. oneidensis* DSP-10 cultures were harvested, washed and resuspended to a defined cell density ($1x10^9$ cfu·mL^{-1}). The cells were physisorbed with GF and exposed to tetramethylorthosilicate (TMOS) in vapor phase which undergoes rapid complete hydrolysis in the presence of high concentrations of water. Further condensation and cross-linking of the hydrolyzed silica monomers in the presence of high concentrations of salt (in the reaction), leads to gelation and particulate growth. The resulting matrix of silica particles immobilizes the bacterial cells directly to the GF (Si/cells-GF). The vapor-phase process eliminates the use of co-solvents or catalysts which are commonly used in sol-gel synthesis.[70] It is also likely that silica interacts directly with the cell membranes due to electrostatic interactions and hydrogen bonding leading to effective immobilization.[75] Control electrodes were physisorbed to GF with no subsequent TMOS exposure (Cells-GF).

4.2 Methods & Materials

‡*S. oneidensis* DSP-10 was cultured in Luria Bertani broth containing rifampicin (5 $\mu g \cdot mL^{-1}$) at 30°C, 100 rpm. Cells were harvested at late stationary phase (OD_{600} ~4-5) by centrifugation, washed (3x) and resuspended in phosphate buffered saline (PBS) to a final OD_{600} of 5. Corresponding colony forming units (cfu per mL) were determined by serial dilution and plate counts. Graphite felt (GF) (5 cm, 1/8", Morgan AM&T, Inc. Greenville, SC) electrodes were woven with ~20 cm titanium wire (0.25 mm, Goodfellow, Oakdale, PA) allowing ~10 cm for connections and sterilized in PBS before use. Sterilized GF was placed into a glass petri dish (100 x 10 mm) modified with a central glass well designed to hold the GF electrode. 5 mL of the harvested and washed culture was applied to the top of the graphite felt and TMOS (1 mL, Sigma Aldrich, St. Louis, MO) was deposited in the outer ring. Glass beads were added to the outer well to increase the surface area for evaporation. The dish was covered and incubated for 30 min at 37°C.

MFC were prepared in plastic funnels with anode and cathode separated by a polycarbonate membrane (0.2 μm) (Fig. S1). All experiments were maintained at room temperature (~22°C) unless otherwise stated. Sterile defined media[76] with lactate (20 mM) was used as MFC feed unless described otherwise. Open circuit electrode voltage (OCV) was measured using a Personal Daq/54 (IOtech, Cleveland, OH). Polarization potentials were measured on a VersaSTAT 3 potentiostat/galvanostat (Princeton Applied Reseach, Oak Ridge, TN) by varying the potential and recording steady state current values. Power was calculated using Ohms law and normalized, based on a geometric surface area of 21 cm^2. Samples were cut from the electrodes (in triplicate) and

incubated in NaOH (0.1N, 90°C, 30 minutes) to cause cellular lysis and release immobilized protein. Total protein content of cells was determined using the bicinchoninic acid protein (BCA) assay according to the manufacturer's instructions (Pierce Biotechnology, Rockford, IL).

4.3 Results & Discussion

Silica-coated bacterial cells were visible on the fibers of GF by scanning electron microscopy (SEM) (Fig. 4.1). Energy dispersive spectroscopy (EDS) conducted during SEM analysis confirmed that the particulate structure consisted of silicon and oxygen (data not shown). Samples of Si/cells-GF were subcultured to fresh growth medium and grew to pure culture, confirming that silica encapsulation did not hinder the viability of the cells.

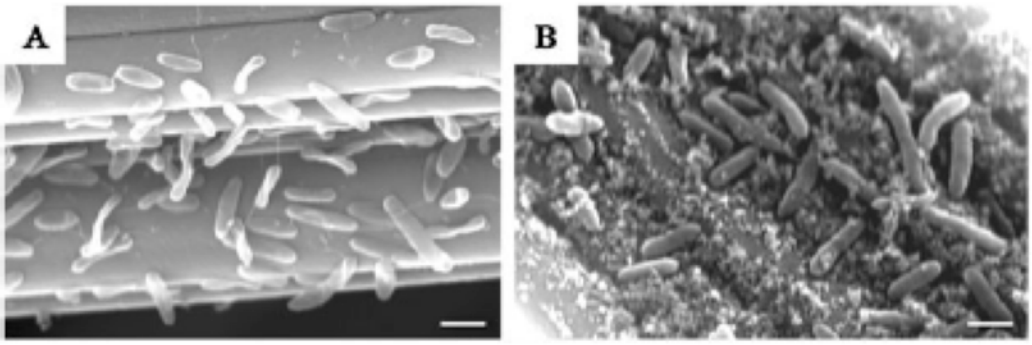

Figure 4.1: SEM of bacterial cells on GF electrodes in the absence (A) and presence (B) of silica matrix. Scale bars are 1 µm.

Although physisorbed cells were retained on the carbon fibers, (Fig. 1) the silica immobilization is expected to enhance reproducibility and association of cells at the electrode surface. Electrodes were assembled as anodes in a simple flow-through MFC with unmodified GF as cathode. A stabilized open circuit voltage (OCV) of 430±29 mV

(*n*=11) for Si/cells-GF and 385±117 mV (*n*=9) for Cells-GF was obtained with lactate as electron donor, in agreement with previous studies.[66] Si/cells-GF electrodes retained stable OCV for 48 hours (445±22 mV, *n*=6) whereas Cells-GF decreased over 48 hours (340±11 mV, *n*=5). The standard deviation for Cells-GF was significantly greater than for

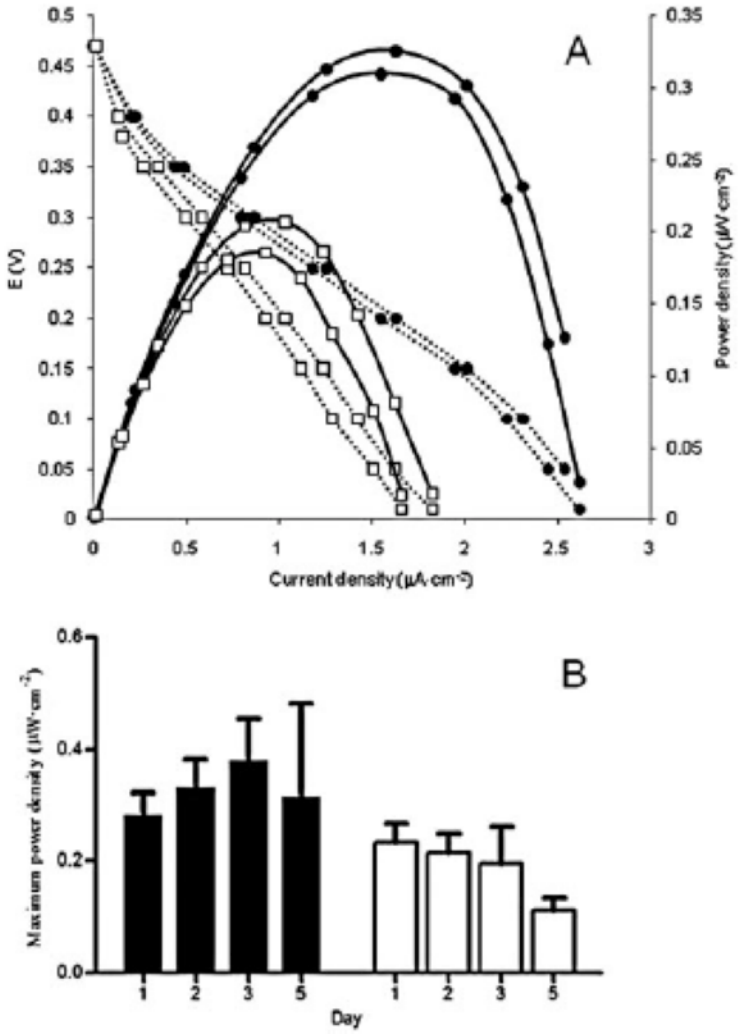

Si/cells-GF, confirming that the silica-encapsulation does provide a reproducible means for fabrication of MFC anodes. Maximum power density for Si/cells-GF (0.358±0.03 $\mu W \cdot cm^{-2}$) was higher than for Cells-GF (0.236±0.03 $\mu W \cdot cm^{-2}$). In addition, Si/cells-GF anodes retained a higher maximum power density with no loss of activity after 5 days of operation (Fig. 4.2).

Figure 4.2: (A) Power (solid lines) and polarization (dashed lines) curves for duplicate MFCs at 24 hours: Si/cells-GF (•) cells-GF (■). (B) Maximum power density over 5 days, Si/cells-GF (black bars), cells-GF (white bars).

Increased power density for Si/cells-GF is attributed to a greater number of active cells on the electrode surface. Protein determination assays confirmed that more cells were associated with Si/cells-GF (~3.45 mg protein·cm^{-2} after 5 days) than for Cells-GF (~2.05 mg protein·cm^{-2}). The loss of protein is attributed to cells being flushed from the MFC during the addition of medium, which results in a loss of power density and long term stability. Increased power output in Si/cells-GF may also be attributed to more efficient passage of electrons as the cells are tightly associated with the electrode.

The loss of cells due to flow-through elution was confirmed by varying the flow rate through the MFC. Under continuous flow, Si/cells-GF produced higher OCV, less variability in output and significantly higher voltage under load (330Ω) than Cells-GF (Table 4.1). The difference in output voltage under load was less significant at higher flow rates (1 mL·min^{-1}) but the maximum voltage sustained was higher for Si/cells-GF than for Cells-GF.

Silica-encapsulation of *S. oneidensis* clearly provides reproducible loading on GF that can be used to standardize anodes for further MFC stduies. As a proof of concept, we investigated the electrocatalytic activity of *S. oneidensis* in response to a range of potential electron donors (Table 4.2). The influence of electrolyte was determined in the same manner by substituting buffer for growth medium (Table 4.2). Glucose (under anaerobic conditions) was a comparatively poor substrate for power generation relative to

lactate, in agreement with previous studies.[77] Acetate and pyruvate demonstrated comparable power output to lactate, but was dependent upon substrate concentration and electrolyte (i.e. growth medium or buffer). There was no significant variation in protein

Table 1 Output potentials for MFC with *S. oneidensis* anodes under continuous flow

			Potential under 330 Ω load/mV		
	Flow rate/mL min^{-1}	OCV/mV	Min.	Max.	Mean ± SD
Cells–GF	0.5	92 ± 31	0.012	0.11	0.05 ± 0.24
Si/cells–GF	0.5	162 ± 4	0.256	0.47	0.35 ± 0.05
Cells–GF	1.0	146 ± 13	0.073	0.32	0.14 ± 0.04
Si/cells–GF	1.0	189 ± 6	0.036	0.71	0.14 ± 0.08

Table 2 Open circuit voltage and maximum power density for MFC with Si/cells–GF anodes and various electron donors

	OCV in media/mV		OCV in buffer/mV		
Electron donor	5 mM	20 mM	5 mM	20 mM	Max. power[a]/μW cm^{-2}
None	174 ± 83		188 ± 19		0.008
Glucose	196	314	ND[b]	268 ± 52	0.018
Acetate	245	219	ND	395 ± 50	0.035
Pyruvate	304 ± 74	367 ± 75	385 ± 39	446 ± 14	0.220
Lactate	398 ± 107	474 ± 25	431 ± 79	386 ± 33	0.129

[a] Max power in buffer (Note: power output in growth medium with lactate is given in the text). [b] ND = not determined.

density for Si/cells-GF electrodes incubated with growth media or buffer (296±42 and 306±42 μg·mL^{-1} protein (n=6) with 20 mM lactate in media and PBS respectively).

Tables 4.1 and 4.2

Silica-immobilization of *S. oneidensis* appears to provide protection against cell lysis. In-fact, when the incubation temperature for the MFC was varied much above physiological norm for *S. oneidensis*, Si/cells-GF allowed for an extended operating range and a shift in maximum power output to 45^{o}C and sustained ~65% of maximum power output up to 50^{o}C (Fig. 4.2). Cells-GF, in comparison, exhibited a typical bell-curve response to temperature, with maximum power output at 37^{o}C.

4.4 Conclusions

The vapor-deposition of silica creates a particulate matrix that enhances bacterial association with surfaces and negates the solvent toxicity of conventioanl aqueous sol-

gel techniques. The resulting silica matrix provides a stable and defined microbial community. In MFC, the ability to stabilize and standardize populations of *S. oneidensis* with repsect to electrocatalytic performance provides a platform for a range of characterization studies. Although the proof of concept demonstrated in this communication has an emphasis on MFC research, the methodology described can be readily applied to immobilizing other microorganisms for industrial applications. The silica matrix, in essence, mimics the exopolysaccharide 'glue' that binds cells in a natural biofilm. This synthetic process, however, eliminates the significant cultivation times and variability typically associated with natural biofilm formation, thereby facilitating electrochemical studies on a standardized platform.

Chapter 5 – Facile Fabrication of Scalable, Hierarchically Structured Polymer/Carbon Architectures for Microbial Fuel Cell Electrodes

Co-authors: Heather R. Luckarift, Susan R. Sizemore, Karen E. Farrington, Carolin Lau, Plamen Atanassov, & Glenn R. Johnson

5.1 Abstract

This research introduces a method for fabrication of biological fuel cells electrodes from porous polymer/carbon composites with hierarchical structure. We demonstrate the fabrication of (3-hydroxybutyrate-*co*-3-hydroxyvalerate) (PHBV) scaffolds doped with carbon materials that provide a conductive three-dimensional architecture with application in microbial fuel cell (MFC) anodes. Composite electrodes from PHBV can be fabricated to defined dimensions by solvent casting and particulate leaching of a size specific porogen (in this case, sucrose). The cellular biocompatibility of the resulting composite material facilitates effective immobilization of a defined preparation of *S. oneidensis* DSP-10 as a model microbial catalyst. Bacterial cells are immobilized via chemical vapor deposition (CVD) of silica to create an "artificial biofilm" that exhibits efficient bio-electrocatalysis of a carbon fuel in a MFC setting (Figure 5.1). DSP-10 functionalized PHBV electrodes demonstrate stable and reproducible anodic open circuit potentials of -320 ± 20 mV (vs. Ag/AgCl) with lactate as the electron donor. Maximum power densities achieved by the hierarchically structured electrodes (~5 mW cm^3) were significantly higher than previously observed for graphite-felt electrodes. The methodology for fabrication of scalable electrode materials may be amenable to other

bio-electrochemical applications, such as enzyme fuel cells, sensors and could easily be adapted to various MFC design concepts.

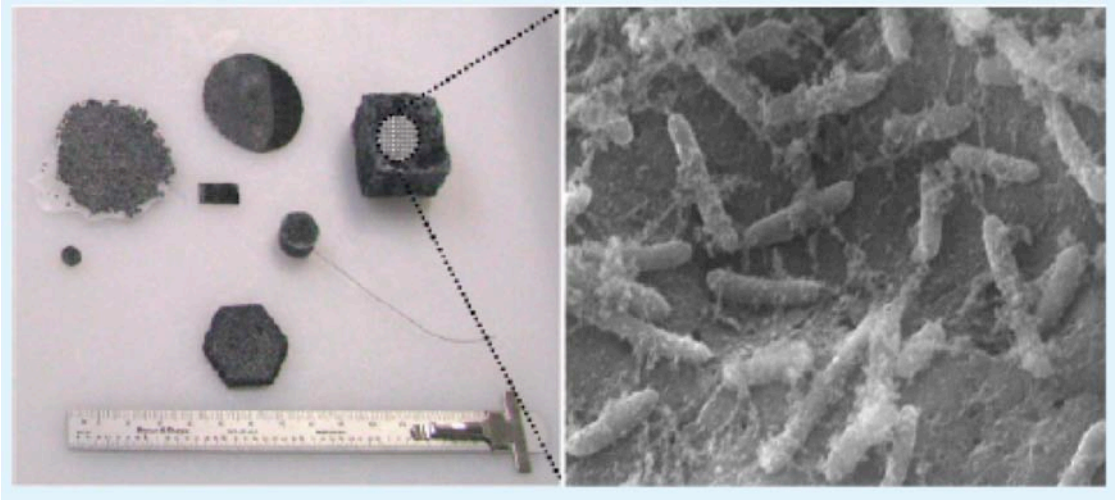

Figure 5.1: Large scale image of assembled electrode in various configurations and SEM image of *S. oneidensis* DSP-10 immobilized in a SiO_2 thin film on the electrode surface

5.2 Introduction

Microbial fuel cells (MFC) have been receiving increased attention because of the ability to integrate controlled bioprocesses with energy harvesting and power generation technology. In a typical MFC anode, dissimilatory metal-reducing bacteria convert chemical energy to electrical energy by transferring electrons from reduced electron donors (e.g. lactate) to insoluble electron acceptors (e.g., the electrode interface).[63,78] In nature, bacteria maximize the use of insoluble electron acceptors (usually Fe or Mn oxides) by excreting extracellular polymers that serve to bind the growing cell population into a structured biofilm.[68,69] Biofilms, however, require significant time to become established, which often leads to variable and irreproducible power density when applied

to MFC design.[65] The variability of natural biofilm formation can be circumvented, however, by attaching bacteria in a manner that preserves the integrity of whole cells and defines the number, activity and physiological status of the bacterial population.[79] Encapsulating a defined population of cells in a silica matrix mimics the natural phenomenon, and provides a rapid and controlled approach to defining an 'artificial biofilm'.[79] Such engineered biofilms can prove facile in designing MFC or devices that integrate bacterial cultures in general, and provide a unique opportunity to fabricate devices with microbial communities that are not traditional biofilm-formers.

Achieving efficient energy transfer to the microbial cells of an MFC biofilm requires an electrode material that is conductive, yet biocompatible enough, to provide an interface for bacterial interactions. Numerous conductive and carbonaceous materials have been investigated to support anodic reactions in MFC development.[78,80] Many potential anode materials, however, are restricted in application by limitations of scalability, cost-effectiveness and conformal manufacturability.[81] Fabricating conductive scaffolds from biopolymers may provide a technology to make three-dimensional composites with tailored structural and mechanical properties. It is desired for such materials to have hierarchically architecture with structured porosity in order to provide ready nutrient access through a large pore volume. At the same time, the architecture requires sufficient surface area to allow a high cell density to be immobilized in a minimal volume in order to maximize the volumetric power density of the MFC. Attempts to integrated biopolymers such as chitosan,[82,83] and cellulose,[84] to form conductive matrices when

doped with carbon nanotubes,[85] have charted the onset of such a materials design strategy.

Bacteria excrete a wide variety of biopolymers that find application in the development of a new class of materials called bioplastics.[86] Polyhydroxyalkanoates (PHA), such as poly (3-hydroxybutyrate) (PHB) and (3-hydroxybutyrate-*co*-3-hydroxyvalerate) (PHBV), are extracellular monomers that serve as carbon and energy stores for bacterial cells.[86,87] These biological polymers are biocompatible with a wide variety of cell types and Therefore find application in tissue engineering.[88] Adding extra functionality to bioplastics extends the versatility of the polymer scaffolds to applications such as drug delivery and biosensing. PHA composites that include ceramic particles for enhanced mechanical strength, anti-oxidative vitamins to enhance biocompatibility, or composites with added carbonaceous materials to provide conductive properties, have all been demonstrated.[89-96]

PHA polymers are stable under typical MFC conditions (neutral pH and ambient temperatures), inexpensive and can be fabricated to conformal shapes and scales. In addition, the biocompatible properties of the polymer encourage cellular retention and provide a scaffold that is amenable to flow through configurations. The porosity of PHA can be controlled by careful choice of the scaffold template. In most cases a water-soluble, low-molecular weight species provides the template or pore-forming agent. Simple solvent casting and particulate leaching of sucrose, for example, provides rapid templating of a pre-determined architecture.[90] The characteristics of scaffold architecture

of a conductive PHA composite are investigated herein in respect to anode performance with *S. oneidensis* DSP-10 as a model organism and used to demonstrate a facile method for fabricating highly reproducible, easily integrated and stable MFC anodes.[97]

5.3 Methods & Materials

5.3.1 Chemicals

Poly (3-hydrobutyate-*co*-3-hydroxyvalerate) (PHBV) with 12% poly (hydroxyvalerate) content, and graphitized carbon nanofibers (CF; hollow fibers 80–200 mm o.d., 0.5–10 nm i.d., length 0.5–20 μm) were purchased from Sigma-Aldrich (St. Louis, MO). Sucrose was purchased as a general grocery item as common household sugar and sieved to a defined size using 30–60 mesh screen sieves (0.250–0.595 mm particle size).

5.3.2 Preparation of PHBV/CF Scaffolds

Wet sucrose was mixed with CF (100:1 w/w), hand-pressed into cylindrical pre-fabricated molds (1.3 x 0.9 cm; volume = 1.195 cm^3) and dried overnight at 37 °C. All sucrose/CF mixtures were pressed around a circle of nickel mesh (40 mesh, Alfa Aeser, Ward Hill, MA) to act as a current collector that was connected externally via a length of titanium wire (0.25 mm diameter, Goodfellow, Oakdale, PA). PHBV was dissolved in chloroform (0.04% w/v), heated to 60 °C and applied to the sucrose/CF template until all of the PHBV solution was incorporated. After overnight drying at 25 °C, the resulting polymer (PHBV/CF) was immersed in deionized water (0.3 L) for 2 hours to dissolve away the sucrose (Scheme 1). The resulting composite electrodes are designated as

$PHBV_{30}$/CF and $PHBV_{45}$/CF for PHBV/CF composites formed with 30 and 45 mesh size sucrose respectively.

5.3.3 Growth and Immobilization of *S. oneidensis* DSP-10

S. oneidensis DSP-10 was cultured in Luria Bertani broth containing rifampicin (5 μg mL^{-1}) at 30 °C, 150 rpm. Cell counts were determined by conventional serial dilution, plating and counts of colony forming units per mL (cfu mL^{-1}). Cells were harvested at late stationary phase (OD_{600} ~4-5), washed (x 3) and resuspended in phosphate buffered saline to a defined cell density (1 x 10^9 cfu mL^{-1}). DSP-10 was immobilized to the PHBV/CF composite electrodes using a method for silica-encapsulation described previously.[79] Briefly, PHBV/CF electrodes were placed in a glass Petri dish (4.5 cm diameter) modified with a central glass well (1.7 cm diameter) to accommodate the electrode. The cell suspension (1 mL) was added to cover the PHBV/CF electrode and tetramethylorthosilicate (TMOS; 0.2 mL) was added to the outer well. TMOS in vapor phase undergoes rapid hydrolysis in contact with aqueous solvents of high salt concentration and leads to rapid formation of particulate silica. The resulting matrix of silica particles immobilizes the bacterial cells directly on the PHBV/CF surface. For control experiments, PHBV/CF electrodes were incubated with a suspension of DSP-10 as prepared above, but in the absence of TMOS. Cell viability and loading on PHBV/CF electrodes was determined using a microbial cell viability assay based on relative luminescence units (RLU) for direct quantification of ATP according to the manufacturer's instructions (BacTitre-Glo® Reagent, Promega, Madison, WI).

5.3.4 Electrochemical Measurements

Electrochemical measurements were made in a one-compartment electrochemical cell (50 mL European 5 neck flask with 3 14/20 fittings and 2 #7 threads; Ace Glass, Vineland, NJ) containing 30 mL electrolyte (potassium phosphate buffer/ KCl, 0.1 M, pH 7.0) with lactate (20 mM) as electron donor (fuel), unless otherwise stated. Electrolyte was purged continuously with nitrogen to ensure anaerobic conditions. Measurements consisted of the PHBV/CF anode as working electrode, a glassy-carbon counter electrode (Metrohm USA, Riverview, FL) and a standard Ag/AgCl reference electrode (CH Instruments Inc., Austin, TX). Cyclic voltammetry and polarization studies were controlled using a potentiostat (Versastat 3; Princeton Applied Research, Oak Ridge, TN). Power was calculated using Ohms law and values normalized to the geometric volume (1.195 cm^3).

5.3.5 Porosity and Contact Angle Measurements

Pore size distribution was determined (triplicate samples) using a surface area analyzer (Micromeritics Gemini, Norcross, GA) based on adsorption isotherms over various relative pressure ranges according to the manufacturer's instructions. Pore measurements were interpreted by applying Brunauer-Emmett-Teller (BET) and Barrett-Joyner-Halenda (BJH) algorithms to determine micropores ($P/Po < 0.05$) and meso-pores ($P/Po > 0.05$). Contact angle measurements were obtained using the sessile drop method with a drop shape analyser (DSA100 Krűss, Mathews, NC) according to the manufacturer's instructions.

5.3.5 Imaging and Microscopy

Scanning electron microscopy (SEM) was used to visualize the interior and exterior features of the composite materials. PHBV/CF anodes with bacteria were fixed with 2.5% glutaraldehyde in cacodylic buffer (0.1M), dehydrated in ethanol, and fixed by critical point drying according to the manufacturer's instructions (Autosamdri®-815, Tousimis Research Corp. Rockville, MD). Non-conductive samples were sputter-coated with gold (Denton Desk-V, Denton vacuum LLC, Moorestown, NJ) and all samples were examined by SEM (Hitachi HTA, Pleasanton, CA).

5.4 Results & Discussion

5.4.1 Fabrication of 3D Hierarchically Structured Polymer/Carbon Electrodes

Hierarchically structured 3D electrodes were fabricated from PHBV/CF composites using a method of solvent casting and particulate leaching, with sucrose as a template/porogen (Figure 5.2). The mesh size of the sucrose was controlled by size-selective sieving, and sucrose of 30 mesh (<595 μm) and 45 mesh (<354 μm) were found to be optimal in respect to ease of fabrication. Increasing the sucrose mesh size resulted in packed template scaffolds that were too dense for polymer to penetrate. In contrast, decreasing the mesh size of the sucrose (or using sucrose that was not sieved) resulted in a polymer matrix that was poorly interconnected and Therefore mechanically brittle. The crystal size of the sucrose defines the porosity within the final structure and dictated the formation of a primarily macroporous/mesoporous internal structure (Figure 5.2, Table 5.1). For MFC applications, an open porous structure is desirable to ensure unrestricted acess of nutrients (fuel) through convective flow and diffusion, combined with large

surface area of the porous matrix to encourage interaction between bacterial cells and the anode interface.[81]

The PHBV/CF composites are formed directly around a nickel mesh current collector, thereby providing an electrode that can be fabricated without the need for any further

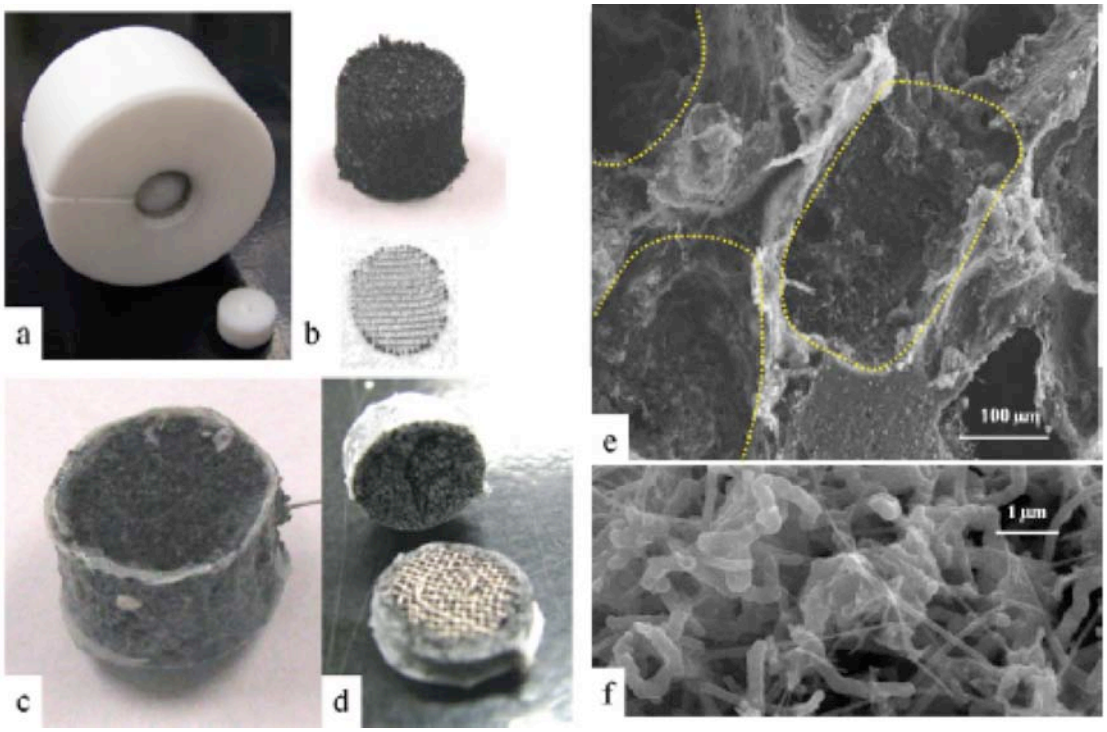

Figure 5.2: Schematic of polymer/carbon (PHBV/CF) composite fabrication. (a) A die is used to (b) pack sucrose/CF around a nickel mesh current collector. (c) The resulting sucrose/CF scaffold is intercalated with polymer and (d) the sucrose removed to form a porous scaffold. Final electrode cut to show the interiorer nickel mesh. (e) The sucrose dissolves and leaves a hole of a size comparable to the original particles (yellow dashed lines) that is (f) interconnected with carbon fibers.

supporting material. The resulting PHBV/CF composites provide a lightweight structure with a hierarchical porosity as observed by SEM (Figure 5.3). By initially mixing the CF with the sucrose, the conductive carbon becomes an integral part of the porogen scaffold and creates a homogenous distribution of carbon throughout the final matrix. The

presence of CF within the microstructure of the PHBV composites is clearly evident from SEM when compared to PHBV polymer prepared in the absence of CF. The addition of CF adds a surface roughness to the polymer matrix that increases the surface area.

Table 5.1: Materials Characterization of PHBV/CF Composites

	Unprocessed carbon nanofibers (CF)	$PHBV_{30}$/CF	$PHBV_{45}$/CF
BET[a] (m^2/g)	ND[d]	4.69	4.41
micropore surface area[b] (m^2/g)	ND	2,906	0.102
conductivity (Ω/g)	20.4	51.2	36.8
EASA (cm^2/g)	ND	667	454
density (g/cm^3)	ND	0.14	0.15

[a]BET specific surface area. [b]Micropores <2 nm, [c]EASA: electrochemically accessible surface area. [d]ND: not determined

Static contact angle measurements of the composites confirmed the hydrophobic nature of the unmodified polymer (contact angle of 106.2 ± 8.7 and 101.1 ± 13.4 for $PHBV_{30}$ and $PHBV_{45}$ mesh respectively, n = 6) in agremment with previous reports.[91] The wetability of the composites increased significantly when carbon fibers (CF) were included in the structure and decreased the contact angle to essentially zero (Table 5.1). The additional effective roughness of the CF within the polymer matrix may add to the increased hydrophilicity of the matrix. A similar observation was previously noted for the inclusion of bioactive glass within composites of PHB.[91]

The conformal distribution of CF with the polymer matrix also renders the matrix conductive (Table 5.1). The presence of CF resulted in an increase in capacitance current

attributed to the formation of an interconnected network of CF that provides conductivity throughout the matrix. As expected, for such a porous material, the conductivity increases with compression (Table 5.1). Increased compression forces the CF within the porous structure into close proximity and thereby increases the bulk conductivity.

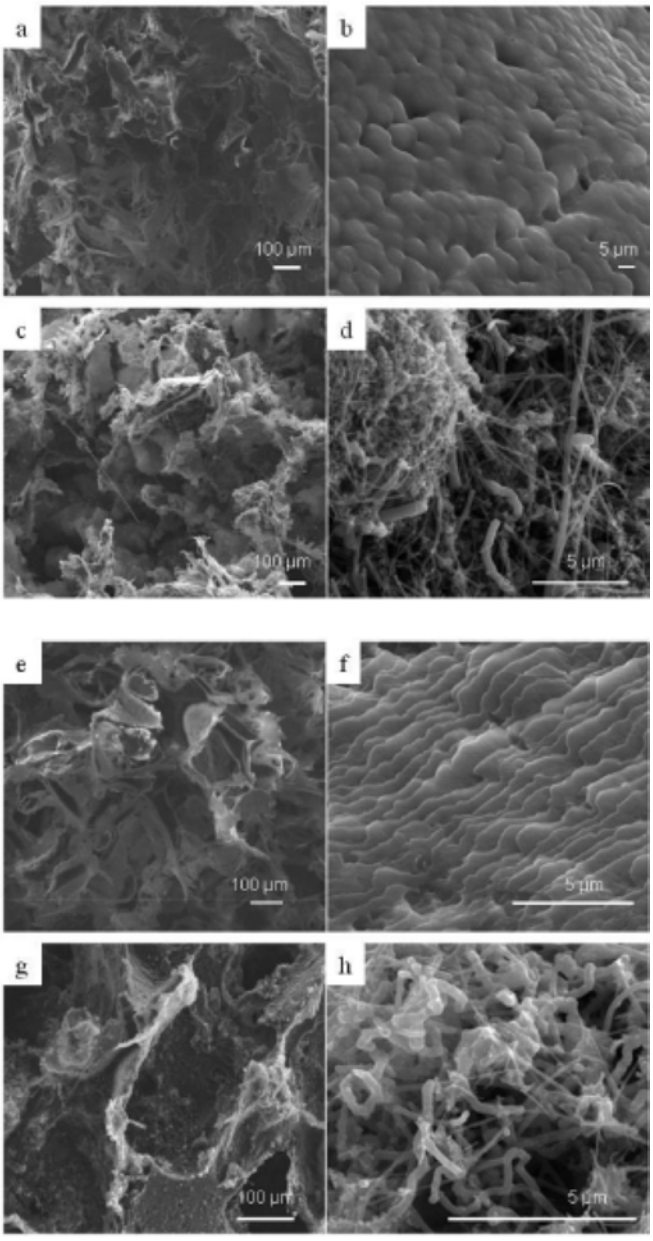

Figure 5.3: SEM micrographs of cross-sections of PHBV composites with and without CF. (a,b) $PHBV_{30}$ (c,d) $PHBV_{30}$/CF, (e,f) $PHBV_{45}$ (g,h) $PHBV_{45}$/CF

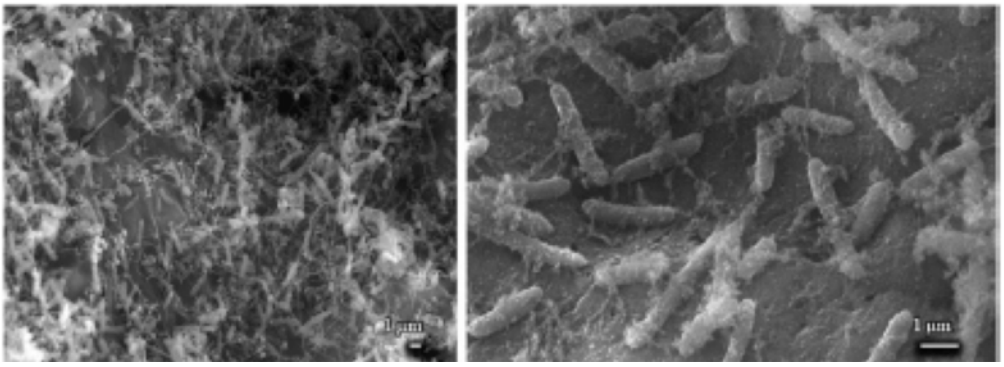

Figure 5.4: SEM micrographs of *S. oneidensis* DSP-10 immobilized to PHBV/CF composites via silica vapor deposition.

5.4.2 Characterization of Hierarchically-Structured PHBV/CF Electrodes as Anodes for MFCs

Initial characterization of the PHBV/CF electrode materials confirmed the fabrication of a conductive polymer composite with properties that would be advantageous for MFC applications. As such, MFC anodes were prepared by immobilizing *S. oneidensis* DSP-10 to the surface of PHBV/CF via silica encapsulation.[79] The stabilized open circuit potential (OCP) of the bacterial anodes was -322 ± 18 and -328 ± 16 mV (vs Ag/AgCl) (n = 4) for $PHBV_{30}$/CF and $PHBV_{45}$/CF respectively, with lactate as the electron donor. OCP values were highly reproducible across replicate electrodes, even when fabricated from distinct bacterial cultures prepared days or weeks apart. Control anodes in the absence of cells exhibit no electrocatalytic activity besides Faradic capacitance and OCP of ~150 mV (vs Ag/AgCl) (data not shown). The high reproducibility of the MFC anodes prepared in this manner is attributed to the silica 'binder' – an inorganic, highly porous encapsulation matrix, which serves to create an 'artificial biofilm' of a defined cell density at a specific

metabolic state.[79] The short time required to achieve a stable and reproducible MFC anode is advantageous and significantly reduces the time delay (often several days) typically required to establish a natural biofilm and achieve maximum cell potential.[65,81] The physical entrainment of bacterial cells at the anode surface could be visualized and verified by SEM and indicated homogenous distribution when analyzed at various cross-sections throughout the matrix (Figure 5.3). As SEM imaging is only qualitative, quantitative enumeration of viable microbial cells on the anode was further determined by using ATP as an indicator of metabolically active cells. Cell counts of $2.4 \times 10^7 \pm 1.2 \times 10^7$ and $6.8 \times 10^7 \pm 2.1 \times 10^7$ cfu mg^{-1} polymer were determined for $PHBV_{30}$/CF and $PHBV_{45}$/CF composites respectively and confirmed high cell loading on the composite material.

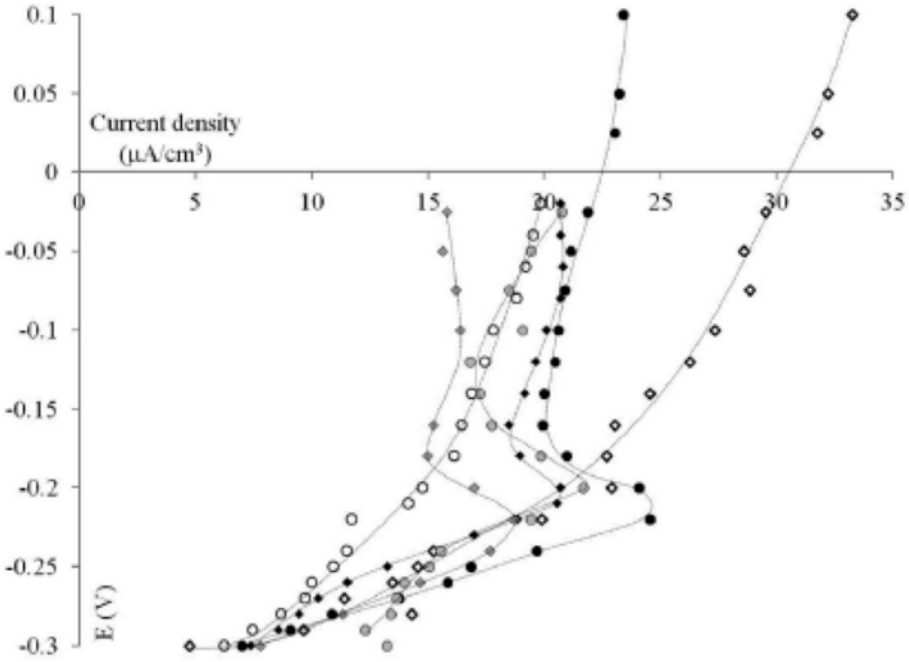

Figure 5.5: Polarization curves for $PHBV_{30}$/CF (circles), $PHBV_{45}$/CF (diamonds) with immobilized DSP-10.

Control PHBV/CF electrodes incubated with DSP-10 to allow the formation of a natural biofilm on the electrode surface confirmed that the electrocatalytic characteristics of DSP-10 are reflective of native electron transfer processes and not artifacts of the immobilization procedure. Physisorbed cells attained a maximum OCP of ~ -300mV (vs Ag/AgCl), but required significantly longer incubation times (>5 hours) to reach stable output potentials.

Electrochemically active microbial species, such as DSP-10 are known to excrete redox active mediators that aid in electron transfer.[66] The bacterial cell cultures used in anode preparation were washed thoroughly before encapsulation to remove any soluble mediators. Washed cells, however, retain electrocatalytic activity and generate electrical current from the onset. *S. oneidensis* sp. are often reported to exhibit a redox response associated with the production of riboflavin as a soluble mediator, but no such flavin was observed (E^o = -405 mV vs Ag/AgCl at pH 7.0) following the immobilization protocol described herein.[98] Initial current output is Therefore attributed to mechanisms for direct electron transfer, arising due to interaction between the cells and the electrode surface.

The maximum current density of the DSP-10 functionalized PHBV/CF anodes was comparable irrespective of the template mesh size (22.02 ± 2.37 and 22.18 ± 6.69 $\mu A/cm^3$ [n = 3], for PHB_{30}/CF and $PHBV_{45}$/CF respectively) and produced maximum power densities approaching 5 $\mu W/cm^3$ (4.23 ± 1.22 and 4.38 ± 0.18 $\mu W/cm^3$ [n = 3] for $PHBV_{30}$/CF and $PHBV_{45}$/CF mesh respectively) (Figure 5.5). This is in agreement with the hypothesis that the pore-forming/templating ensures the macropore structure and the

biological catalyst immobilization capacity is determined by the meso-porosity obtained from the CF component of the polymer/carbon composite matrix. Current density reaches a maximum that is sustained between -0.2 and 0 V and any further increase in current output is limited by mass transport effects. The internal resistance of the MFC anodes 6.6 ± 1.0 and 8.8 ± 3.8 Ω (n=3) were calculated from the slope of the polarization curve during the linear region (-0.3 to -0.2 V) for $PHBV_{45}$/CF and $PHBV_{30}$/CF respectively [62].

Under potentiostatic conditions (-0.15V vs Ag/AgCl), $PHBV_{30}$/CF and $PHBV_{45}$/CF anodes maintain a stable current for 8 hours with no loss in efficiency and confirm the stabilization of the bacterial population at the anode surface (Figure 5.6).

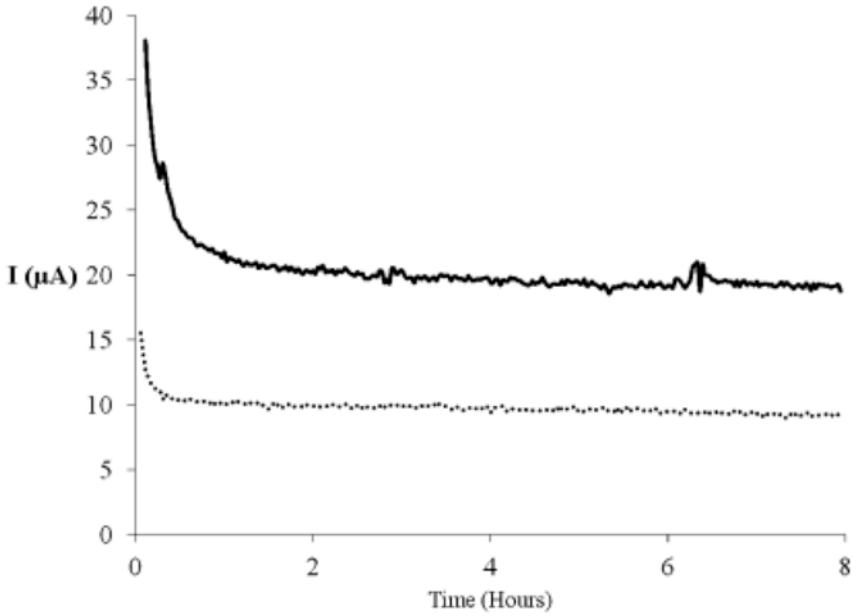

Figure 5.6: Chronoamperometry of PHBV30/CF (dashed line) and PHBV 45/CF (solid line) at -0.15 V vs Ag/AgCl (3 M KCl)

5.5 Conclusions

We demonstrate the facile fabrication of a conformal, 3D porous carbon/polymer material that provides a structure amenable to microbial attachment in an MFC anode. The materials exhibit hierarchical porosity and structure that can be controlled by the size of the pore-forming agent (sucrose) and by the characteristics of the carbon fiber (or other carbonaceous material) used. Immobilization of *S. oneidensis* DSP-10 via encapsulation in a CVD grown silica matrix creates an 'artificial biofilm' that provides rapid and reproducible electrocatalytic activity as evidenced by replicate MFC anodes. The biocompatibility of the PHBV facilitates interaction between the microbial population and the electrode surface and establishes efficient electron transfer between the immobilized biocatalysts (the artificial biofilm' of DSP-10) and the polymer/carbon electrode interface. The fabrication methodology makes a free form or a cast form anode that can be integrated with numerous cathode configurations and is conformal to system design and versatile in various applications. The techniques described herein provide a platform for designing MFC anodes that may also be extended to cathode design or for microbial or enzyme-based fuel cell electrodes.

Chapter 6 – Microbial-Enzymatic-Hybrid Biological Fuel Cell with Optimized Growth Conditions for *S. oneidensis* DSP-10

Co-Authors: Carolin Lau, Heather R. Luckarfit, Susan R. Sizemore, Karen E. Farrington, Plamen Atanassov, & Glenn R. Johnson

6.1 Abstract

In this work we present a biological fuel cell fabricated by combining a *S. oneidensis* microbial anode and a laccase-modified air-breathing cathode. This concept is devised as an extension to traditional biochemical methods by incorporating diverse biological catalysts with the aim of powering small devices. In preparing the biological fuel cell anode, novel hierarchical-structured architectures and biofilm configurations were investigated. A method for creating an artificial biofilm based on encapsulating microorganisms in a porous, thin film of silica was compared with *S. oneidensis* biofilms that were allowed to colonize naturally. Results indicate comparable current and power densities for artificial and natural biofilm formation, based on growth characteristics. As a result, this work describes methods for creating controllable and reproducible bio-anodes and demonstrates the versatility of hybrid biological fuel cells.

6.2 Introduction

Microbial fuel cells (MFCs) present a novel energy harvesting technology with potential applications in municipal, agricultural and industrial wastewater treatment processes.[58] MFCs may be coupled with a range of biological catalytic material to extend utility to a new generation of bioelectrochemical devices with potential application in biosensors or

other small-scale devices. In this work we present a "hybrid" biological fuel cell assembly with lactate as a fuel that is oxidized by *S. oneidensis* at the anode, in concert with a laccase modified air-breathing cathode for cathodic oxygen reduction. By combining these two electrode technologies, we create a true biological fuel cell with no inorganic catalysts or exogenously added electrochemical mediators. Previous reports of a hybrid microbial–enzymatic biofuel cell demonstrate the proof-of-concept.[99,100] The aim of the work described herein is to address the formation of *S. oneidensis* biofilms optimized for such systems.

The anodic catalyst, *S. oneidensis* DSP-10, is a model dissimilatory metal reducing bacterium (DMRB) with a known ability to reduce insoluble electron acceptors in the environment and, as such, is commonly used in MFC studies at the laboratory scale.[20] The exact pathway of insoluble electron acceptor respiration in these organisms is disputed; however, it is known that environmental stimuli will cause a metabolic shift towards metal oxide respiration.[21,30,101] This puts into question the ability, or more specifically, under which conditions *S. oneidensis* will form biofilms active in metal oxide respiration, or in this case, biological anode reduction. Herein, we compare specific physiological environments (i.e. aerobic *vs.* micro-aerobic) and culture conditions (complex Luria broth *vs.* defined medium) to determine the effect on biofilm formation and electrochemical response. For comparison, planktonic cells cultured in the same growth media were artificially attached to an electrode by chemical vapor deposition (CVD) of the silicon precursor tetramethyl orthosilicate (TMOS) that forms a thin film of

silica over the microorganisms; effectively binding the bacterial population to the electrode.[102]

The effect of different anode architectures was also investigated for reticulated vitreous carbon (RVC), RVC modified with a surface coverage of multi-walled carbon nanotubes (RVC-CNT) and a hierarchically-structured biocompatible poly-hydroxybutyrate-co-valerate polymer/ carbon fiber electrode (termed PHBV/CF). The PHBV/CF electrode was elected as the optimal anode material due to the apparent higher bioelectrocatalytic activity and stability when compared with the other materials.

6.3 Methods & Materials

6.3.1 Chemicals

All chemicals were obtained from Sigma-Aldrich (St. Louis, MO) and of highest available purity unless otherwise stated.

6.3.2 Anode Material Fabrication

PHBV/CF electrode fabrication was reported previously.[103] Briefly, 1 g sieved (354 mesh) sugar "porogen" was mixed with 0.02 g graphite nanofibers by adding 2 drops of DI H_20. The mixture was pressed in a size-specific mold around a Ni mesh current collector. The compressed porogen scaffold was removed from the mold and allowed to dry overnight in a low-humidity environment. To form the PHBV polymer matrix, 0.2 g polymer (poly-3-hydroxybutyric acid-co hydroxyvaleric acid; PHV content 12%) was dissolved in chloroform (3 mL) and heated to ~60 °C. The polymer mixture was applied drop-wise to the porogen scaffold (with additional chloroform as required) until all

polymer was deposited into the scaffold. The polymer was allowed to dry overnight, and the sugar porogen was dissolved out of the electrode by the soaking in ~0.5 L DI H_20. The resulting polymer electrode was dried and any excess polymer trimmed from the edges. Reticulated vitreous carbon (RVC) was from Electrolytica, Inc of Amherst, NY. Multi-walled carbon nanotube modified-RVC (RVC-CNT) was fabricated in-house, based on previous established methodology.[104]

6.3.3 Cathode Preparation

The gas-diffusion cathode was prepared by a modified method described previously.[105] The cathode structure was prepared by pressing 100 mg of hydrophobized carbon black (Vulcan XC72®, Cabot, MA, USA) at a pressure of 1000 psi for 5 minutes onto a Ni mesh current collector. The hydrophobized carbon black contained 35% by weight of Teflon® to form a hydrophobic layer on the Ni mesh current collector. One side was treated with 0.1 mL isopropyl alcohol (IPA) for 30 minutes to form a hydrophilic-catalytic layer. A solution of laccase (from *Trametes versicolor*) was prepared in chloride-free phosphate buffered saline (pH 6.3) to a final concentration of 4 $mg \cdot mL^{-1}$. The electrode was incubated in the laccase solution for 5 hours at room temperature to allow physisorption of the enzyme onto the hydrophilic side.

6.3.4 Bacterial Culturing and Biofilm Formation

S. oneidensis DSP-10 was cultured aerobically in Difco Luria broth (LB; Fisher Scientific, Pittsburgh, PA) containing rifampicin (5 $\mu g \cdot mL^{-1}$) at 30 °C, with shaking (120 rpm). Cells were harvested at late stationary phase (OD_{600} ~4) by centrifugation, washed (3x) and resuspended in PBS to a defined cell density (OD_{600} =5; equivalent to ~1 x 10^9

cfu/mL). The cell suspension was immobilized to the electrode by CVD of silica using methodology described previously.[102] Electrodes prepared in this manner are defined Si-biofilm-LB. For natural biofilm formation, electrodes were incubated in growing cultures and recovered from solution at a time equivalent to the late stationary phase of growth (biofilm-LB).

S. oneidensis DSP-10 was similarly cultured in a defined medium (DM) previously described, [40] containing rifampicin (5 μg·mL-1) at 30 °C, with shaking (120 rpm) and modified to contain sodium fumarate (30 mM) as a terminal electron acceptor. The culture was incubated in a capped shaker flask to simulate micro-aerobic metabolism; as oxygen is consumed, fumarate acts as an alternative electron acceptor. The resulting culture was harvested at late stationary phase (OD_{600} ~0.3) by centrifugation, washed (3x) and resuspended in PBS. The washed cell suspension was encapsulated onto the electrode as described above and defined Si-biofilm-DM. For natural biofilm formation, electrodes were incubated in growing cultures and recovered from solution at a time equivalent to the late stationary phase of growth (biofilm-DM).

6.3.5 Electrochemical Characterization

All biofilm anode formulations were allowed to stabilize in a solution of PBS purged of saturated O_2 by sparging with N_2. The open circuit potential (OCP) was measured against a Ag/AgCl [sat'd KCl] reference electrode using a data acquisition device. Similar measurements were made for the OCP of the cathodes in solution saturated with O_2 to confirm the oxygen reduction activity of the enzyme. When individual electrodes exhibited stabilized OCP, they were combined in a modified stack cell,[106] (Figure 6.1)

with a separation of approximately 1.5 cm, (Note: no membrane was used in this data set). The N_2-sparged analyte consisted of 50 mM sodium phosphate buffer with 20 mM sodium lactate as the fuel source. Chronoamperometry and potentiometry measurements were performed using a potentiostat, either a Versastat or Bio-Logic. Polarization and power curves are reported normalized to the geometric volume of the anode; the limiting

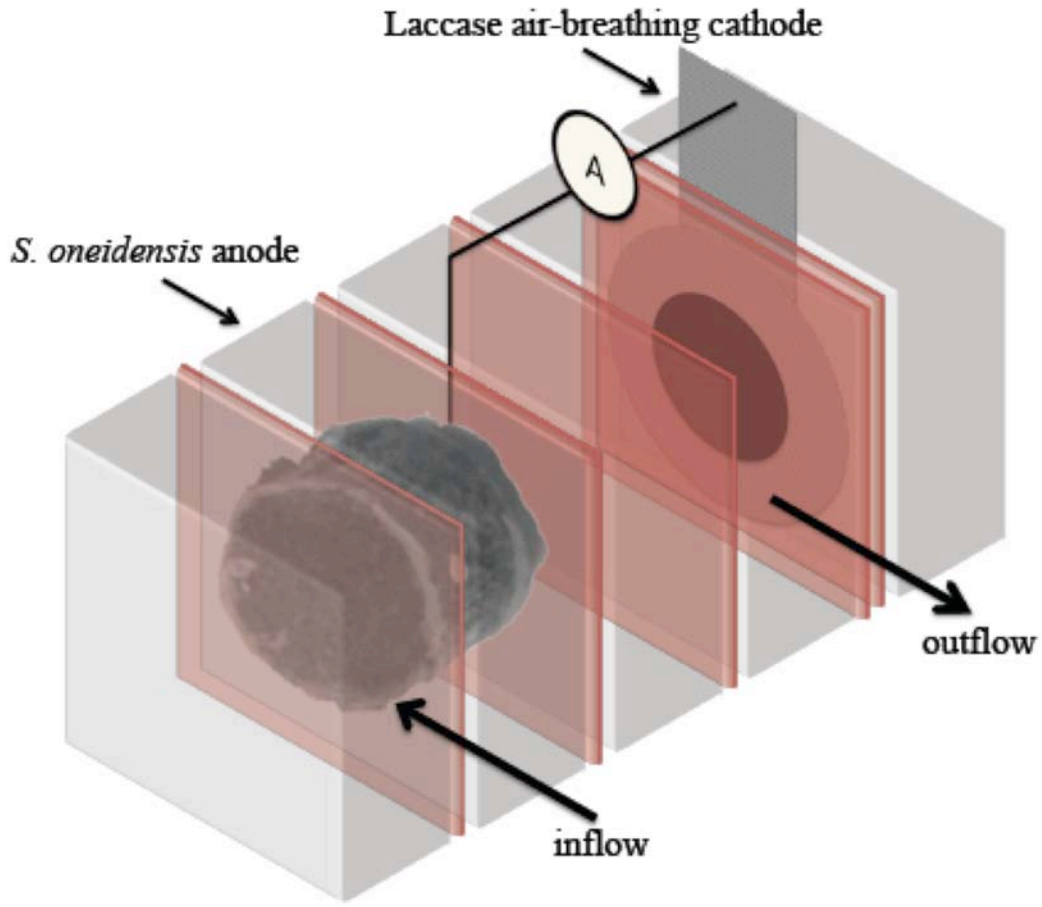

electrode in these experiments. Experiments to determine the operating conditions of the biological fuel cell were conducted in the stack cell with a suitable load, calculated from polarization curves and the OCP, again measured using a data acquisition device.[107]

Figure 6.1: Diagram of stack cell configuration of the final fuel cell assembly. Each component of the inter-changeable stack is separated by a rubber gasket (in pink), the anode and cathode are connected by an external current collector, at 3 cm apart.

6.3.6 SEM Characterization

After electrochemical characterization, anodes were dissected for SEM preparation with the biomass being fixed to the electrode by soaking for 1 hour in 0.1 M cacodylate buffer containing 2.5% glutaraldehyde. Samples were soaked in increasing concentrations of ethanol in water for 10 minutes each (50, 60, 70, 80, 90, 100 %). The samples were then preserved by critical point drying according to the manufacturer's instructions (Tousimis®, Rockville, MD) and coated with gold using a Denton V sputter-coater (Denton Vacuum, LLC, Moorestown, NJ) to a thickness of ~10 nm.[38,108] Once the samples were prepared for SEM examination, imaging was performed using a Hitachi model S-2600N scanning electron microscope.

6.4 Results & Discussion

6.4.1 Anode Material Selection

In an effort to optimize biofilm formation at the anode, three types of hierarchical materials were investigated as electrodes; all are three-dimensional and provide increased surface area for biomass attachment. *S. oneidensis* DSP-10 was grown aerobically in LB and allowed to directly form a biofilm on the surface of three materials: i) RVC, ii) RVC-CNT and iii) PHBV/CF. After biofilm formation on the respective electrodes, OCP was measured over time. The RVC anode stabilized at -100 mV vs Ag/AgCl [sat'd KCl] (Figure 6.2). In contrast, RVC-CNT initially exhibits a relatively low OCP of about -350 mV. However, this electrode was unable to sustain this thermodynamic potential and the OCP was relatively inconsistent over the measurement period, rising in a final OCP of

approximately -250 mV. Finally, the PHBV/CF anode attained an initial open circuit potential of -250 mV that was stabile and sustained for >16 hours.

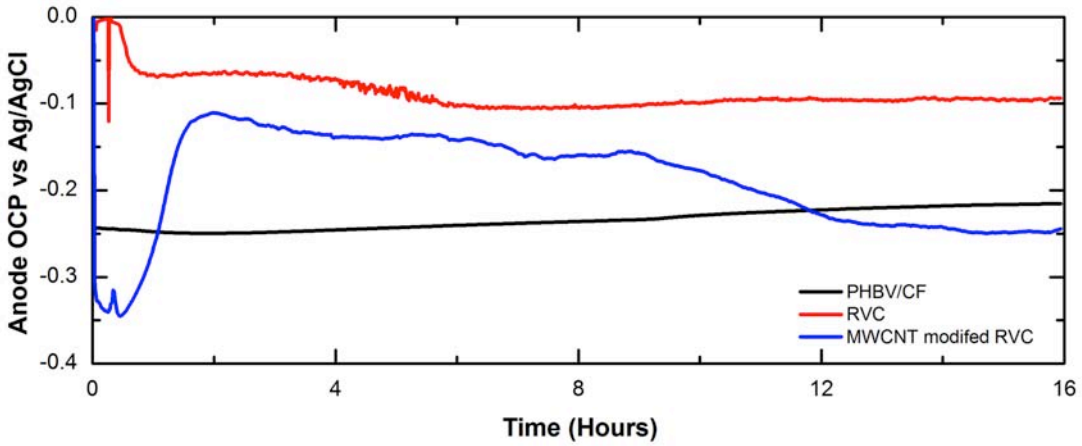

Figure 6.2: Open circuit potential measurement of *S. oneidensis* DSP-10 biofilms on various electrode materials

The inability of the RVC anode to produce a lower OCP is attributed to the lack of surface area and this is validated by the poor attachment and surface coverage of bacteria observed on this material by SEM (Figure 6.3a). From SEM images, biological nanowires are clearly visible on the surface, but the biomass concentration was not high enough to produce an effective anode respiring biofilm. The RVC-CNT, by comparison, exhibits a much larger surface area due to the deposition of carbon nanotubes; however, due to the geometry of the base material, consistent surface coverage of carbon nanotubes is difficult (Figure 6.3b). This inconsistency in the modified RVC-CNT material does not allow for complete surface coverage by the biofilm, and limits application for development of a biological fuel cell.

The PHBV/CF electrode material was able to sustain a stable OCP that was clearly related to a high biofilm density on the surface, as confirmed by SEM. PHBV/CF can be

fabricated with scalable meso/microporous porosity, defined by the desired application and determined by the size of the scaffold porogen.[103] PHBV/CF provides porosity suited to microbial attachment and a large internal surface area for biofilm development across the entirety of the material surface (Figure 6.3c). As PHBV/CF electrode showed stable performance after biofilm attachment, this electrode material was utilized as the anode for subsequent studies.

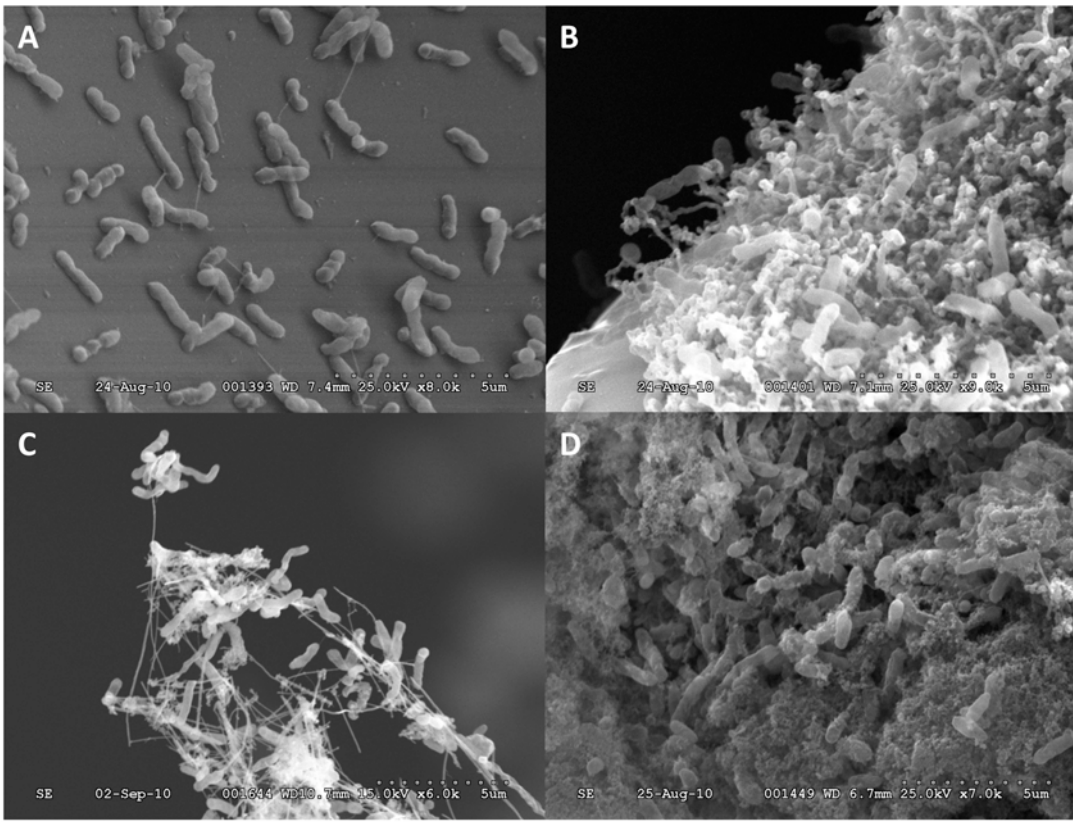

Figure 6.3: SEM images of *S. oneidensis* DSP-10 biofilms formed on (A) reticulated vitreous carbon (RVC), (B) multi-walled carbon nanotube modified RVC, (C) PHBV/CF, and (D) PHBV/CV with the biofilm being encapsulated on the surface with a silica thin film.

6.4.2 Biological Fuel Cell Operation

Biological fuel cells were fabricated by combining a laccase-modified air-breathing cathode with a *S. oniedensis* functionalized PHBV/CF anode. The effect of growth conditions on anode performance was investigated by varying the growth medium used during biofilm development on PHBV/CF electrodes. Anodes were thus prepared from i) *S. oneidensis* biofilm cultured in LB, directly on a PHBV/CF electrode (biofilm-LB), ii) the same in DM (biofilm-DM) and iii) *S. oneidensis* cultured in LB and immobilized in silica (Si-biofilm-LB), iv) and the same in DM (Si-biofilm-DM). Naturally-formed and silica-immobilized DM biofilms consistently reached steady state OCV of ~0.9 V., Alternatively when a culture was prepared in LB and then encapsulated on the electrode by silica the measured OCV was 0.7 V (Figure 6.4a). Polarization curves for biological fuel cells prepared with biofilm-LB and biofilm-DM demonstrated comparable electrochemical characteristics and maximum current densities approaching ~40 $\mu A \cdot cm^3$. Under potentiostatic conditions, the silica-immobilized biofilm anode (Si-biofilm-DM) appears to suffer from diffusion limitations and is presumably due to the silica thin film that binds the bacterial population to the electrode surface, potentially inhibiting diffusion of lactate to the microorganisms. In contrast, Si-biofilm-LB exhibits a mostly ohmic limitation; with little contribution coming from the anode as seen from the OCV.

Interestingly, anodes prepared with biofilms that were allowed to develop naturally exhibit significantly higher current densities. Biofilm formation during batch-cultivation, occurs primarily during stationary phase (data not shown), when population density reaches a critical mass. Literature reports suggest that environmental oxygen saturation

plays a role in *S. oneidensis* metabolism.[30,31] During bacterial cultivation in LB cultivation, cell density increases exponentially and rapidly removes all available oxygen, creating an oxygen-limited environment. A similar scenario was established in DM by creating a micro-aerobic environment for cultivation. In theory, limited oxygen environments could promote higher current densities, as it has been suggested that during anaerobic respiration outer membrane cytochromes (multi-heme cytochromes), play a role in insoluble electron acceptor reduction.

As a biofilm develops, an oxygen gradient is created within the matrix, and the microorganisms nearest to the electrode surface are essentially anaerobic, and Therefore capable of effectively reducing the electrode. To further illustrate this point, Si-biofilm-LB consists of aerobically cultured planktonic cells bound to the surface of the electrode by silica and shows poorer electrochemical characteristics compared to other configurations. We speculate that since these organisms were cultured aerobically, the metabolic pathways for anaerobic metabolism are not active and the ability to utilize an insoluble electron acceptor is compromised. In contrast, when the PHBV/CF electrode is present during cultivation, a biofilm forms directly on the surface, creates an oxygen gradient within the matrix and this population does have the metabolic capacity for electrode respiration. The physiological characteristics of the differing metabolic states are evidenced by the bioelectrocatalytic activity. Furthermore, *S. oneidensis* cultured micro-aerobically establishes metabolic mechanisms for respiration, such that when the planktonic culture is immobilized to the electrode surface by silica, anode respiration is

observed. This is clearly visible in the current and power densities of the resulting biological fuel cell (Figure 6.4).

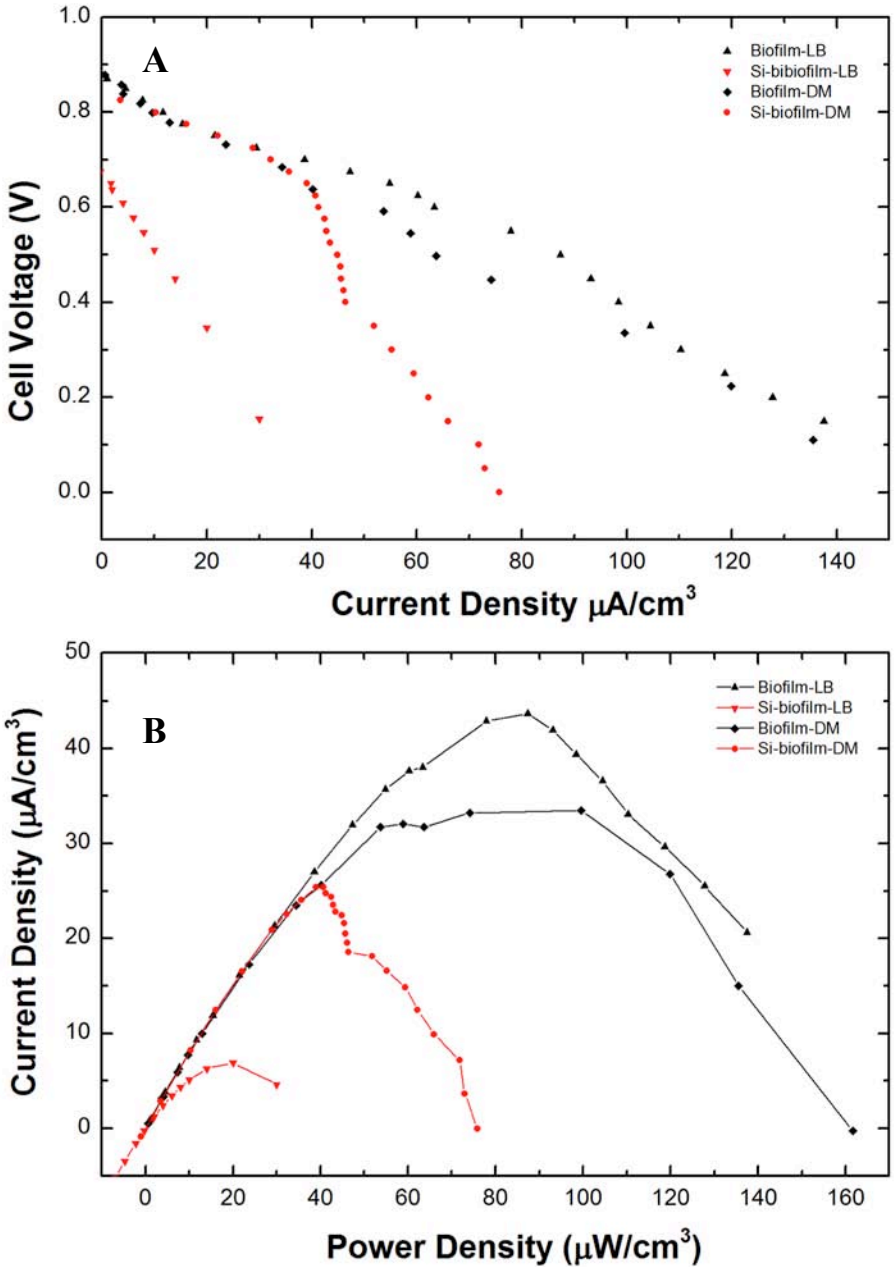

Figure 6.4: (A) polarization and (B) power curves of the hybrid biological fuel cell incorporating laccase cathodes and various *S. oneidensis* DSP-10 biofilms on PHBV/CF electrodes

After polarization and power curves were obtained for each hybrid biological fuel cell, an external load of 20 kΩ was applied to evaluate the stability of each anode configuration (Figure 5). The resistance was determined empirically by extrapolation from the polarization curves, based on a value corresponding to one-third of the maximum current density for biofilm-LB. The biofilm-LB anode/laccase cathode fuel cell sustained an OCV of ~0.3 V for >18 hours (equivalent to 30 $\mu W \cdot cm^3$) under load. In contrast, the Si-biofilm-LB anode/laccase cathode fuel cell sustained 0.15 V (15 $\mu W \cdot cm^3$). Both the minimal media cultured silica-encapsulated and non-encapsulated anodes sustained a cell voltage of approximately 0.20 V (20 $\mu W/cm^3$). This confirms the findings from the power curves in Figure 6.4. After the load was removed from the fuel cells, the cell voltage for all 4 types of anodes versus the laccase cathodes returned to approximately 0.80 to 0.85 V.

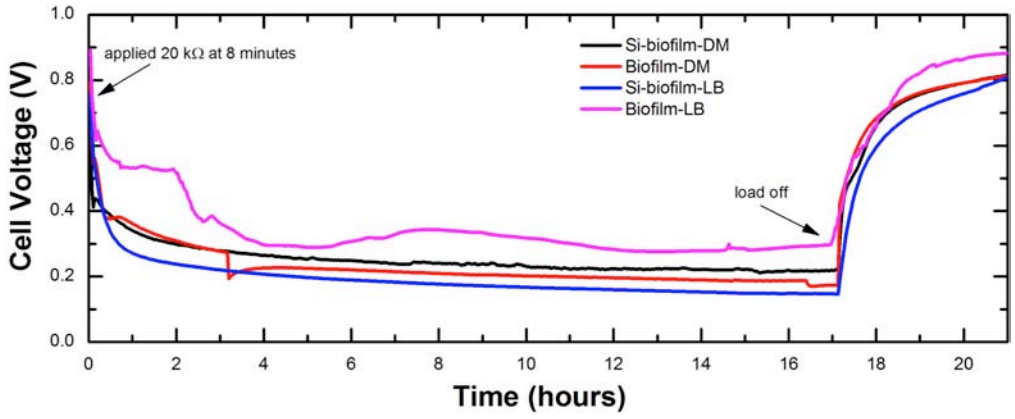

Figure 6.4: Stability study of the hybrid biological fuel cell with externally applied load, measuring the cell voltage

6.5 Conclusions

This research provides a methodology to build a hybrid biological fuel cell by combining enzymatic and microbial electrocatalytic activity. More specifically, the method for allowing biofilm formation in creating *S. oneidensis*-based anodes in such systems is demonstrated. Environmental stimuli and physiological growth conditions influence biofilm formation, as the culture begins to populate the surface of the electrode at the onset of stationary phase. Therefore, we can conclude that if the biofilm is formed naturally, there is little difference in power performance between *S. oneidensis* cultured in a defined media (aerobically) versus a complex media (allowing for micro-aerobic cultivation). Variation in the current and power densities may be present from the concentration of microorganisms on the surface, as the cultures will have different population densities at stationary phase (LB vs defined media or aerobic vs micro-aerobic). *S. oneidensis* cultivated under specific conditions may be forced into a biofilm by the encapsulation of silica onto the electrode. Providing a viable option for the construction of a biological anode.

Chapter 7 – A Study of the Flavin Response by *S. oneidensis* Cultures in Carbon Limited Environments

Co-Authors: Heather R. Luckarift, Carolin Lau, Akinbayowa Falase, Kristen E. Garcia, Linnea K. Ista, Privthiraj Chellamuthu, Ramaraja P. Ramasamy, Venkataramana Gadhamshetty, Greg Wanger, Yuri A. Gorby, Kenneth H. Nealson, Orianna Bretschger, Glenn R. Johnson & Plamen Atanassov

7.1 Abstract

Mediated electron transfer has been implicated as a primary mechanism of extra-cellular electron transfer to insoluble electron acceptors in anaerobic cultures of the facultative anaerobe *S. oneidensis*. In this work, planktonic and biofilm cultures of *S. oneidensis* exposed to carbon-limited environments trigger an electrochemical response thought to be the signature of an electrochemically active metabolite. This metabolite was detected via cyclic voltammetry for *S. oneidensis* MR-1 biofilms. The observed electrochemical potentials correspond to redox potentials of flavin-containing molecules. Chromatographic techniques were then used to quantify concentrations of riboflavin by the carbon-limited environmental response of planktonic *S. oneidensis*. Further evidence of flavin redox chemistry was associated with biofilm formation on multi-walled carbon nanotube-modified Toray paper under carbon-starved environments. By encapsulating one such electrode in silica, the encapsulated biofilm exhibits riboflavin redox activity earlier than a non-encapsulated system after media replacement. This work explores the electrochemical nature of riboflavin interaction with an electrode after secretion from *S. oneidensis* and in comparison to abiotic systems

7.2 Introduction

S. oneidensis MR-1 is a dissimilatory metal reducing bacteria (DMRB) that is widely utilized as a model organism in microbial fuel cell (MFC) research.[17,109-111] *S. oneidensis* appears to use a combination of mechanisms for extracellular electron transfer (EET) to insoluble electron acceptors.[112] These mechanisms include: (i) direct electron transfer (DET) through outer membrane cytochromes;[30,31,39,113] (ii) direct electron conduction via extracellular appendages described as bacterial nanowires,[29,38,108] and (iii) mediated electron transfer (MET) (or shuttling) through exogenous metabolites.[26,114] Each of these mechanisms has been associated with electrochemical activity and, as such, exploited to produce power in MFCs.

MFC power production is a fortuitous result of microbial metabolism in which the fuel cell performance is dictated by microbial EET processes, acting either individually or in concert. The ability to effectively transfer electrons is intrinsically linked to microbial metabolism and DMRB exhibit versatile EET mechanisms that allow the bacterium to respond to changes in physiological conditions. It is unclear, however, how EET mechanisms are controlled by physiological constraints or how environmental conditions may dictate each mode of EET.

Elucidating and understanding these relationships may lead to improved MFC systems by: 1) guiding the rational development of engineered surfaces to improve the physical association between microbes and products of metabolism; 2) determining microbial

culture conditions that provide reproducible redox processes; and thereby 3) define optimal operational conditions for MFCs.

In this work we explore the phenomena of riboflavin production by *S. oneidensis* MR-1 in electron donor-limited conditions,[115] and investigate the influence of riboflavin redox chemistry within biofilms formed on the electrode. One inherent problem in the study of *S. oneidensis spp.* is the apparent rapid detachment of biomass from the biofilm under certain environmental stimuli.[54] A method to artificially bind a culture to an electrode to mimic biofilm formation is investigated by immobilizing a defined population of *S. oneidensis* MR-1 cells to an electrode by means of silica coating. This technique overcomes potential limitations of investigating riboflavin redox reactions within a *S.* oneidensis biofilm by preventing a loss of biomass during medium exchange. In either case, natural biofilm formation or silica immobilized biofilm formation, the subsequent adsorption of riboflavin onto electrode materials and the biofilm surface is predicted to dominate the electrochemical character of an *S. oneidensis* MR-1 populated bio-anode under operating conditions defined within this study.[116]

The work described here further elucidates the role of riboflavin within *S. oneidensis* EET. In terms of MET, for example, studies originally reported by Marsili *et al*. and corroborated by others show that *S. oneidensis spp.* will use flavin compounds as a dominant redox mechanism in EET anaerobic respiration.[26,32,43,117] Recently however, there is evidence to suggest the role of electron shuttles that mediate taxis of organisms towards insoluble electron acceptors; perhaps leading to biofilm formation on these

surfaces once an environmental stimulus is present; for example, carbon or oxygen limitation, as described herein.[118] A mechanism to hydrolyse cytoplasmic synthesized flavin mononucleotide (FMN) to flavin adenine dinucleotide (FAD) and riboflavin has also recently been described via the periplasmic protein UshA.[32] This supports the idea of metabolic release of riboflavin into the environment where these environmentally bound flavins may serve in cell-to-cell signalling, sensing of redox gradients, or other non-respiratory functions.[117] Furthermore, an idea of mediated energy taxis has been proposed in which *S. oneidensis* not only uses riboflavin as a mediator but as a signal to direct cell populations to insoluble electron acceptors.[118] This idea becomes significant in the context of *G. sulfurreducens* biofilms, which have been shown to produce higher current densities compared to biofilms of *S. oneidensis*.[4] As of yet, no such electrochemical endogenous metabolite has been identified for *G. sulfurreducens* biofilm formation.

7.3 Methods & Materials

7.3.1 Bacterial Strain and Culture Conditions

S. oneidensis MR-1 was inoculated from frozen culture stocks onto tryptic soy (Sigma-Aldrich 22092) agar plates and incubated at 30°C. Colonies were then re-cultured in Luria-Bertani (LB) (Sigma-Aldrich L3022) broth and incubated aerobically for approximately 18 hours and then washed in 50 mM sodium phosphate buffer (pH 7). All glassware and mediums were autoclaved for 20 minutes at 15 psi and 121°C prior to use. Experimental cultures of *S. oneidensis* MR-1 were grown in chemically defined medium (M1), from an original specification.[40] This composition included 30 mM sodium fumarate for oxygen-limited cultures. Note: the vitamin solution used in the chemically

defined medium contains no riboflavin. Washed (8000 rpm for 5 minutes, 3 repeats) LB cultures of *S. oneidensis* MR-1 were sub-cultured into flasks containing chemically defined medium and were capped with a rubber stopper and incubated for approximately 48-60 hours (30°C, 150 rpm) until the optical density at 600 nm was ~0.3. These planktonic cultures were then washed in 50 mM sodium phosphate buffer and re-suspended in the buffer to an optical density of 0.3 at 600 nm. Electrodes were incubated in this solution (exposed to filtered ambient air) for 24 hours at 30°C for biofilm formation. Note: the culture at this point is under carbon limitation.

Cell counts were determined by conventional serial dilution, plating and colony counting to determine colony-forming units per mL (CFU mL^{-1}).

7.3.2 Electrode Preparation and Population

Toray® carbon paper TGP-H-060 (TP; Fuel Cell Earth, Stoneham, MA) was augmented with multi-walled carbon nanotubes (TP-CNT) using a modified technique described previously.[104] Briefly, TP was plasma-treated for 12s, and then placed in a standard 3-electrode configuration electrochemical cell with TP as the working electrode, a nickel mesh counter electrode and Ag/AgCl (saturated KCl) reference electrode (CH Instruments Inc.). The electrolyte contained an equimolar (14 mM) mixture of cobalt acetate, nickel acetate and boric acid in DI water and metal nanoparticles were deposited on the TP by subjecting the cell to -1.3 V for 12 s. The paper was removed and sonicated in DI water, dried and placed in a tube furnace (Lindberg/Blue model TF55035A). TP

samples were reduced in 5% hydrogen/95% nitrogen atmosphere and the temperature ramped from room temperature to 620°C, at which point the H_2 feed was replaced with 33% ethylene in nitrogen for the remainder of the temperature ramp to 750°C, and held for 1 hour to allow CNT growth.

TP-CNT electrodes were again plasma treated for 10s to sterilize the surface and to increase surface wettability. TP-CNT electrodes were incubated in 10 mL of an *S. oneidensis* MR-1 cell suspension in sodium phosphate buffer overnight at 30°C with no agitation. The culture is starved of a carbon source at this time. Following biofilm development, the electrodes were removed and used in electrochemical characterization experiments and visualized by scanning electron microscopy (SEM). Biofilm coated TP-CNT electrodes were further encapsulated in silica by chemical vapor deposition (CVD) of tetramethylorthosilicate (TMOS) as described previously.[102]

7.3.3 Bioreactor Cultures

M1 growth medium (pH 7.0) was used in all bioreactor studies. *S. oneidensis* MR-1 plates were previously prepared and colonies were washed from the plate using M1 growth medium and used as the bioreactor inoculum.

The bioreactor was a Bioflow 110 (New England Biosciences) operated in semi-batch mode at 30°C, with stirring (600 rpm) and maintained at pH 7.0 (by addition of 1N HCl).

The gas flow into the bioreactor was controlled at 5% dissolved oxygen by mixing ultra high pure N_2 and compressed air. Cell density was monitored by measuring optical density of the culture at 600 nm. To identify physiological conditions that affect riboflavin production, the bioreactor was also operated in semi-batch mode under anaerobic conditions; at which time 40 mM of sodium fumarate was added to the medium as the terminal electron acceptor.

7.3.4 Riboflavin Quantification

Culture samples were periodically (and aseptically) removed from the bioreactor and clarified by filtration (0.2 μm). The concentration of riboflavin was measured using a 96 well fluorescent plate reader (FlexStation 3; Molecular Devices) with an excitation wavelength of 440 nm and observed fluorescence measured at 520 nm. Riboflavin concentrations are reported as the mean of 10 replicate samples and correlated to a standard curve (in the range 25 nM to 1mM).

7.3.5 HPLC Analysis

Organic acid content of culture samples was determined using high pressure liquid chromatography (HPLC). Filter clarified supernatant was acidified to a final concentration of 12.5 mM H_2SO_4 and analyzed using an Agilent HPLC (Agilent 1200, Agilent) with a reverse phase C18 column (Synergi-Hydro, Phenomenex). Chromatographs were generated using a multiwavelength detector (Agilent 1200, Agilent) set to 210 nm. A 20 μL sample of each electrolyte was injected into the sample loop and eluted using an isocratic sulfuric acid mobile phase (2.5 mM, pH 2.0) at a flow rate of 0.5 mL/min and at a column temperature of 25°C. Peak areas were integrated and

concentrations calculated by comparison to peak areas and retention times of known standards for lactate, pyruvate, and acetate.

7.3.6 Electrochemical Testing

All electrochemical measurements were conducted in a standard 3-electrode electrochemical cell containing a platinum wire as the counter electrode and Ag/AgCl (3M KCl) reference electrode in 10 mL of sodium phosphate buffer (50 mM, pH 7.0), with 20 mM sodium lactate as the carbon source. TP-CNT electrodes populated with *S. oneidensis* MR-1 biofilms were secured to glassy carbon (GC) rods (CH Instruments Inc., 3 mm diameter) as the working electrode. All electrochemical measurements were obtained using a Gamry 600 Potentiostat/Galvanostat/ZRA. The presence of riboflavin was determined by cyclic voltammetry (CV) (from -0.60 V to -0.30 V) at a 10 mV/s scan rate. The diffusive behaviour of riboflavin was characterized by varying the scan rate from 0.20 V/s to 0.001 V/s. For the purposes of this study, peaks at approximately -0.45 V are of interest, as defined by the theoretical potential for riboflavin at pH 7.0.[26] Measurements were taken in an electrochemical cell purged with N_2; but exposed to ambient air. This system design creates a micro-aerobic environment since full removal of dissolved O_2 is not required.

7.3.7 Silica Encapsulation

Washed cell suspensions were physically adsorbed to TP-CNT electrodes and exposed to 100 μL of TMOS in the vapor phase for 10 minutes. The TMOS precursor undergoes hydrolysis in aqueous solvent upon contact with high salt concentrations in the liquid medium and leads to sol-gel and silica particulate formation at the substrate surface.[102]

7.3.8 Scanning Electron Microscopy

For SEM analysis, cells were chemically fixed on the electrode in a 2.5% glutaraldehyde solution for approximately 12 hours and then exposed to increasing concentrations of ethanol, culminating in three final washes at 100% ethanol. The samples were then subjected to critical point drying,[38] using an automated critical point dryer, (Seevac Inc., Florida, USA) before coating with a 5 nm layer of gold-palladium using an Emitech K950X sputter coater (Emitech, USA). Fixed samples were viewed using an FEI Quanta 3D FEG microscope (FEI Company, Hillsboro, Oregon) at accelerating voltages ranging from 5–10 kV and the elemental composition was characterized by energy-dispersive X-ray spectroscopy (EDS) analysis.

7.3.9 Electrochemical Characteristics of Riboflavin

The number of electrons, involved in the redox processes observed for riboflavin, was calculated using the following expression:

$$z = \frac{56.5}{E_p - E_{p/2}} \qquad \textbf{(Equation 7.1)}$$

Where the peak potential (E_p) and half peak potential ($E_{p/2}$) are expressed in millivolts. Using the calculated value of z, the number of moles of oxidized or reduced electrochemical species was calculated using Faraday's Law:

$$n = \frac{Q}{zF} \qquad \textbf{(Equation 7.2)}$$

Where charge (Q) is obtained from analyzing the redox peaks from CV. Since the standard contains a known bulk concentration of riboflavin (C_b), the apparent diffusion

coefficient (D_{app}), of riboflavin was estimated using the expression:

$$Dapp = \left[\frac{i_p}{269000 z^{1.5} A C_b \nu^{0.5}} \right]^2 \qquad \textbf{(Equation 7.3)}$$

Where A is the porous area of the electrode, ν is the sweep rate in mV/s, and i_p is the peak current density. Finally the redox potential (E_{redox}) was obtained by midpoint evaluation.

The peak potential (E_p), peak current (I_p), half peak potential ($E_{p/2}$), and charge (Q) were obtained by analysis of the redox peaks, while the number of electrons (z), moles of riboflavin reacted (n), apparent diffusivity (D_{app}) and redox potential (E_{redox}) were obtained by calculation.[57]

7.4 Results & Discussion

7.4.1 Riboflavin Production in Cell Cultures

During time course experiments riboflavin production was observed to accumulate as a function of physiological state and population density (Figure 7.1). In addition, results indicate that riboflavin production increases with respect to a defined cell density; particularly under micro-aerobic growth conditions (i.e. 5% dissolved oxygen).

The maximum concentration of riboflavin produced was 391 nM, which corresponded with the stationary phase of cell growth (cell density of 1.6 x 10^8 CFU mL^{-1}). HPLC analysis of culture supernatants confirmed that volatile fatty acids were completely oxidized at this point and indicated that maximum levels of riboflavin production occurred immediately after all electron donors were consumed. This correlation may

imply that riboflavin production in *S. oneidensis* is a response to intracellular carbon fluxes as has been proposed for other bacterial species.[115] The onset of riboflavin production corresponds with depleted lactate at a point when acetate and pyruvate oxidation by-products begin to accumulate within the culture. A second kinetic increase in riboflavin production then occurs after pyruvate was consumed and acetate concentrations began to decrease (Figure 7.1). Riboflavin production reaches a stable maxima (equivalent to 2.55 nM/cell) once residual acetate has been consumed.

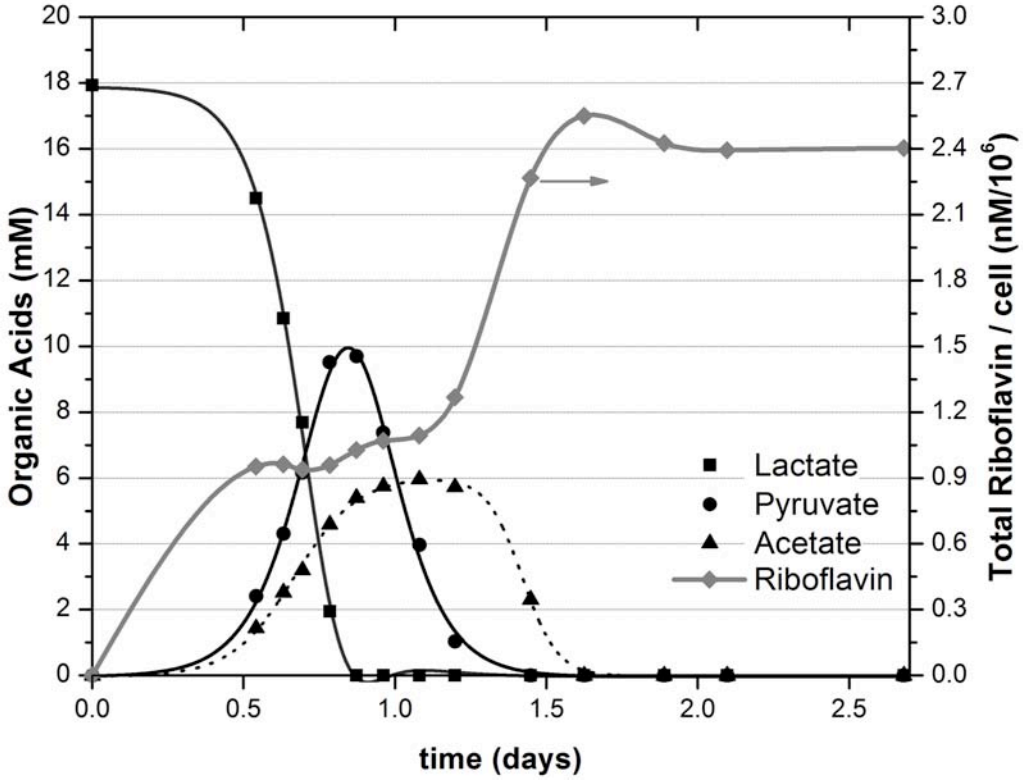

Figure 7.1: Conversion of lactate to oxidation products (acetate and pyruvate) and production of riboflavin during cell growth of *S. oneidensis* MR-1.

In contrast, when sufficient concentrations of an alternative electron acceptor are present in anaerobic cultures (e.g. sodium fumarate), no riboflavin is synthesized by *S. oneidensis*

(data not shown). Under steady state anaerobic conditions, (cell density decreased to ~0.6 x 10^8 CFU mL^{-1} and riboflavin was no longer detected in the medium (considering a fluorescence detection limit of 25 nM). The correlation between riboflavin production and the presence of oxygen as an electron acceptor is in agreement with previous studies showing that aerobic conditions promote higher riboflavin and FMN production in *S. oneidensis* MR-1.[119] However, the results are incongruent with the idea that flavin molecules play a role in mediated electron transfer to insoluble electron acceptors in anaerobic conditions, e.g. in the MFC anode.

7.4.2 Abiotic Riboflavin/Electrode Interaction

To understand the proposed biocatalytic interactions of microbial excreted riboflavin and the electrode, we must first consider any abiotic association between riboflavin and the electrode in an electrochemical system. The electrochemical characteristics of riboflavin were determined by CV studies and used to demonstrate the relationship between riboflavin concentration and redox activity in sterile electrolyte. The riboflavin concentrations selected for study were based on molar amounts typically reported in MFC studies.[120] The symmetrical response of CV anodic and cathodic sweeps irrespective of riboflavin concentration indicates fully reversible redox behaviour (Figure 7.2A). The redox potential (E_{redox}) for riboflavin was -0.45 V vs Ag/AgCl for all concentrations investigated, in agreement with the standard thermodynamic potential of the flavin molecule.[121] The amperometric response was proportional to riboflavin concentration and this behaviour is apparent once the non-Faradaic background capacitance of the graphite felt electrode is subtracted from the data set (Figure 7.2A).

The relationship between the reduced and oxidized species at the onset of electrode

polarization ($n_{oxidized}/n_{reduced}$) was consistent (~1.26) and indicated that riboflavin in an abiotic system yields a reversible electrochemical response that can serve as a baseline for comparison to measurements in a microbial biofilm.

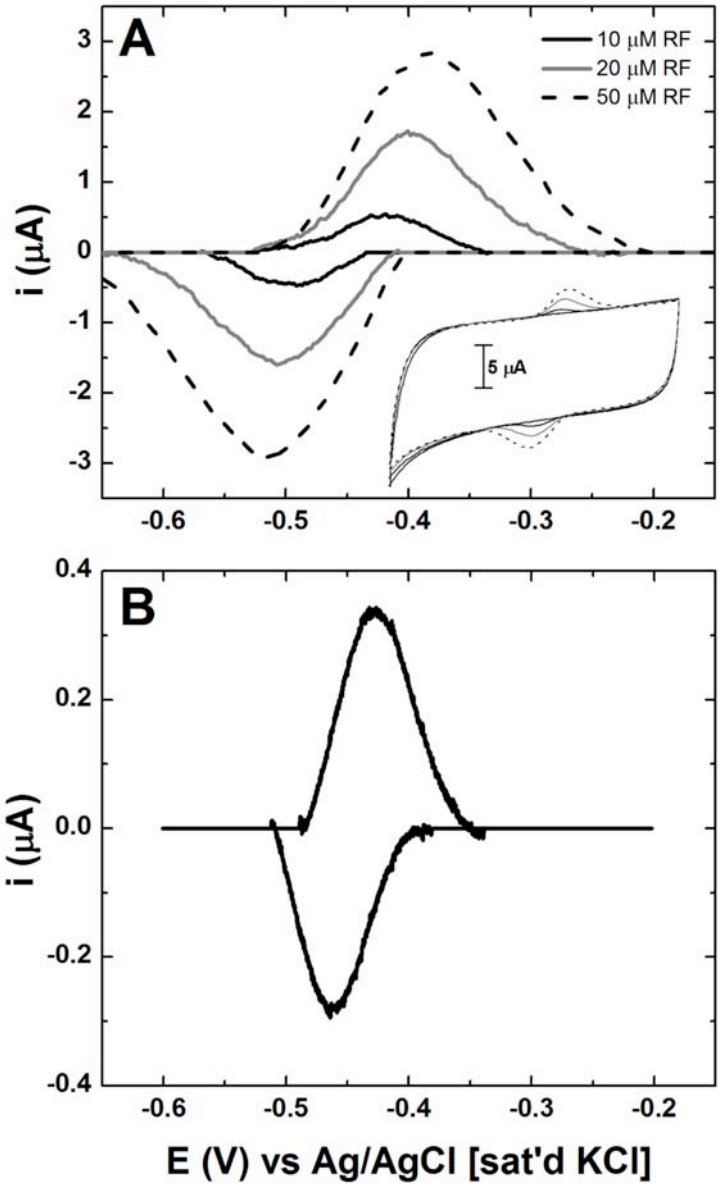

Figure 7.2: Riboflavin voltammetry associated with (A) abiotic systems containing known concentration in the bulk and (B) associated with *S. oneidensis* MR-1 biofilms on TP-CNT. Data in panels A and B is shown with background subtraction to remove the effects of capacitive current on the electrode. Inset to panel A shows CV of riboflavin without background subtraction.

These results confirm that CV can be used as a quantitative tool to analyse the electrochemical response of riboflavin. Parametric analysis was then performed on biofilms by extracting electrochemical parameters from CV and comparing the data to that of the flavin standards (Table 7.1). For consistency only the region between -0.60 V and -0.30 V was considered for peak analysis; the region above -0.30 V was discarded from analysis because of the mixed contribution from metabolite oxidation and other non-mediator related processes in this region.

Table 7.1: Electrochemical parameters of riboflavin derived from abiotic standards and from *S. oneidensis* MR-1 biofilms on carbon electrodes.

Extracted Parameters	10 µM Riboflavin		20 µM Riboflavin		50 µM Riboflavin		MR-1 on TP-CNT	
	Oxidation	Reduction	Oxidation	Reduction	Oxidation	Reduction	Oxidation	Reduction
E_p (V)	-0.418	-0.491	-.400	0.507	-0.382	-0.516	-0.433	0.465
I_p (µA)	0.59	0.62	1.70	1.76	2.89	3.09	0.48	0.344
E_p-$E_{p/2}$ (mV)	41	46	47	55	65	75	24	32
z	1.38	1.23	1.20	1.03	0.87	0.75	2.35	1.76
Q (µC)	5.7	6.4	20.3	22.3	42.3	47.2	2.84	2.12
n (mol)	0.4×10^{-10}	0.5×10^{-10}	1.8×10^{-10}	2.2×10^{-10}	5.0×10^{-10}	6.5×10^{-10}	1.3×10^{-11}	1.2×10^{-11}
D_{app} (cm^2/s)	0.6×10^{-8}	0.9×10^{-8}	1.9×10^{-8}	3.2×10^{-8}	2.3×10^{-8}	4.0×10^{-8}	ND	ND
$I_{p,c}/I_{p,a}$	1.05		1.04		1.07		0.72	
$\eta_{oxidized}/\eta_{reduced}$	1.25		1.22		1.30		0.92	

[a]Footnote: Two values of D_{app} were determined from each CV, one for the diffusion of reduced flavin from the electrolyte to the electrode surface (oxidation) and a second for the diffusion of oxidized metabolite away from the electrode surface into the electrolyte (reduction).

Although the riboflavin redox reaction theoretically involves two electrons, the actual redox response from measurement of standard solutions yielded values ranging from 0.73–1.38 and indicate a low Faradaic conversion of the compound. The empirical calculation of the number of electrons involved in the redox reaction of riboflavin appears to decrease with increasing riboflavin concentration. The apparent diffusivity (D_{app}) was estimated to be between 0.6–4 x 10^{-8} cm^2/s, which compares favourably with values reported in the literature.[122] Since D_{app} was empirically obtained based on peak

current (i_p), factors such as surface-bound riboflavin, ionic properties of the electrolyte, activation of the graphite felt, transfer coefficients and exchange current density may all indirectly influence D_{app} but are not directly addressed by equation 7.3. The analysis does confirm, however, that riboflavin is an electrochemically active species when interacting with carbonaceous materials and that in the presence of a biofilm is seen to accumulate at concentrations within the detectable range.[123,124]

7.4.3 Microbial Riboflavin Production and Electrode Interaction

Riboflavin production in *S. oneidensis* MR-1 biofilms (on TP-CNT) was confirmed by CV (typical example shown in Figure 7.2B) where distinct oxidation and reduction peaks were observed at -0.45 V vs Ag/AgCl in agreement with riboflavin standards (Table 7.1). As no exogenous riboflavin is added to the system, the redox-active flavin is clearly synthesized by the biofilm. Peak current was observed to correlate with riboflavin concentration, and when plotted and integrated using linear regression (oxidation current slope = 0.053 ± 0.014, r^2 = 0.933; reduction current slope = 0.057 ± 0.013, r^2 = 0.945) can be used to extrapolate an apparent concentration of riboflavin in the biofilm of ~85 µM (79.6–90.9). The measurement can only be deemed 'apparent' as no consideration is taken for surface-confined affects within the biofilm compared to bulk diffusion of riboflavin in standard solution measurements.

When considering the relationship between reduced and oxidized species ($n_{oxidized}/n_{reduced}$), values >1 indicate a higher concentration of the oxidized species, with the opposite being true of vales less than 1. For the abiotic systems, $n_{oxidized}/n_{reduced}$ was greater than 1 and constant at ~1.26 for all evaluated concentrations of riboflavin in the

bulk media. In comparison, $n_{oxidized}/n_{reduced}$ for a biofilm-modified electrode was less than 1, indicating a higher concentration of the reduced species. This observation is consistent with the hypothesis that biologically secreted riboflavin leaves the cell in a reduced form either by interaction with terminal electron acceptor proteins or by some other unknown mechanism.[125] Consequently the reduced riboflavin interacts with the electrode through indirect electron transfer.[117,126]

7.4.4 Silica Encapsulated vs. Natural Biofilms

In previous work within our group, microbial fuel cell anodes were prepared by capturing biofilms in a silica matrix that provides enhanced operational longevity by preventing a loss of biomass. For this study, silica-encapsulated biofilms were again used and results indicated earlier electrochemical activity associated with riboflavin in comparison to non-encapsulated biofilms after media replacement. These silica encapsulated biofilms displayed increased current density that was initially attributed to a high cell density. Subsequent studies, however, and further analysis indicated that the enhanced current density of the silica-encapsulated system may be attributed to accumulation of secreted riboflavin at the electrode surface and subsequent increased surface area due to the silica matrix allowing for increased riboflavin adsorption. Therefore to examine the diffusive and adsorptive behavior of riboflavin, cyclic voltammetry was evaluated for biofilms on TP-CNT electrodes that were populated naturally and compared to biofilms artificially bound to the electrode via silica encapsulation.

Physical and chemical characterization of the anodes identified distinctions between the two populations. When incubated with TP-CNT, *S. oneidensis* MR-1 forms a biofilm on

the material surface (Figure 7.3A). The distribution of individual cells indicates that cells integrate with the CNT structures directly. Following silica encapsulation of the biofilm, EDS confirmed the introduction of silica and oxygen compared to a non-silica control (data not shown). Furthermore, SEM images of the silica-encapsulated biofilm revealed the preserved microbial cells and extracellular structures (Figure 7.3B).

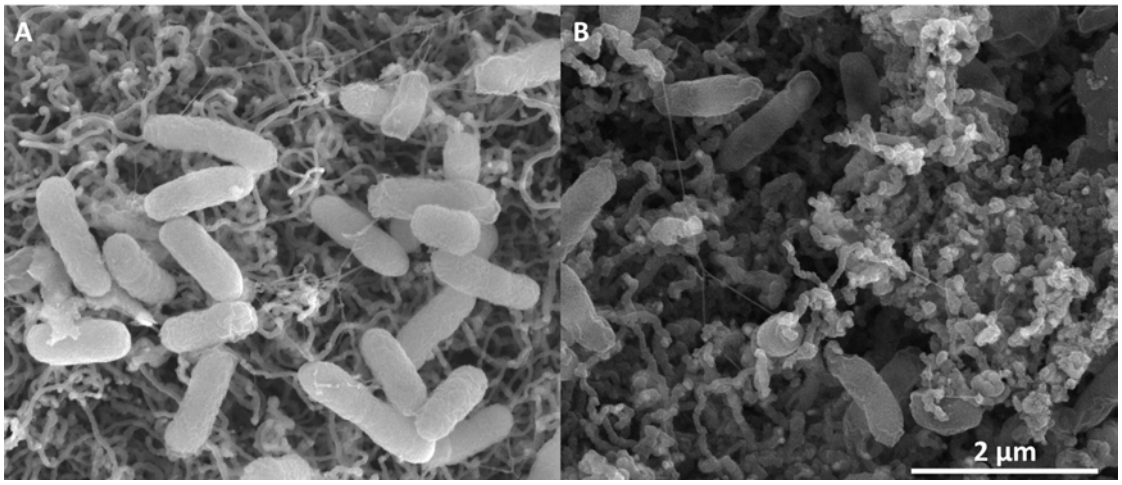

Figure 7.3: SEM image of carbon source limited *S. oneidensis* MR-1 natural biofilms on TP-CNT (A) and silica encapsulated cells (B).

Both natural and silica-encapsulated biofilms demonstrate reversible peaks at a midpoint potential of -0.45 V irrespective of scan rate (Figure 7.4). Peak currents plotted against scan rate yield a linear dependence (Figure 7.4B), from which we conclude that a significant concentration of riboflavin must be adsorbed to the electrode surface in agreement with the Laviron model.[127]

Additionally, the peak currents of each oxidative and reductive peak were plotted against the square root of the scan rate, yielding linear relationships in both electrode systems and indicating diffusion-based limitation (Figure 7.4C). While the two observations

appear to be contradictory, it is possible that the redox process could be controlled by the diffusion of counter ions to maintain electro-neutrality on the electrode surface.[124]

Observations from previous studies outside of this group provide information suggesting that the removal of surrounding medium reduces electrocatalytic activity of the anode by removal of the mediator, riboflavin. Electrodes housing naturally formed biofilms and silica-encapsulated biofilms underwent medium replacement with carbon substrate free electrolyte. CVs of the natural biofilm did not yield any redox peaks at the onset; after 24 hours of residence time in the electrochemical cell containing no carbon source, however, oxidation and reduction peaks appear near a midpoint potential of –0.45 V indicating the accumulation of riboflavin at the electrode surface (Figure 7.5A). Additionally, the capacitive current of the system increased despite the lack of essential compounds required for cell proliferation. This increase in electrode capacitance was attributed to the microbial secretion of riboflavin and the associated redox behaviour of that metabolite with the electrode under carbon-limiting conditions. In comparison, *S. oneidensis* MR-1 populated electrodes that had been encapsulated in silica exhibited a fully reversible redox peak at approximately -0.45 V vs. Ag/AgCl (Figure 7.5B) from the onset. After 24 hours residence time, the capacitive current of the system increased as observed for the natural biofilm. In essence, the natural biofilm must reach a cell density sufficient to act as a binding matrix for the riboflavin, with the density of the natural biofilm being compromised during media replacement. When the biofilm is artificially prepared by silica immobilization, the cell density is high from the onset and any riboflavin production is readily captured by the dense cell and silica matrix. Once the biofilm

population stabilizes, electrocatalytic performance is comparable for both systems.

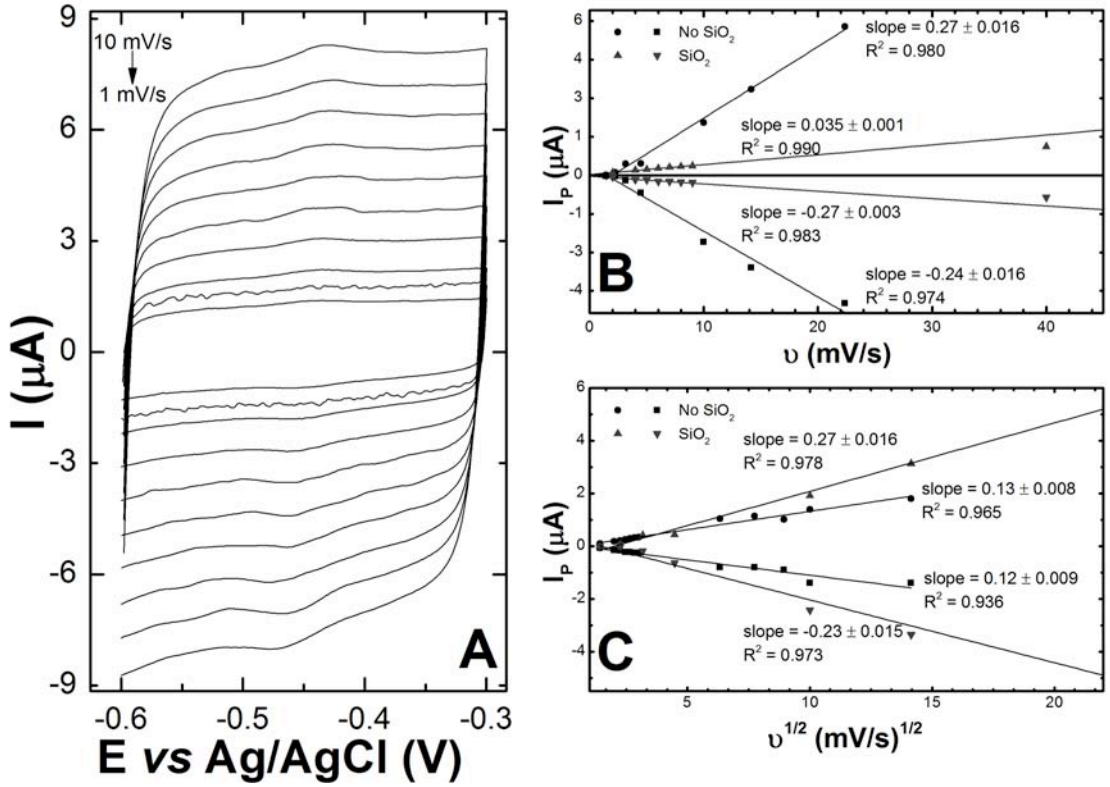

Figure 7.4: (A) Cyclic voltammetry of riboflavin associated with *S. oneidensis* MR-1 with varying scan rates. Peak currents for both natural biofilm and silica encapsulated biofilms plotted against (B) the scan rate and (C) the square root of the scan rate.

7.4.5 Electrode Reduction Performance Influenced by Riboflavin

Silica-encapsulated and natural biofilm populated electrodes were analysed by galvanostatic polarization to evaluate the performance in terms of current density of the electrode systems over time (Figure 7.6). At the onset of medium replacement (M1 medium), the natural biofilm anode exhibits an open circuit potential (OCP) of approximately – 0.15 V vs Ag/AgCl that increases dramatically over the following 24 hours to a final OCP approaching –0.35 V, consistent with the establishment of a stable,

electrochemically active biofilm. Prolonged incubation results in a slight decrease of the

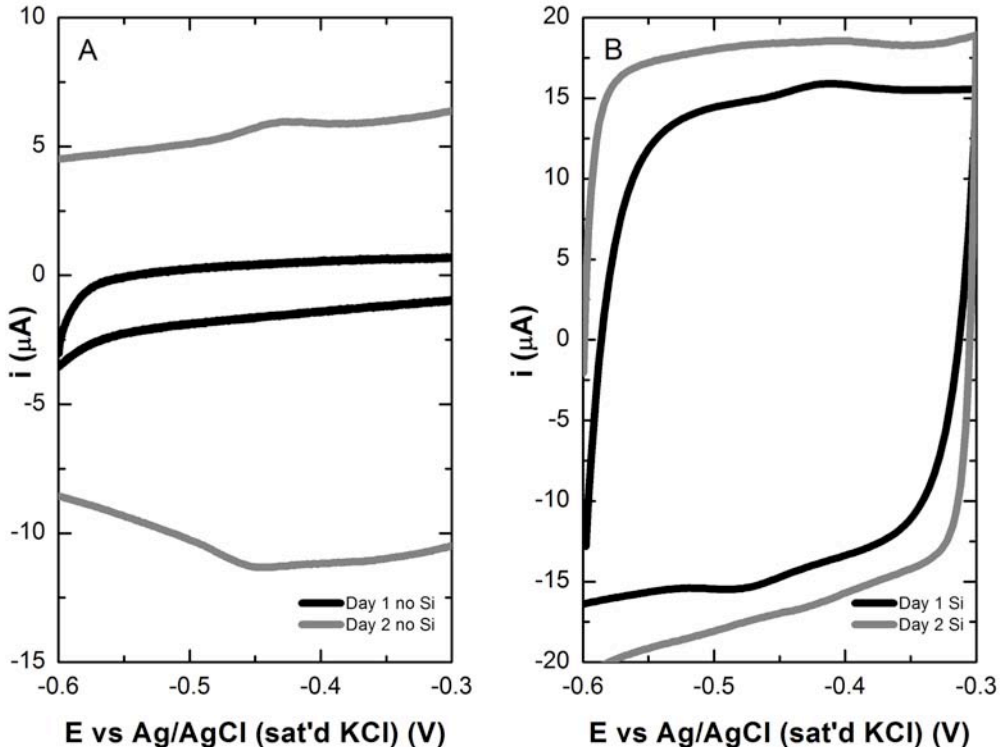

Figure 7.5: Cyclic voltammetry of *S. oneidensis* MR-1 biofilm (A) and silica encapsulated biofilm (B) on TP-CNT after 1 (black) and 2 (gray) days in a carbon-limited environment.

OCP (–0.32 V) that may be attributed to diffusion and mass transfer limitations across such a dense cellular matrix. The silica-encapsulated biofilm electrode exhibits an OCP of approximately – 0.37 V immediately after medium replacement. The galvanostatic polarization curves vary little over the following 2 days, but again on day 4, a slight decrease in anodic performance is observed. These results indicate that the silica film was able to retain concentrations of biomass and potentially riboflavin that affect the performance of the electrode. In summary, when comparing the two systems, the natural biofilm requires ~24 hours after media replacement to re-establish critical biomass on the electrode for measurable performance difference. At that point, riboflavin is present but

the relationship between EET processes is vague. The silica-encapsulated electrode, however, shows superior electrocatalytic activity at the onset due to the preservation of the biomass on the surface. In fact, silica-encapsulation produced current output at the onset that surpassed that of the natural biofilm. Furthermore, the initial OCP for the silica-encapsulated electrode indicates that riboflavin may be retained on or near the electrode surface, as the OCP measurements approached the midpoint potential of riboflavin.

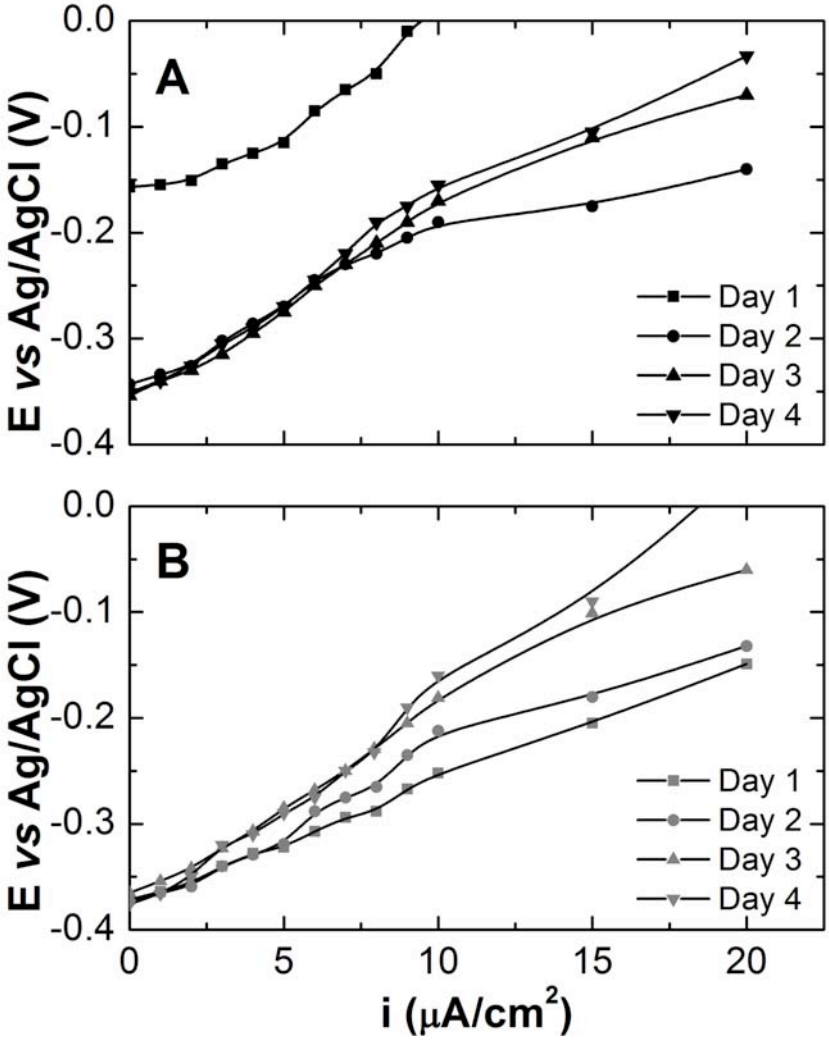

Figure 7.6: Polarization curves for *S. oneidensis* MR-1 biofilms without (A) and with silica encapsulation (B).

Silica-encapsulation may also induce changes in the micro-environment relative to electron donor availability, pH, biofilm life-cycle, and oxygen diffusion that will unequivocally influence physiology and in turn, likely affect electrochemical response. Future explorations should address these factors as they relate to improved electrochemical performance of encapsulated biofilms. Nonetheless, the data collected here suggest that silica-encapsulation may inhibit electrochemically active metabolite diffusion from the surface, and provide increased surface area for riboflavin adsorption.

7.5 Conclusions

The results within this study provide insight into the phenomenon of extra-cellular riboflavin associated with *S. onidensis* MR-1 metabolism and subsequent electrochemical interaction on the electrode. Riboflavin production appears at a maximum for *S. oneidensis*, under micro-aerobic and electron donor-limiting conditions. Riboflavin production clearly varies in response to specific growth condition (e.g. aerobic vs. anaerobic conditions, electron donor versus electron acceptor limitations) suggesting that riboflavin synthesis or release is regulated and responsive to the physiological state of the organism. The redox behaviour of riboflavin under abiotic conditions was essentially identical to the populated anodes.

The electrochemical response after the MFC medium (electrolyte) was removed and replaced was consistent with the presence of a soluble redox mediator. In biotic systems with an established biofilm on an electrode, removal of the surrounding medium results in a significant decrease in electrochemical activity. This could be attributed to the loss of riboflavin near the surface of the electrode, the perturbation of the biofilm from the act of media replacement, or both. After subsequent incubation in fresh electrolyte that is free

of carbon substrate, the capacitance of the electrode is increased and riboflavin redox chemistry is observed after a refractory period. The refractory time is somewhat overcome with silica-encapsulated cells on the electrode surface. The silica likely limits perturbation of the biofilm by media replacement and preserves electrochemical activity. For both encapsulated and non-encapsulated biofilms there is no exogenous carbon source in solution during the 24-hour retention time. Despite this, the capacitive currents of the voltammograms increases, and the concentration of riboflavin appears to increase, further suggesting that *S. oneidensis* riboflavin production stimulated by carbon limitation. Based on these observations we speculate that riboflavin secretion is a response to changes in local environment other than electron acceptor availability. Accordingly, the organism has not adapted a regulatory mechanism that promotes riboflavin-mediated electron transfer dominating in anaerobic environments. Instead, the special environmental circumstances of the MFC allow *S. onedensis* to take advantage of riboflavin as a redox shuttle for indirect extra-cellular electron transfer to insoluble electron acceptors.

7.6 Acknowledgements

This study was funded by the Material Science Directorate of the U.S. Air Force Research Laboratory and the Air Force Office of Scientific Research. Venkataramana Gadhamshetty was supported through a postdoctoral fellowship from Oak Ridge Institute for Science and Education. Jared Roy was supported through a pre-doctoral fellowship from Oak Ridge Institute for Science and Education.

Chapter 8 – Applied Electrode Potential Leads to Biofilm Formation for *S. oneidensis* MR-1

Co-authors: Kristen E. Garcia, Heather R. Luckarift, Akinbayowa Falase, D. Matthew Eby, Andrew J. Schuler, Glenn R. Johnson & Plamen Atanassov

8.1 Abstract

Model organisms such as *S. oneidensis sp*. and *G. sulfurreducens* sp. are often utilized in the study of extra-cellular electron transfer to insoluble electron acceptors (electrode respiration) with the belief that the physiological characteristics present within these species will provide fundamental insight into energy harvesting processes involved in biological based remediation. Energy harvesting is typically associated with the formation of bacterial biofilms, but the precise physiological conditons for this process are not fully elucidated, particularly for the facultative anaerobe *S. oneidensis* MR-1 when cultured under anaerobic conditions. In this study, electrodes were incubated with anaerobic cultures of *S. oneidensis* MR-1 while being exposed to a defined applied potential. The choice of applied potentials were based, in part, on the electrochemical characteristics of riboflavin, which is known to play a role in cell-to-cell signaling. Cyclic voltammetry and electrode polarization were then used to interrogate the electrochemical interaction of biofilms developed under these conditions. In particular, a prolific biofilm developed on the electrode when subjected to an applied potential of -0.3 V vs Ag/AgCl; corresponding to the redox potential for surface-bound oxidized riboflavin. These biofilms display a non-reversible oxidation at 0.2 V. By using a double deletion mutant, ΔMtrC/OmcA, that lacks specific multi-heme cytochromes, the

oxidation species at 0.2 V was determined to be the terminal heme-protein complex in the Mtr pathway. Scanning electron microscopy provided visual confirmation of complex biofilm structures, including the presence of microbial nanowires that developing on the electrode surface under an applied potential of -0.3 V, and during anaerobic cultivation. This study culminates in a hypothesis of *S. oneidensis* biofilm formation as related to cellular metabolic response to changes in environmental conditions.

8.2 Introduction

S. oneidensis is a model organism used in the study of extra-cellular electron transfer (EET) to insoluble electron acceptors with direct application towards the development of microbial fuel cells (MFCs). The phenomenon of EET is associated with organisms deemed to be "dissimilatory metal reducing bacteria" (DMRB), which have been implicated in natural metal and nutrient cycling throughout the environment.[113,128] In other DMRB model organisms such as *G. sulfurreducens* spp., outer membrane-bound c-type cytochromes are known to be involved in direct electron transfer (DET) to metal oxide or electrode surfaces.[18,31,129] In terms of EET for *S. oneidensis,* the mechanisms for electron transfer are less clear, as a combination of effects may be present, including DET via outer membrane bound cytochromes, and/or mediated electron transfer (MET) via biologically synthesized electron shuttles.[26,32,117] One commonality between these two organisms, however, is the apparent utilization of conductive biological nanowires within biofilm communities.[29,38,130,131]

Under anaerobic conditions, *G. sulfurreducens sp.* have been shown to populate the surface of electrodes by forming complex biofilms, in which increasing biofilm thickness leading to greater current density[46]. Conversely, *S. oneidensis* MR-1, as a facultative anaerobe, is also able to form large biofilms, but in the presence of oxygen; removal of oxygen results in a significant reduction in biomass attached to the electrode.[2,53,54] This experimental observation may be one reason for the perception that *S. oneidensis* biofilms do not typically produce the high current densities associated with *G. sulfurreducens* biofilms.[3,4,132] The capability of *S. oneidensis* to form biofilms in anaerobic environments is investigated herein with the aim of increasing current density in model MFCs. The task of addressing the issue of biofilm formation for *S. oneidensis* may be complicated, however, by a number of physiological constraints. First, *S. oneidensis* is a facultative anaerobe containing essential mechanisms to survive in a range of different physiological environments[20]. Secondly, it is well known that *S. oneidensis* MR-1 can express outer membrane proteins capable of metal oxide reduction,[30,39] but MET via redox molecules such as riboflavin appear to dominate the electrochemical character of anaerobic insoluble metal oxide respiration for *S. oneidensis*.[26,32,39,107,117,120,133] Furthermore, recent studies proposed an additional function for riboflavin as an extra-cellular secreted metabolite within *S. oneidensis* cultures. A mediated energy taxis role for riboflavin within *S. oneidensis* cultures was suggested, based on the observation of apparent taxis of planktonic *S. oneidensis* within riboflavin concentration gradients.[118] The use of riboflavin as a redox-sensing metabolite has been observed previously, specifically within *Escherichia coli*, but primarily limited to species that exhibit no known natural ability for metal oxide reduction.[134,135] Parallel studies within our group

identified extra-cellular riboflavin secretion by *S. oneidensis* under carbon limitation and within a range of electron accepting conditions.[136] Most notably, extra-cellular riboflavin is observed in aerobic and micro-aerobic culture under carbon limitation. However, riboflavin concentrations were below the limit of detection for anaerobic cultures exposed to similar carbon limitation. This led to the hypothesis that *S. oneidensis* MR-1 triggers a stress-response as the culture transitions from aerobic to anaerobic metabolism with simultaneous carbon substrate consumption.

In this work, we utilized electrochemical methods, specifically cyclic voltammetry, to probe the electrochemical communication between a developing *S. oneidensis* MR-1 biofilm and an electrode surface in an anaerobic environment. We propose that riboflavin is secreted by *S. oneidensis* MR-1 (potentially as a stress-response to changes in environment) and has the capacity to sense redox changes within its environment and lead the culture into the formation of conductive biofilms on the surface of an electrode (schematic in Figure 8.1A), corroborating the findings in Li et al.[118] We investigated the effect of different potentials applied to the electrode in respect to the attachment and subsequent electrochemical interaction of an *S. oneidensis* MR-1 biofilm. The applied potentials were based on the theoretical electrochemistry of riboflavin, with comparison to non-polarized electrodes as control studies. The findings herein provide insight into the initial phases of biofilm attachment and development for *S. oneidensis* MR-1.

8.3 Methods & Materials

8.3.1 Strain & Culturing Conditions

Frozen stocks of *S. oneidensis* MR-1 were stored in a glycerol solution at -80°C. Cultures were maintained on Luria broth (LB) agar plates and incubated for 24 hours at 30°C. Isolated colonies were subcultured into LB and incubated aerobically at 150 rpm and 30°C for approximately 18 hours corresponding to late exponential growth / early stationary phase and an optical density (OD_{600}) of approximately 4. A 250 mL, 3-neck flask, was modified to fit a 3-electrode electrochemical cell configuration by wiring electrodes through a rubber stopper. A syringe containing glassy wool served as the filter for out-flow gas. Defined medium was prepared as previously reported,[40] and modified to contain 30 mM sodium fumarate as an electron acceptor for anaerobic experiments. 100 mL of defined media was introduced into the electrochemical cell and sparged with nitrogen to achieve anaerobic conditions. *S. oneidensis* MR-1 (MR-1) was subcultured from the initial LB stock into defined medium (1:1000 v/v) and continuously sparged with nitrogen.

Similarly, measurements were made for aerobic cultures by inoculating the electrochemical cell with MR-1 in 50 mM sodium phosphate buffer containing 20 mM sodium lactate to a final OD_{600} of ~0.2 and continually sparged with oxygen. Aerobic cultures were allowed to incubate for 24 hours before electrochemical measurements were made.

8.3.2 Electrochemical Testing

The electrochemical experiments were conducted in the modified 3-neck electrochemical cell containing a reference electrode (Ag/AgCl wire within a saturated solution of KCl), a platinum wire mesh counter electrode and a gold disk utilized as the working electrode (1.5 cm diameter). A low surface area gold electrode was utilized in part of this study to examine exchange current density of the MR-1 biofilms. The same gold electrode was used in multiple experiments and polished before each use to ensure consistency in surface area. Large surface area electrodes (1 cm^3 of graphite felt; Morgan AM&T Grade VDG) were also utilized in this study to examine current density of relevant MR-1 biofilms. The graphite felt electrodes were wired with 10 cm Ni wire as a current collector. All measurements and applied potential experiments were done on a Gamry Reference 600 Potentiostat/Galvanostat/ZRA. Cyclic voltammograms (CVs) were measured between -0.8 V (vs Ag/AgCl) and 0.8 V at a scan rate of 10 mV/s. CVs reported within this study are the first scan unless otherwise noted. Polarization curves were first measured by potentiostatic polarization based on the open circuit potential after biofilm formation. Galvanostatic polarization were subsequently measured based on the current obtained under potentiostatic polarization. Galvanostatic polarization curves are reported within this study. All electrochemical experiments reported herein were measured in the culturing media without removing the working electrode to prevent perturbation of the biofilm from media replacement.

8.3.3 Scanning Electron Microscopy

Scanning electron microscopy (SEM) analysis was used for visual confirmation of biofilm formation on graphite felt electrodes after electrochemical characterization. Cells

were chemically fixed to the electrode using a 2.5% glutaraldehyde solution for approximately 12 hours and then exposed to increasing concentrations of ethanol (30, 40, 50, 60, 70, 80, 90%) ending in 3 separate washes of 100% ethanol. The samples were then exposed to critical point drying using an automated critical point dryer (Seevac Inc.) before coating with ~5 nm layer of gold-palladium using an Emitech K950X sputter coater. Electron microscope manufactured by FEI Company (model Quanta 3D FEG microscope) was used to image the samples at 5 to 10 kV accelerating voltages.

8.4 Results & Discussion

8.4.1 Biofilm Development

The initial investigation was to determine the ability of MR-1 to form a biofilm on an insoluble electron acceptor (gold electrode in this case) under anaerobic conditions. No external potential was applied and the culture was maintained at room temperature (approximately 27°C) for 36 hours. After this time, CVs were obtained (Figure 8.1B; non-polarized biofilm) but no apparent change in capacitive current was observed versus the abiotic control. This is indicative of a lack of electrochemically active biomass accumulation on the surface of the electrode. Biomass was clearly visible in solution as a suspension of planktonic cells, with an optical density of approximately 0.2 (corresponding to ~10^4 CFU mL^{-1}). Additionally there was no measureable concentration of riboflavin observed by CV (at the theoretical standard potential of -0.450 V vs Ag/AgCl), confirming observations that riboflavin is not present in an extra-cellular form under anaerobic growth conditions.

Subsequent experiments were aimed at elucidating the effect of changes in the local redox environment in respect to biofilm formation. An applied potential corresponding to that of riboflavin (near -0.450 V vs Ag/AgCl) was applied to the working electrode under anaerobic conditions for ~36 hours (corresponding to reduced riboflavin on the

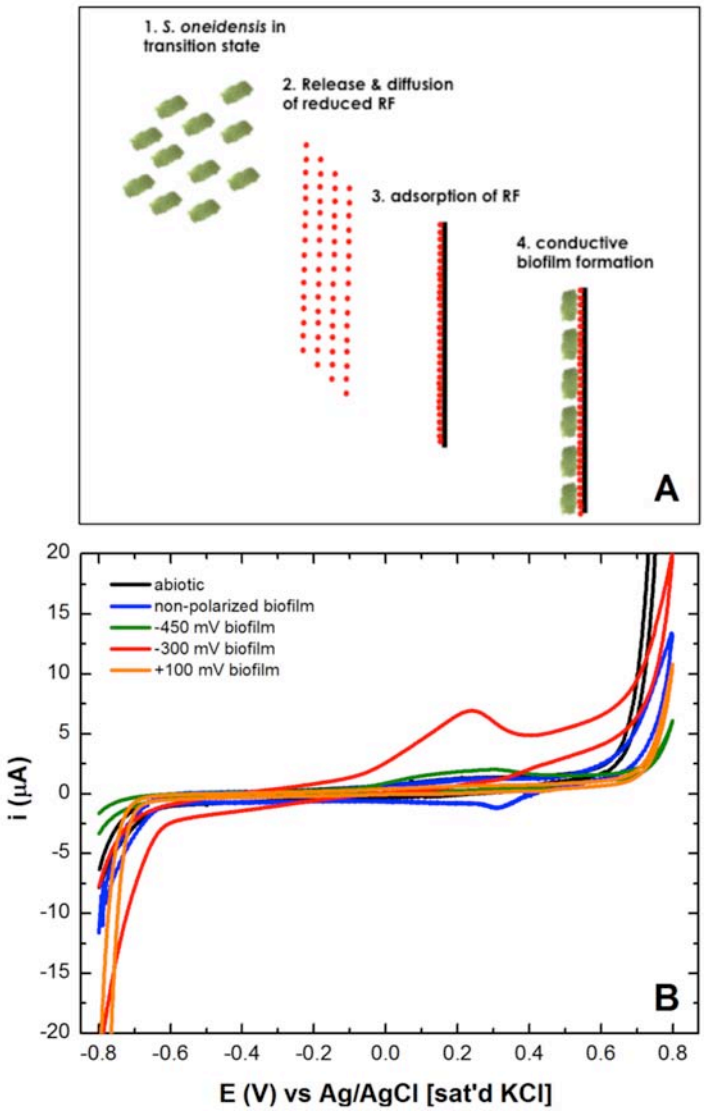

Figure 8.1: (A) An illustration depicting proposed attachment and biofilm formation onto an electrode surface and (B) cyclic voltammograms of biomass-electrode interaction after 36 hours of applied potential biofilm formation.

electrode surface). The CV of the resulting electrode, however, exhibited little evidence of biomass accumulation or the presence of electrochemically-active metabolites (Figure 8.1B, -0.45 V biofilm). The experiment was repeated, with an applied potential of -0.3 V on the working electrode (this time, corresponding to a greater concentration of oxidized riboflavin on the surface).

The CV obtained for this system (Figure 8.1B, -300 mV biofilm) provided evidence for the accumulation of biomass on the electrode surface, based on higher capacitance relative to the abiotic CV. Interestingly, a non-reversible oxidation peak centered at 0.2 V was also observed and this oxidation species was investigated using further experiments (described below). As a point of reference, a further experiment was performed with an applied positive potential of 0.1 V vs Ag/AgCl. The CV obtained (Figure 8.1B, +100 mV biofilm) for this system also lacked any evidence for biomass accumulation on the electrode surface, despite planktonic biomass being present in solution. In all four cases, no oxidation or reduction species near -0.45 V vs Ag/AgCl was detected via CV, indicating the lack of riboflavin in all biofilms.

The specific response of the MR-1 culture to an applied potential of -0.3 V led us to speculate that redox gradients may play a role in biofilm formation under anaerobic conditions. It is plausible that cell-to-cell signaling may be utilized by *S. oneidensis* to form biofilms, triggered by the release of specific metabolites under changes in environmental conditions. Electrochemically active metabolites, such as riboflavin, may be retained at the electrode surface and thereby create a redox gradients that directs cell

attachment to insoluble electron acceptors. This taxis-like behavior has been previously reported for *S. oneidensis* in response to riboflavin gradients.[118]

8.4.2 Electron Transfer Mechanism in Anaerobic Biofilms

Building on the evidence that MR-1 can form biofilms under specific growth conditions, the nature of EET was explored, with possible connections to the oxidation species observed at 0.2 V (Figure 8.1B, -300 mV biofilm). A mutated form of *MR-1* (ΔMtrC/OmcA) contains a double deletion mutant lacking the MtrC/OmcA multi-heme cytochrome complex, MtrC/OmcA is the terminal protein in the Mtr pathway of *S. oneidensis,* proposed as the electron pathway for DET, linking the metabolic system of the cell to an insoluble electron acceptor.[16,125,137] When cultured in the electrochemical cell at an applied potential of -0.3V vs Ag/AgCl for 36 hours, the ΔMtrcC/OmcA provided compelling insight into the involvement of specific cytochromes in EET. First, there was only a minor change in capacitance between the abiotic electrode and the electrode populated by the ΔMtrcC/OmcA mutant MR-1 (Figure 8.2A), indicating a lack of biomass attachment at the electrode surface. This puts into question the ability for the biofilm to electrochemically communicate with the electrode when lacking this terminal protein. Secondly, the oxidation peak centered at 0.2 V vs Ag/AgCl was no longer apparent (Figure 8.2B), indicating that the observed oxidation species is likely the terminal protein complex in the Mtr pathway, MtrC/OmcA.

Interestingly, after anaerobic cultivation of the native MR-1 at -0.3 V vs Ag/AgCl, the distinct non-reversible oxidation species at 0.2 V was clearly present on the first scan of

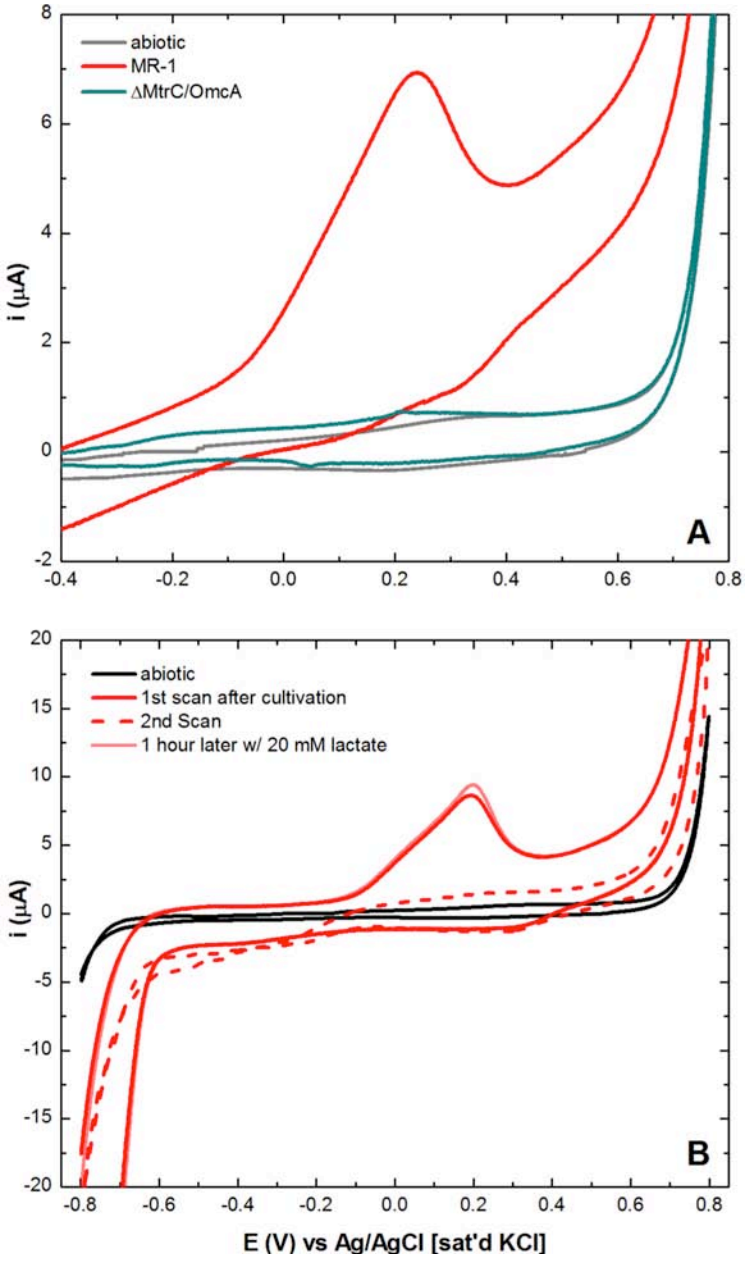

Figure 8.2: (A) Cyclic voltammograms of native strain *S. oneidensis* MR-1 (red), the ΔMtrC/OmcA mutant (blue), and abiotic control (grey) after 36 hours of applied potential at -0.3 V vs Ag/AgCl; and (B) Cyclic voltammograms of native strain *S. oneidensis* MR-1 after 36 hours of applied potential biofilm formation. First scan (red), second scan (dashed red) and after an hour of open circuit potential with addition of 20 mM lactate in solution (light red).

the CV (Figure 8.2B). However, after the second scan, the oxidation event was severely depleted or absent. At this time, lactate (~20 mM) was provided as carbon source and the open circuit potential was observed to stabilize to approximately -0.5 V within an hour (data not shown). The CV measurement was then repeated, and the non-reversible oxidation peak at 0.2 V had returned (Figure 8.2B). We speculate that the apparent non-reversibility of the oxidation species represented by the peak at 0.2 V may be due to the orientation of the terminal protein complex within the outer membrane, such that the process cannot be reversed (or reduced) externally.

In short, the cytochrome complex is not capable of being reduced externally (by driving the potential with a potentiostat) but is oriented in such a way to be reduced in line in the proposed Mtr pathway, as a function of cellular metabolism (and lactate oxidation). The observation of open circuit potential that attained -0.5 V cannot be attributed to the presence of riboflavin, as it was clearly not detected in these anaerobic systems. This negative open circuit potential may, however, be attributed to the proposed idea of a gradient through the biofilm of reduced/oxidized adjacent redox proteins.[42]

8.4.3 Current Density Ascribed to Biofilm Formation

Initial measurements were conducted on low surface area electrode in order to probe the exchange current density during anaerobic biofilm formation, that is to say specific redox couples responsible for EET within these biofilms. Further analyses were performed on large surface area carbon felt electrodes to interrogate current density and polarization performance of the biofilms described above. This is imperative as large surface area electrodes can mask redox couples from the large capacitive current inherent within the material; however, large surface area electrodes will provide a clear range of current

density with large accumulations of biomass. Carbon felt incubated in an anaerobic culture of MR-1 for 24 hours, with no external potential applied, was compared to that of an electrode subjected to an applied potential of -0.3 V during cultivation. Results for galvanostatic polarization curves for the two systems (Figure 8.3) revealed an open circuit potential for the non-poised system of -0.4 V and low current density under polarization (< 25 $\mu A/cm^3$). When compared to the abiotic system, the low current density can be attributed to the presence of biomass on the electrode, albeit a minimal concentration. Electrodes with applied potential at -0.3 V during cultivation clearly exhibited enhanced catalytic activity, with an open circuit potential of -0.5 V, further corroborating the previous discussion.

Interestingly, the current density associated with these biofilms appeared to achieve maximum current within the potential region attributed to the observed MtrC/OmcA oxidation species (0.2 V vs Ag/AgCl). This confirms the hypothesis that the multi-heme cytochromes MtrC/OmcA are involved in reducing the electrode as part of cellular EET. The voltammagrams in the previous sections did not indicate the presence of a measureable concentration of riboflavin (~-0.45 V) for these biofilms. Confirmation for the lack or riboflavin is present within these polarization curves as the bulk of the current density is ascribed to the region near 0.2 V, with little current density occurring at the onset of riboflavin potentials. To that end, the experiment was repeated with the ΔMtrC/OmcA mutant, following 24 hours of anaerobic cultivation with an applied potential of -0.3 V. The observed open circuit potential was approximately -0.4 V, confirming biomass attachment; but no catalytic activity was present in the system under

polarization. Note that the oxidation species near -0.2 V was also present in abiotic systems, and is an intrinsic property of the electrode material.

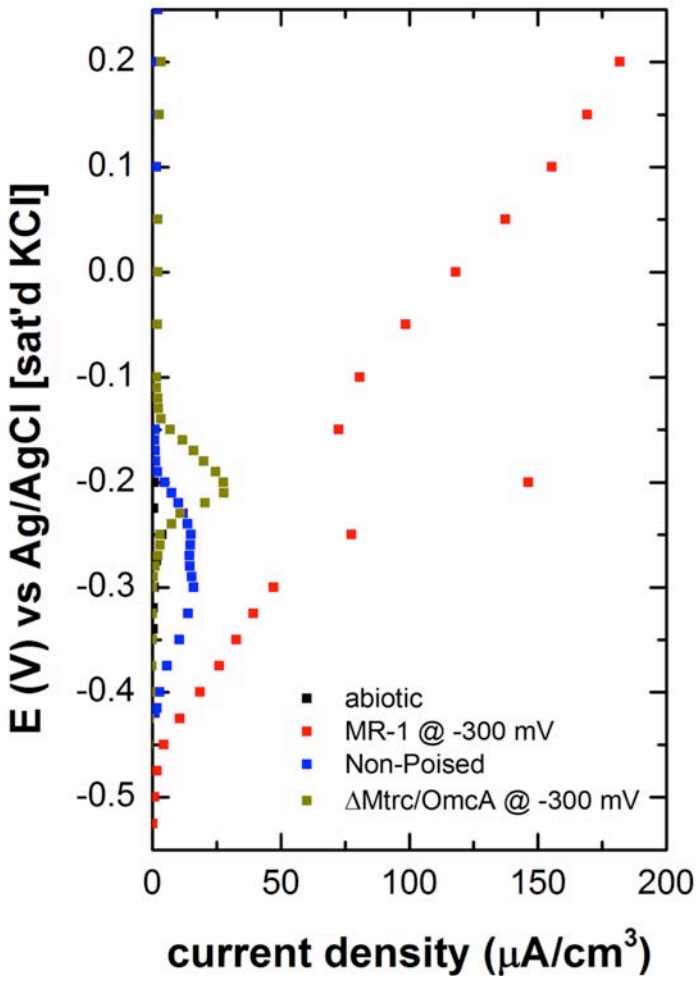

Figure 8.3: Polarization curves of various biofilm formations on carbon felt electrodes

SEM was used to confirm the presence of attached biomass on the electrode surface. For the non-poised anaerobic biofilm (Figure 8.4[A-C]), minimal biomass is visible on the electrode surface and even with increasing magnification the presence of biological nanowires is not observed. In contrast, the biofilm formed anaerobically with applied

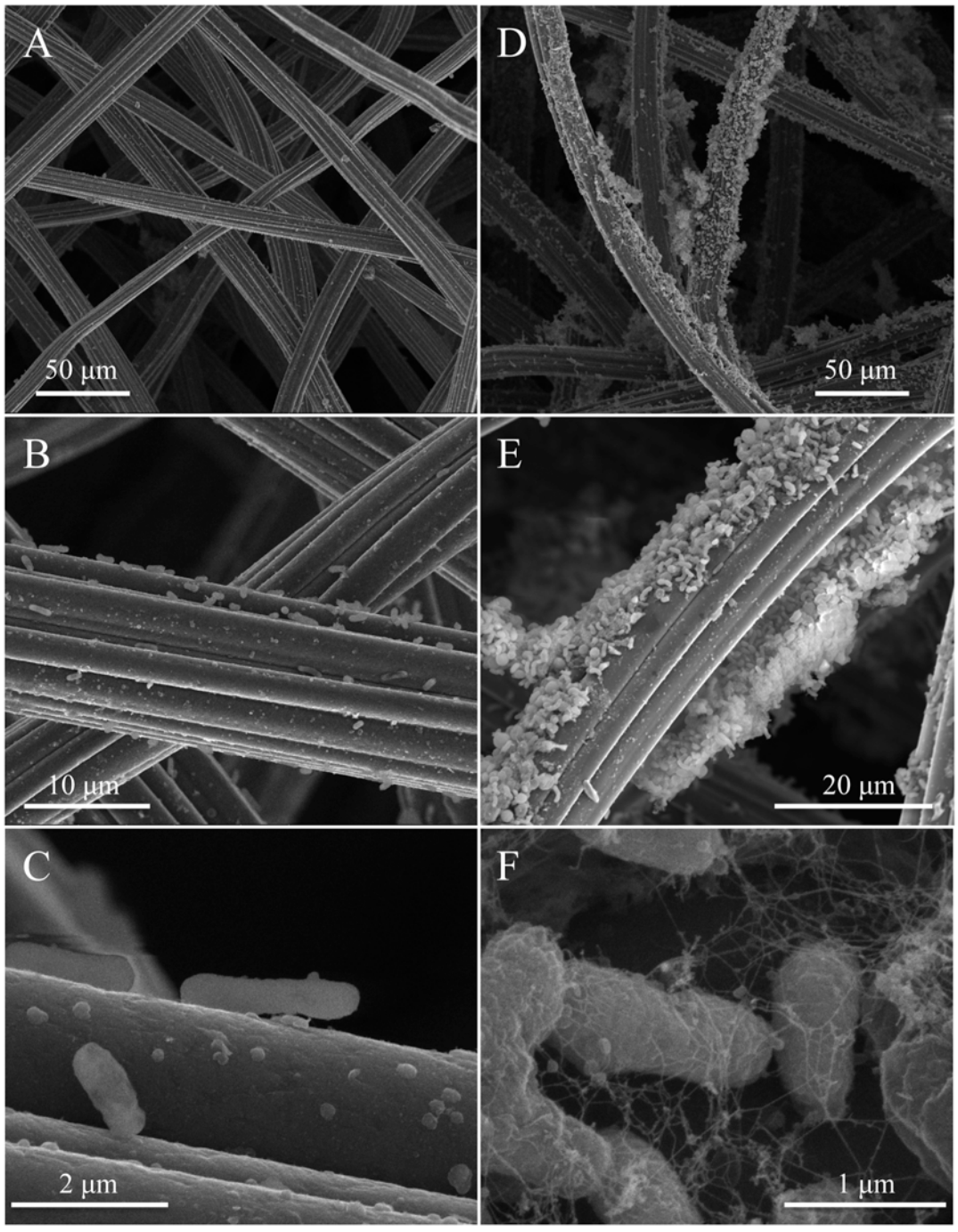

Figure 8.4: Scanning electron microscope images of *S. oneidensis* MR-1 under non-poised potential biofilm formation (A, B, & C) and applied potential (-0.3 V vs Ag/AgCl) biofilm formation (D, E, & F).

potential at -0.3 V yields significantly greater coverage of biomass on the electrode surface (Figure 8.4D). The apparent thickness of the biomass was approximately 10 μm (Figure 8.4E), with visual confirmation of biological nanowires present across the surface of the electrode under greater image magnification (Figure 8.4F). These SEM images provide further visual confirmation to the electrochemical data suggesting preferential biomass attachment and biofilm formation on the surface of the electrode when a potential of -0.3 V vs Ag/AgCl is applied during anaerobic culturing.

8.4.4 Metabolic Transition May Lead to Biofilm Development

As a facultative anaerobe, MR-1 is capable of tolerating different metabolic states governed by growth constituents, more specifically electron acceptors. Based on the observations provided within this study and a parallel investigation of metabolic riboflavin production (Roy et al. 2012), we hypothesize that as the organism transitions from aerobic to micro-aerobic and finally anaerobic metabolism, the electrochemical properties of the biofilm changes, as outlined in Figure 8.5. In ideal batch culture, the organism will proliferate as long as growth constituents (oxygen and carbon substrate, for example) are plentiful.

In aerobic metabolism, there is little or no electrochemical communication with the electrode (or other insoluble electron acceptor). However, as nutrients become limited, it is possible that *S. oneidensis* will secrete cell-to-cell signaling metabolites that signal biofilm formation. We speculate that riboflavin may be one such endogenous metabolite,

as flavin molecules are known to appear at the onset of carbon substrate limitation under micro-aerobic environments. This may lead the organism into forming biofilms on the insoluble electron acceptor for anaerobic, cell sustaining metabolism. This study is an effort to experimentally describe that final anaerobic metabolic state of the organisms on the electrode surface.

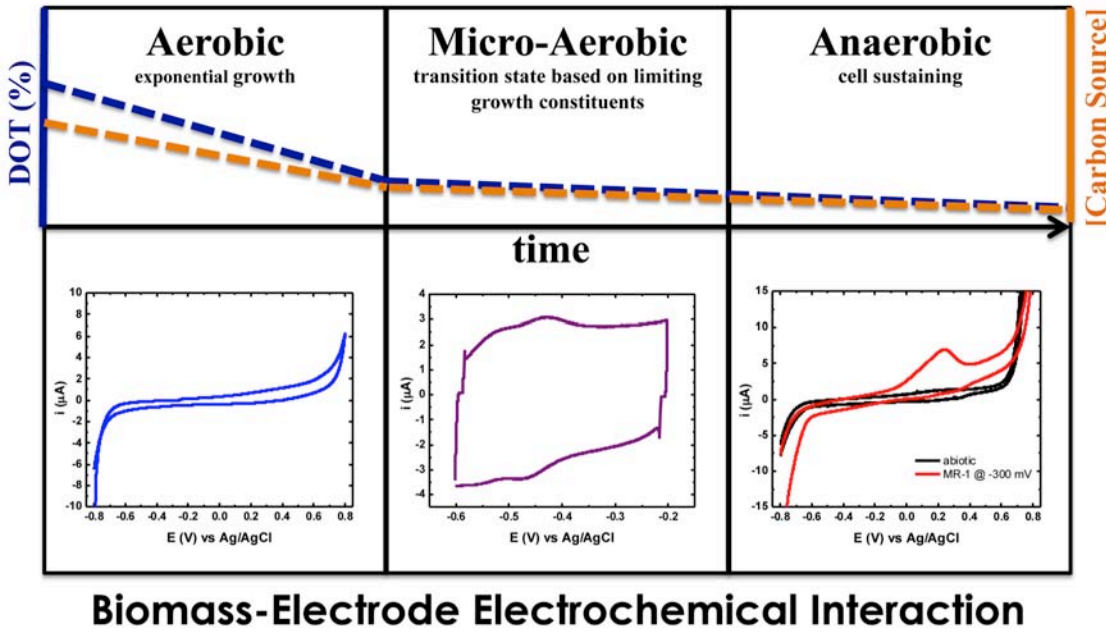

Figure 8.5: Proposed metabolic states of *S. oneidensis* MR-1 leading to biofilm formation and respective electrode interaction as measured by cyclic voltammetry

8.5 Conclusions

The results from this study suggest that anaerobic biofilm formation for *S. oneidensis* MR-1 occurs preferentially on an electrode when subjected to an applied potential of -0.3 V vs Ag/AgCl. Biofilms formed under these conditions yield behavior indicative of DET and a mechanism of EET is supported via the Mtr pathway, with terminal proteins

implicated as the MtrC/OmcA complex. Visual confirmation via SEM in our study also indicated a link between catalytic current and the presence of biomass and biological nanowires on the electrode surface. Direct electrochemical evidence linking biological nanowires and cytochromes will need to be explored further in subsequent studies of these biofilm formations. However, the lack of electrochemical evidence for riboflavin in this anaerobic anode respiring biofilm is clear. First, cyclic voltammetry failed to provide indication of the presence of riboflavin in these biofilms. Second, the observed current density was relatively low within the region of riboflavin standard potentials (~-0.45 V) with large contributions of the current density instead being attributed to the observed MtrC/OmcA potentials (~ 0.2 V). Biofilm formation for *S. oneidensis* appears to correspond to environmental stimuli. More specifically the apparent ability for redox sensing in planktonic cultures leads to biofilm formation on insoluble electron acceptors (metal oxides or electrodes in fuel cells). Relevant redox potentials for this idea coincide with the electrochemically active metabolite, riboflavin (oxidized ~ -0.3 V); which is environmentally relevant for *S. oneidensis* cultures in carbon substrate limitation and limited dissolved oxygen tension.

Chapter 9 – Improved Electrode-Biofilm Formation by *S. oneidensis* MR-1 and Anode Characterization by Expanded Uncertainty

Co-Authors: Kristen E. Garcia, Sofia Babanova & Plamen Atanassov

9.1 Abstract

In this study, high-density planktonic cultures of *S. oneidensis* MR-1 are grown aerobically to early stationary phase. At that time the culture is then exposed to an anaerobic environment in an electrochemical cell. An applied potential of -300 mV vs Ag/AgCl is applied to the working electrode and the corresponding current is measured via chronoamperometry. Current begins to increase within 2 to 3 hours stabilizing at 5 hours. Cyclic voltammetry was measured at 5 hours indicating the initial stages a kinetically limited biofilm and again at 24 hours with an apparently more stable catalytic biofilm. At this point, the biofilm appears to suffer diffusion limitation as the catalytic wave dominates the shape of the voltammogram. A novel biofilm as this is the first such biofilm being reported for *S. oneidensis* MR-1. Polarization curves are also reported herein, further demonstrating a large increase of current near the oxidation potential of the terminal protein complex (MtrC/OmcA) of the trans-membrane cytochrome cascade, the Mtr pathway. Additional characterization and comparison between replicates of the biofilm is made using the idea of expanded uncertainty. This novel approach to reporting obtained results for microbial fuel cells, elucidates specific electrochemical parameters for appropriate comparison between systems and laboratories.

9.2 Introduction

For microbial fuel cells based on the facultative anaerobic model organism, *S. oneidensis* MR-1, forming catalytic biofilms anaerobically is essential for improved current density. In previous studies, we have shown a novel methodology, based on applied potential during anaerobic cultivation which enables *S. oneidensis* MR-1 to grow and populate the surface and employ outer membrane cytochromes in direct reduction of the electrode coupled to the metabolic oxidation of a lactate. We speculate that *S. oneidensis* MR-1 exhibits an electrochemical taxis-like behavior leading the organism to populate the surface. The applied potential identified most effective in surface population was near -300 mV vs Ag/AgCl, near the potential of oxidized riboflavin. Riboflavin, under carbon limitation, has been observed in the extracellular medium by *S. oneidensis* MR-1 cultures in our studies. With these experimental data and observations from others, riboflavin redox potentials likely leads the organism to biofilm formation on substrates that are electron acceptors when EET becomes essential for cell sustaining.[118]

Within this study, *S. oneidensis* MR-1 was cultured aerobically in Luria Broth (LB) to early stationary phase growth, in order to procure a high-density culture. This culture was then exposed to strict anaerobic conditions with an electrode having an applied potential of -300 mV vs Ag/AgCl for varying time increments. The subsequent biofilms formed yielded catalytic activity as characterized by cyclic voltammetry and polarization curves after approximately 5 hours with maximum current density being achieved within 24 hours. The voltammetries reported within this study are the first of this kind to be presented from *S. oneidensis* MR-1 populated electrodes.

With the increasing number of electrochemical investigations metabolic processes of dissimilatory metal reducing bacteria (DMRB), the need to appropriately compare results between different laboratories becomes apparent. Due to the fact that these bioelectrochemical systems' (BES) or biofuel cell performance depends on several factors (metabolic state of the organisms, structure and composition of the biofilm and intrinsic electrode properties) there is not a uniform approach to present the results. Two methods have been unofficially adopted over the years: normalizing the current and power to the electrode geometric surface area or normalizing the gained electrochemical response to the volume of anode/cathode compartment.[138,139] The reason for this is the hypothesis that these two parameters are the main factors influencing the biofuel cell overall current gain.[140] Normalizing the current and power to the electrode cross sectional area holds true only when the electrode is smooth with plain or rod shaped (low surface morphology), in other words, when the geometric surface area is equal to the electrochemical accessible surface area (EASA). It is also proposed that the generated current is reversed proportional to the distance between the electrode and the membrane (two-chambered MFC) or between the anode and cathode (membrane-less MFC), and at the same time is proportional to the diagonal of the anode/cathode chambers. The volume of the fuel cell compartments plays a significant role when the ratio volume/electrode surface is high, otherwise the MFC volume cannot be used as a normalization parameter.

The most common parameters used to represent the electrochemical response of MFCs are the open circuit voltage, maximum power and short circuit current.[59] These

parameters are used to characterize the whole fuel cell performance; however, when electrode (anode or cathode) is individually under investigation these parameters are less appropriate. In these cases other parameters could be selected as the best representation of the system. In this study a statistical examination will help in identifying three defined potentials as being appropriately significant.

Another problem facing MFC studies is the irreproducibility of the gained results. There are two ways to overcome this problem: to minimize the influence of the factors leading to irreproducible results or to normalize the results to the main parameter contributing to the their uncertainty.[141] In both methods the system should be examined in details and the uncertainty of the main factors increasing the expanded uncertainty of the results should be evaluated.

The uncertainty is a term readily understood in other industries, pharmaceutical and food for example; but this concept is new in the microbial fuel cell discipline and perhaps all biofuel cells. In this study we will properly evaluate novel biofilms of *S. oneidensis* MR-1 using the theory of expanded uncertainty and will describe how this methodology can be used to address a variety of standardization problems. This approach consists of: normalization of the current to the electrode electrochemically accessible surface area (EASA) and representation of current as $\mu A/cm^2$ (EASA), accomplished by its expanded uncertainty. Using expanded uncertainty, intrinsic properties of the electrode will be addressed to further explain why EASA is the appropriate parameter in reporting electrode polarization.

9.3 Methods & Materials

All chemicals were obtained from Sigma-Aldrich (St. Louis, MO) and of highest available purity unless otherwise stated.

9.3.1 Strain & Culturing Conditions and Biofilm Formation

Frozen stocks of *S. oneidensis* MR-1 were obtained from a -80 °C freezer and plated on Luria Broth (LB) plates containing 1% agar by weight to ensure continuity of the stock cultures. Individual colonies were isolated and inoculated in 50 mL of liquid LB in 250 mL shaker flasks. The liquid cultures were incubated aerobically at 150 rpm and 30 °C for approximately 18 hours. This time corresponds to the start of early stationary phase corresponding to an optical density measured at 600 nm of 4.5 (~10^{12} CFU mL^{-1}). Cultures were then washed 3 times in 50 mM sodium phosphate buffered saline (PBS) (pH 7) and re-suspended to the original density. 100 mM of sodium lactate and 30 mM of sodium fumarate are added to the culture and the mixture is incorporated into an electrochemical cell. The 3-electrode set up consists of a carbon felt (Morgan AM&T Greenville, SC) working electrode (1.5 cm in diameter) wired with nickel wire as a current collector, platinum mesh (approximately 1 x 2 cm), and an Ag/AgCl [sat'd KCl] reference electrode. Electrodes were connected to a Gamry 600 Potentiostat/Galvanostat/ZRA. The electrochemical cell was sealed and gassed with nitrogen to ensure an anaerobic environment during experiment.

9.3.2 Calculation of Electrochemical Accessible Surface Area

Electrodes were treated with Isopropyl alcohol (IPA) for 10 minutes and rinsed 3 times in sterile 1X PBS to clear away excess IPA, this ensured wettability of the normally

hydrophobic material. Electrochemical accessible surface areas were then determined prior to inoculation with *S. oneidensis* MR-1 culture by measuring a cyclic voltammogram at 0.01 V/s (ν). Corresponding oxidation and reduction currents were used in the following equation to evaluate the EASA for individual electrodes:

$$EASA = \frac{i_{ox} - i_{red}}{2\nu} C$$

With a specific capacitance of the material (C) of 35 μF/cm^2.

9.3.3 Calculation of Expanded Uncertainty

Combined uncertainty (U_c), according to the National Institute of Standards & Technology, is expressed as the uncertainty of many measurements and an be assumed to be the estimated standard deviation. However, for some commercial, industrial or regulatory applications, expanded uncertainty (U) may be more appropriate. Thus expanded uncertainty can be obtained by multiplying U_c by a coverage factor (k):

$$U = kU_c \qquad \textbf{Equation 9.1}$$

With k typically being in the range of 2 to 3 with a k value of 2 corresponding to the 95% confidence interval and a k value of 3 corresponding to a confidence interval of 99%. For this study, a k value of 2 was used, yielding our expanded uncertainty to be within a confidence interval of 95%.

9.4 Results & Discussion

9.4.1 Biofilm Formation

Planktonic cultures were inoculated into the electrochemical cell with an applied potential of -300 mV vs Ag/AgCl on the working electrode (via chronoamperometry) in an anaerobic environment, the current measurement obtained was 0 for approximately 2.5 hours (Figure 9.1). At that point the current started to increase and stabilized at 5 hours. It is likely that this time is required for the culture to transition to an aerobic respiration basted metabolism to one that is capable of electrode reduction as a function of metabolic oxidation of lactate. Biofilm formation is likely to start during this time.

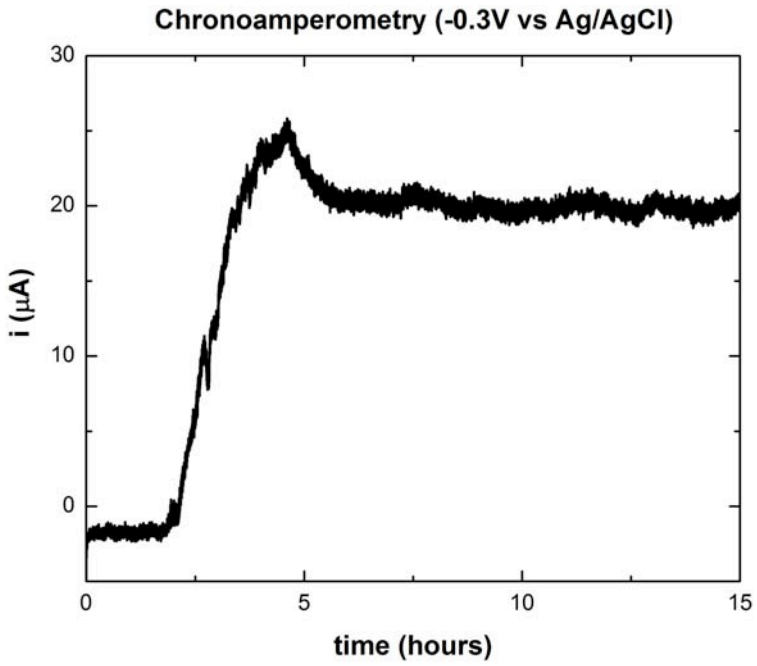

Figure 9.1: Chronoamperometry measurement of the working electrode during first 15 hours of biofilm formation of *S. oneidensis* MR-1 from planktonic cultures in an anaerobic electrochemical cell

The high-density culture (~10^{12} CFU mL^{-1}) contains 100 mM sodium lactate and 30 mM sodium fumarate at the onset with addition of only lactate (100 mM) after 10 hours. The idea to add fumarate initially is to prevent the death of the culture during the beginning of the aerobic to anaerobic change. This prevents the death of the biomass from an arrested metabolism (inability to respire) until the biological structures are in place to begin biofilm formation and electrode respiration. With the addition of lactate after approximately 10 hours, the measured current increases again and stabilizes within an hour.

9.4.2 Cyclic Voltammetry of Biofilms

After 5 and 24 hours, cyclic voltammetry was measured for the system to evaluate redox characteristics of the developing biofilm (Figure 9.2A). The 5-hour voltammogram (obtained in turnover conditions) measured the beginning stages of a catalytic biofilm that appears to be engaged in kinetic limitation. In terms of a beginning biofilm, for this system, one must look at the voltammogram of the biofilm after a longer period has passed under anaerobic applied potential biofilm formation. After 24 hours, the same measurement is made on the biofilm (again, under turnover condition). The biofilm now appears to be under a diffusional-based limitation, reaching saturation current above +0.40 V vs Ag/AgCl. When comparing the two time frames, we speculate that the 5-hour biofilm is in the initial stages of biofilm formation, leading to a system that suffers kinetic limitations. This is likely caused, at least in part, in the lack of catalyst on the surface (low population density), with the orientation of the terminal reeducates playing a role.

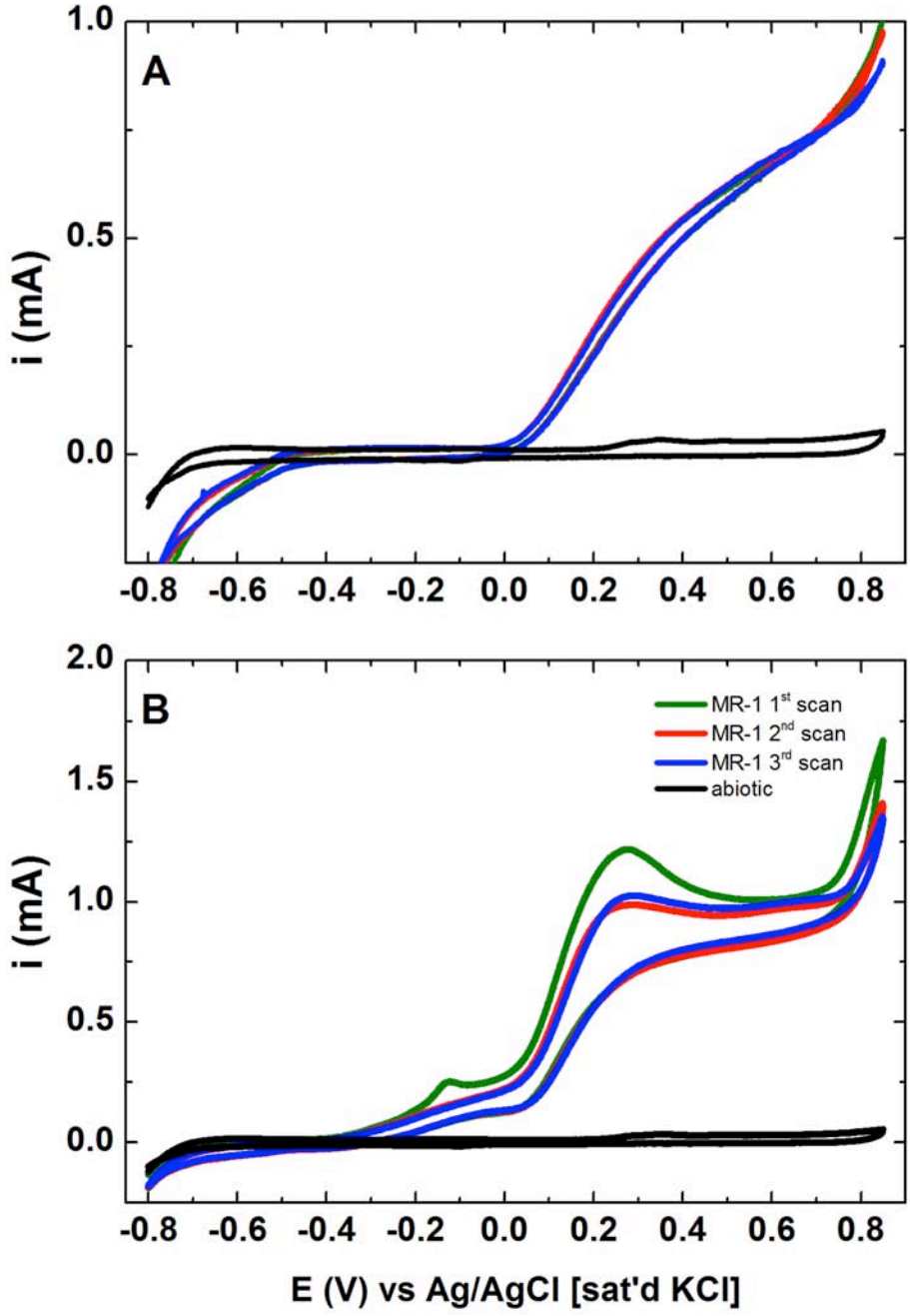

Figure 9.2: Cyclic voltammograms of 3 consecutive scans under turnover conditions including an abiotic control for a 5-hour biofilm (A) and a 24-hour biofilm (B)

The CV for the 5-hour biofilm exhibits catalytic activity beginning at 0 V vs Ag/AgCl and this is consistent with previous findings that anaerobically formed *S. oneidensis* MR-

1 biofilms on an electrode with applied potential (-0.3 V) do not exhibit MET features consisting of the presence of riboflavin (consistent with chapter 7) as others have speculated. Additionally, the catalytic nature of this biofilm appears to be dominated by DET mechanisms consistent with previous findings (chapter 8). However, as the biofilm becomes more developed, complex and indeed larger (after 24-hours of formation) the presence of a second EET mechanism appears at the onset of -0.3 V. This multi-step electrode reduction cascade may be attributed to a mediator. Likely, this is riboflavin, as the potential of the new catalytic feature corresponds to an onset potential near the redox potentials of riboflavin. The sudden appearance of riboflavin is consistent with the theories outlined within our broader study, the theory that riboflavin becomes electrochemically detectable within carbon source limited cultures of *S. oneidensis*. Thus, as this particular biofilm becomes more complex as a function time and applied potential on the electrode, the biofilm achieves greater thickness; likely causing organisms near the electrode surface to switch to a carbon source limited metabolism (as have been proposed in previous chapters) and subsequent secretion of riboflavin influencing the electrochemical character of the system.

9.4.3 Electrode Polarization

To elucidate the achievable current densities of these biofilm systems, potentiostatic polarizations were measured beginning with the stabilized open circuit potential after the applied potential had been removed from the working electrode. Under turnover conditions, the open circuit potentials for both systems stabilized within an hour to near -0.5 V vs Ag/AgCl. This low open circuit seems to correspond to the findings of other groups which propose an electron gradient perpendicular to the surface as the biofilm is

no longer able to respire with the electrode during open circuit conditions.[42] Multiple repeats of the same conditions on identically prepared electrodes (for both 5-hour and 24-hour biofilms) were evaluated and are plotted in Figure 9.3.

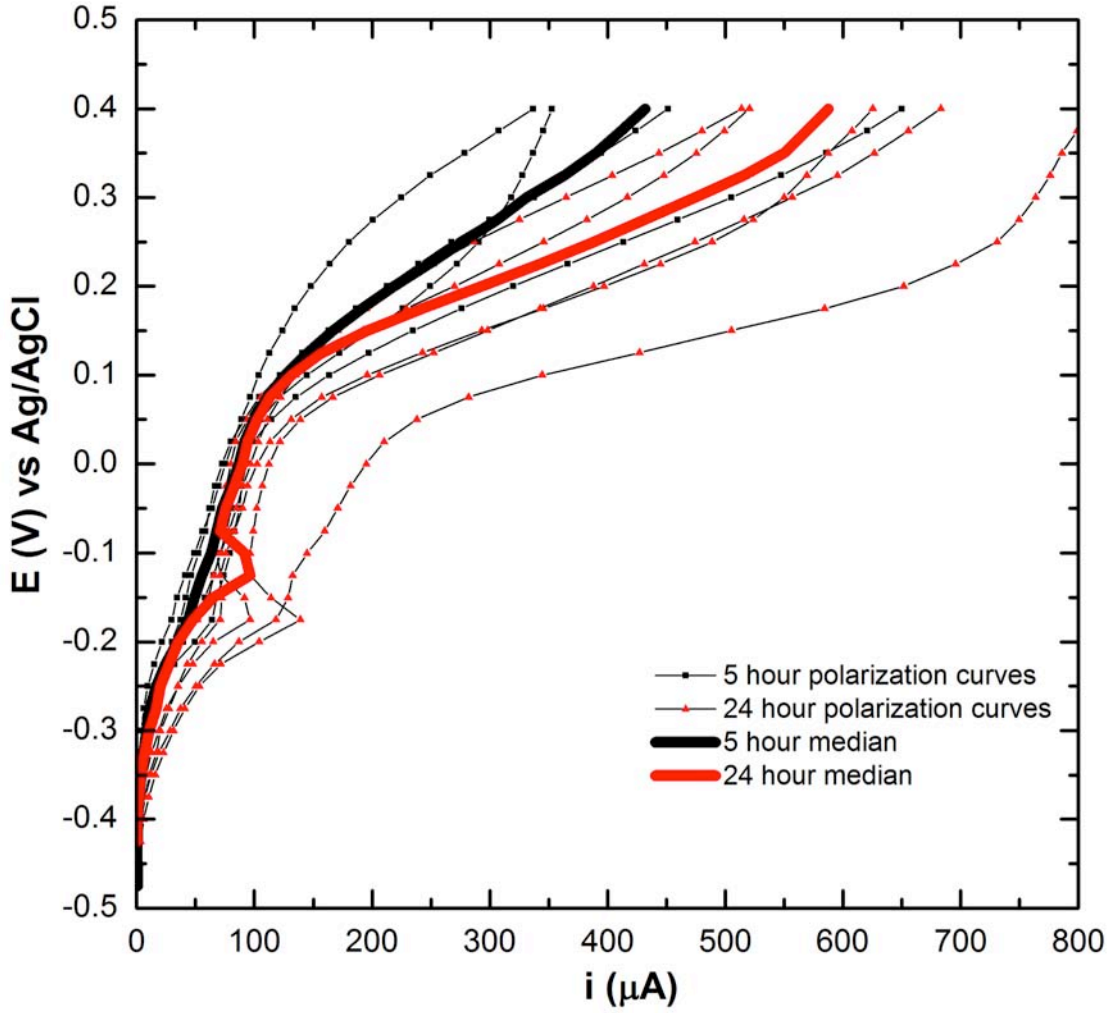

Figure 9.3: Multiple repeats of potentiostatic polarization curves for 5-hour (black circles) and 24-hour (red circles) biofilms, including the median of all measurements for 5-hour (black solid line) and 24-hour (red solid line) biofilms

The 5-hour biofilms show little contribution towards current at potentials lower than -0.2 V vs Ag/AgCl, with increased current measured near -0.1 to 0 V consistent with the previously measured CVs. Confirming results from the 24-hour CVs are the 24-hour

polarization curves, with observed measurements increasing the current (compared to the 5-hour biofilm) beginning at -0.3 V. However, the overall contribution to the total measured current within the region (riboflavin redox potential region ~ -0.350 V) is little compared to the measured current contribution from the MtrC/OmcA terminal reductatases (onset at 0 V). Indeed the 24-hour biofilm contributes to increased current within this region (above 0 V) compared to the 5-hour biofilm, consistent with our hypothesis of a more developed, catalytic biofilm at this time point. The oxidation event near -0.2 V vs Ag/AgCl in the 24-hour biofilms is likely an intrinsic material property as this is evident in abiotic controls (data not shown).

9.4.4 Expanded Uncertainty Evaluation of Abiotic Electrodes

As previously shown, variation of the measured current is congruent between biofilms that are cultivated and grown in the same way on identically prepared electrodes. In order to determine an appropriate way to normalize the measured current to achieve less variability in the system, we first looked at the intrinsic material properties of the electrodes that were identically prepared. The uncertainty of the electrodes inhomogeneity was determined by measuring the mass of fifty carbon felt electrodes. The resistance and the EASA of the same electrodes were also established. The uncertainties of these parameters were evaluated using Robust statistics and the results are found within table 9.1. It is obvious that the uncertainty due to differences in electrochemical accessible surface area has the highest value - fifteen times higher than the uncertainty due to variation in electrodes mass and more than three times higher than the electrode resistance uncertainty. Thus electrochemical accessible surface area is the major factor limiting the results reproducibility.

Table 9.1: Measured intrinsic electrode material properties with average, standard deviation, expanded uncertainty value and percent change of the expanded uncertainty from the average value

Parameter	Average	Standard Deviation	Expanded Uncertainty	Expanded Uncertainty (%)
Internal Resistance	3.28 Ω	± 0.25 Ω	± 0.49 Ω	14.9 %
EASA	22.25 cm^2	± 7.03 cm^2	± 14.06 cm^2	63.2 %
Mass	0.1039 g	± 0.0025 g	± 0.0050 g	4.9 %

It is obvious that the uncertainty due to differences in electrochemical accessible surface area has the highest value - twelve times higher than the uncertainty due to variation in electrodes mass and more than four times higher than the electrode resistance uncertainty. Thus this parameter is the major factor limiting the results reproducibility. Therefore, normalizing the gained electrochemical results from the biocatalysts, one must consider the electrochemical accessible surface area as the most appropriate value.

9.4.5 Expanded Uncertainty Evaluation of the Biofilms

In order to represent the results gained from the polarization curves in a statistically meaningful way, according to the requirements of the chemical metrology, and to define their reproducibility, the expanded uncertainty of the current at each point of the polarization curves were evaluated, for both of the studied electrode systems – 5-hour and 24-hour biofilms (Figure 9.3). Because of the complicated character of the studied system Robust or nonparametric statistic were used as a statistical tool. An estimation of the measured value the median of all replicates is applied. The uncertainty is related to the median of absolute deviation (MAD) and normalized median of absolute deviation.

When polarization curves are taken, the generated current is established. This current is used as a parameter describing the electrochemical behavior of the system. There are three major problems connected with it: (i) representation; (ii) comparison; (iii) and reproducibility. Resolving the last one will give us the answers to the other two. For current reproducibility evaluation, the uncertainties of the main factors leading to irreproducible results were estimated, building an uncertainty budget. The main factors having an impact on the current uncertainty, for the examined *S. oneidensis* anodes are: (i) electrode inhomogeneity; (ii) electrode resistance; (iii) electrode electrochemical accessible surface area; and (iv) biofilm growth and development. We can say that the last two factors must be connected. The number of the cells attached to the electrode surface depends on the electrode surface area. Because of the fact that we observe direct electron transfer within *S. oneidensis* biofilms, the amount of cells, which can utilize the electrode as final electron acceptor, is proportional to the EASA. Thus, for the purposes of the current uncertainty estimation the uncertainty due to the biofilm growth and development will not be discussed. We assumed that this uncertainty would be strongly correlated with the uncertainty due to differences in EASA. Definitely the factors previously described are not the only factors determining the anode electrochemical behavior; however, they are the parameters that can have a substantial impact on the results' uncertainty.

Before the uncertainty evaluation, the data from the polarization curves was checked for outliers using the linear dependence between current and EASA. For each point of the polarization curves, the gained current is linearly proportional to the electrochemical

accessible surface area (data not shown), which is further evidence that this parameter has a large impact on the results' reproducibility.

As it can be seen from Figure 9.4A, the calculated expended uncertanty is extreamly high, especially, at higher potentials (blue bars), where a higher current is produced. This could be expected, due to the "living" characteristic of the anode, or from the high uncertainty due to variation in electrodes ECSA as discussed in the previous section. The current densities uncertanties were Therefore, reevaluated once normalized to the EASA (Figure 9.4B) and it is obvious that the uncertainties are significantly decreased, espessially for the 24-hour biofilm median polarization. This is further proof that this parameter (EASA) is having a significant impact on the results uncertainties. The decrease of the uncertanty when the current is normalized to the EASA for the 5-hour biofilm median polarization curve indicates that at the beginning of the biofilm formation, the number of electrode respiring bacterial cells (catalysts) on the electrode surface has an impact on the current generation and at that phase of the biofilm formation is still not fully limited by the EASA. Consistent with the interpretation of the CV results. After 24 hours when the biofilm is likely covering the entire electrode surface, the number of celles attached to the surface can now be mostly defined by the EASA and the uncertanty decresed significantly normalazing current to that parameter (Figure 9.4B). Thereforee the MFC`s electrochemical operational characteristics should be represented and compared when normalizing to the electrode's electrochemical accessible surface area as a primary factor influencing the electrode's electrochemical behavior. This is

especially recommended when the electrode material is inhomogenous and the geometrical surface area is inconsistent with the EASA.

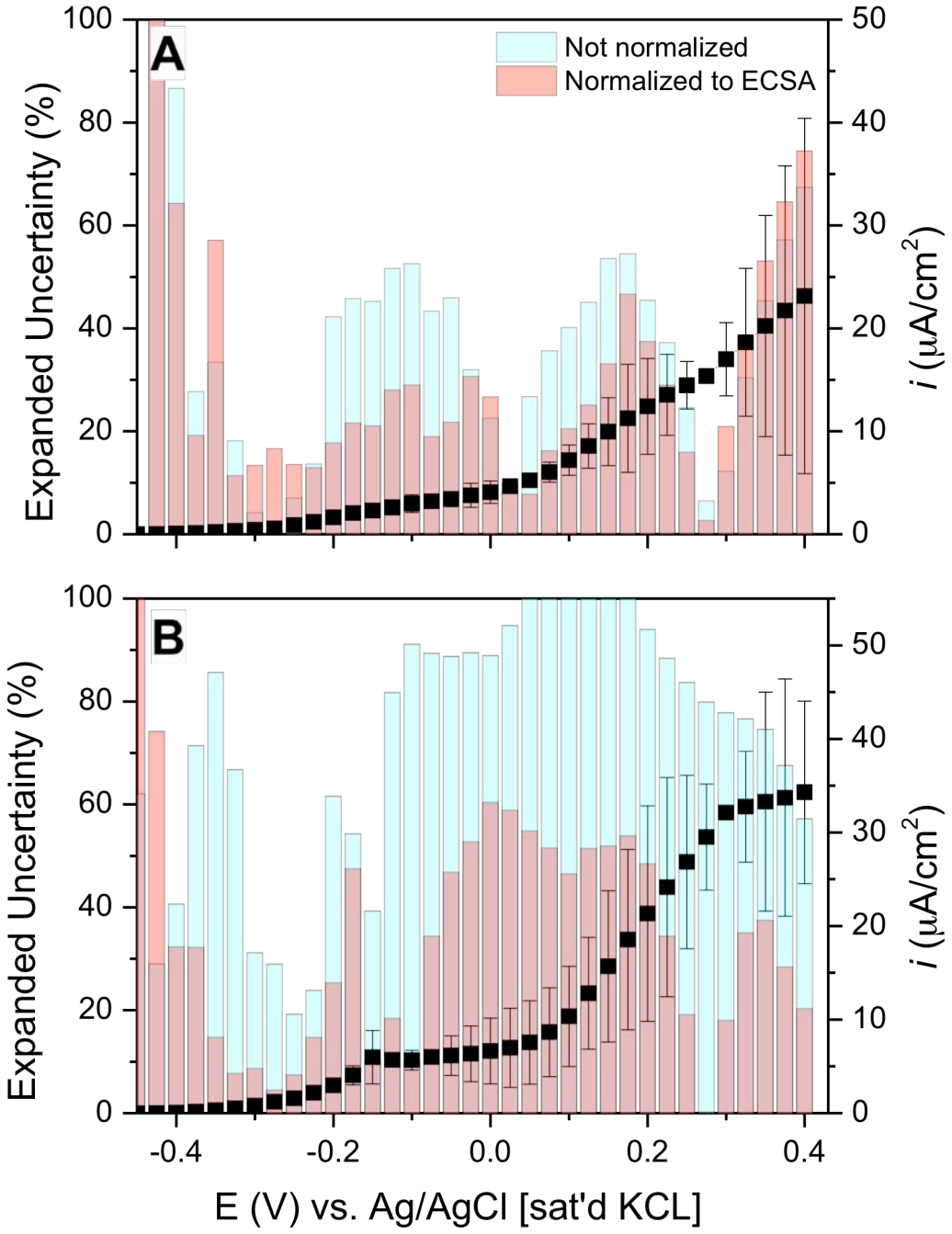

Figure 9.4: Median polarization curves for 5-hour biofilms (A) and 24-hour biofilms (B) with corresponding percent uncertainty for non-normalized current (red bars) and electrochemical assessible surface area normalized current density (blue bars)

It is interesting to noutice that three points with much lower uncertainty can be seen (Figure 9.4). These points are approximately at the same potentials for both types of electrodes. For the 5-hour biofilm they are at -0.225 V, 0.05 V and 0.275 V; and for the 24-hour biofilm they are at -0.275 V, -0.10 V and 0.275 V. The first potential value can be associated with overcoming the activation overpotential (η_{act}). The second point is the potential at which the activation losses are swiched to ohmic losses (η_{ohm}) and the current starts to increase rapidly. The more well developed biofilm after the 24 hour polarization leads to a decrease of overpotential in the region where the activation losses are dominant (Figure 9.4B).

The third point is at potential corresponding to the onset of diffusional limitation. However, due to the nature of the electron transfer (DET, in this case), these limitations are no longer diffusional. We speculate that instead of the system suffering a diffusion limitation (based on lactate and/or migration of ions from the biofilm/electrode interface) this potential is the region of "metabolic limitations". Meaning, that the microorganisms are transferring electrons to the electrode at higher rates than they are produced by metabolic substrate oxidation. In essence, the electrons are consumed faster at the electrode (at higher potentials during polarization) than they are metabolically accumulated in the living cells, and as a result the current densities are being truncated.

In regards to the range of uncertainties corresponding to individual potentials, the fact that there are three potentials values with dramatically lower current density uncertainties (normalized or not), and that these potentials are connected with defined electrochemical changes; means that the current densities generated at these potentials should be used for

results comparison. In doing so, current densities can be associated with particular changes in the system and at the same time these current densities are reliable with high reproducibility. The results from this expanded analysis using the theory of uncertainty are summarized in Table 9.2.

Table 9.2: Current densities (reported vs electrochemical accessible surface area) associated with specific potentials based on activation limitations (E_{act}), Ohmic limitations (E_{ohm}), and "metabolic limitations" ($E_{metabolic}$) for 5 and 24-hour biofilms

Electrode	E_{act}	E_{ohm}	$E_{metabolic}$
5-hour biofilm ($\mu A/cm^2$)	1.20 ± 0.08	3.42 ± 0.37	15.37 ± 0.21
24-hour biofilm ($\mu A/cm^2$)	1.60 ± 0.04	6.02 ± 0.31	32.15 ± 0.04

The two electrodes are generating current using one and the same mechanisms, there is no difference in the nature of the electrochemical reaction occurring at the electrode, and due to that there are no drastic differences in the current densities at the beginning of the polarization measurements for both 5-hour and 24-hour biofilms. The current is increased by approximately 30% for the first comparison point (E_{act}). But with the increase of the potential during electrode polarization (chronoamperometry), the current densities produced from the 24-hour biofilm are significantly higher (75% E_{ohm} and 109% $E_{metabolic}$) due to the enhanced amount of electrochemically active microorganisms are attached at or near the electrode surface. This is our final evidence to co-borate our previous discussion that the 24-hour biofilm (anaerobically formed on an electrode with

applied -0.3 V potential for 24 hours) is a more well-developed, complex and catalytic biofilm than the 5-hour biofilm.

9.5 Conclusions

In this study, high-density planktonic cultures of *S. oneidensis* MR-1 are grown in a rich medium aerobically. The culture is then removed from this media and placed in an electrochemical cell, containing lactate and electrolyte and the culture is transitioned into an anaerobic metabolism. The biofilm was then formed by applying an external potential of -0.3 V vs Ag/AgCl on the working electrode for up to 24 hours. At the onset of inoculation into the electrochemical cell/batch bioreactor, the measure current was 0 for approximately 2.5 hours when an increase was apparent. This increase of current reached stable maxima at approximately 5 hours for multiple repetitions. The subsequent electrochemical characterization of the biofilms included CVs and polarization curves at time points of 5 and 24 hours under turnover conditions. The 5-hour biofilm exhibited a large current with the shape of the voltammogram lending to the analysis that at this particular time point the biofilm is in a region of kinetic limitation. This kinetic limitation is defined by a small population in contact with the electrode surface or the initial stages of biofilm formation. The 24-hour biofilm, however, exhibited more catalytic behavior being the first such CV reported for *S. oneidensis* MR-1. We speculate that the CV obtained from the 24-hour biofilm formation exhibits a diffusional-based limitation characteristic. However, despite being initial observation leading to that conclusion, we speculate further that this limitation is in fact one based on the biofilm's (or individual cell's) metabolism. This metabolic limitation is occurring at high potentials in the electrode polarization as the metabolic oxidation of the carbon substrate can no longer

"supply" electrons fast enough to keep pace with electrode respiration, and a truncated current is observed. Polarization curves in this study also confirm the results from the obtained CVs for each biofilm system.

In terms of normalizing the data (polarization curves) between multiple identical experiments, three key concerns were addressed: (i) The generated current depends strongly on the electrochemical accessible surface area and the observed results from the polarization measurements should be represented when they are normalized to the EASA; (ii) There are three defined potentials in the polarization curves, which have much lower uncertainty and can be used for results comparison; (iii) normalizing the current to the EASA leads to significant decrease of the current expanded uncertainty.

In this study, only the current was used as an operational characteristic with the results being analyzed and represented as a current density based on EASA, with its expanded uncertainty. The same approach can be extended for power densities, when a whole microbial fuel cell is examined and other types of biological fuel cells.

Chapter 10 – Summary of Accomplishments & Future Outlook

Model organisms such as *S. oneidensis* are important for researchers in microbial fuel cells, as their known ability to respire with insoluble electron acceptors. This remarkable ability plays a key role in biogeochemical processes throughout the environment and the mechanism of extracellular electron transfer are now being unveiled. Until now, it was generally accepted within the literature that anode respiring biofilms based on *S. oneidensis* were not comparable in terms of current density to those populated by *G. sulfurreducens*. Reasoning for this is partially based on the implication of mediated electron transfer via riboflavin dominating the electrochemical character of the *S. oneidensis* biofilms, with the inability of *S. oneidensis* to form large catalytic biofilms.

The overarching goal of this entire study was to determine if *S. oneidensis* can in fact form biofilms comparable to *G. sulfurreducens* systems, and to shed light on the extracellular electron transfer mechanism within these biofilms. Initially this came in the form of forced encapsulation of *S. oneidensis* cultures within a binding agent, acting as an artificial extracellular polymeric substance (EPS). This novel engineering approach to the fabrication of catalytic biofilms in microbial fuel cells was achieved using the chemical vapor deposition of tetramethyl orthosilicate (TMOS). The silica precursor creates a SiO_2 porous thin film effectively binding the culture to the electrode. These systems not only proved to have increased current density compared to non-encapsulated systems of similar cultures, but the viability of the culture was apparent over a longer period of time. Continuing with the theme of engineering of these systems, a methodology to construct a novel, scalable, hierarchically structured, and biologically compatible electrode was

accomplished within this study (deemed PHBV/CF electrodes). *S. oneidensis* cultures were then successfully incorporated within these versatile electrode assemblies and the subsequent bioelectrocatalytic activity was apparent.

As a way to tie past technology developed within this laboratory to bridge future technology and scientific discoveries; a hybrid biological fuel cell was created based on previously studied laccase catalyzed air breathing oxygen reduction cathodes and *S. oneidensis* (SiO_2 encapsulated and not) anodes formed on PHBV/CF electrodes. These fully biologically catalyzed fuel cells were successful in the oxidation of lactate to generate power in a proof of concept publication. The success of this work led to the collaboration between the University of New Mexico, the Air Force Research Lab, and the Naval Research lab to deploy a proof-of-concept device that could be used as an ocean based sensor that is fully powered by a hybrid biological fuel cell. These first set of accomplishments provide significant contributions to the engineering of systems for microbial fuel cells based on the formation of stable, well bound biofilms on the surface of biocompatible electrodes.

Better engineering of these systems can only be achieved with significant contributions to the fundamental aspects of extracellular electron transfer and biofilm formation of dissimilatory metal reducing microbes such as *S. oneidensis*. Therefore, the next task in this dissertation was to study the partially accepted, dominating EET mechanism of riboflavin-mediated electron transfer (MET). This study successfully showed that riboflavin secretion by *S. oneidensis* into the surrounding medium is a metabolic response

of the culture to carbon substrate limitation. Further complicated by the fact that the cultures were required to be in micro-aerboic environments (dissolved oxygen tension [DOT] less than 5%) and greater (more than 5% DOT) for concentrations of riboflavin to be evident. Anaerobic cultures of *S. oneidensis* carbon substrate limitation did not produce extracellular riboflavin, or the concentration was below limits of detection. Based on these findings, it's difficult to rationalize MET based on riboflavin dominating EET mechanisms in microbial fuel cell operating conditions (i.e. *anaerobic*). This study was successful in characterizing the electrochemical behavior of riboflavin on the electrode, which has an electrochemical signature, irrespective of the presence of *S. oneidensis* or not as the electrode undergoes polarization. Due to this fact, riboflavin may just be a spectator electrochemically active metabolite, incorrectly implicated in MET mechanisms or may play some other non-respiratory, yet electrochemically active role, in anode respiring cultures of *S. oneidensis*.

As an extension of the aforementioned scientific contribution of this thesis, the ability of anaerobic cultures of *S. oneidensis oneidnesis* to form anode respiring biofilms was addressed. This study successfully showed that anaerobic cultures of *S. oneidensis* could not form a biofilm on the surface of the electrode unless an external potential of -0.3 V vs Ag/AgCl was applied to the electrode during cultivation. In fact, these biofilms exhibited oxidation (electrode reduction) phenomena not previously seen within this study. Using mutants, these oxidation events (centered at + 0.2 V) were successfully identified as the terminal proteins in the trans-membrane electron transfer cascade, or Mtr pathway, MtrC/OmcA. Again, no riboflavin was detected via cyclic voltammetry in these

anaerobic biofilms. Further analysis of this methodology for biofilm formation revealed that the MtrC/OmcA proteins dominated the reduction of the electrode and the reduction of the electrode was metabolically coupled to lactate oxidation. Biofilm formation occurring anaerobically at -0.3 V vs Ag/AgCl corresponds to the presence of oxidized riboflavin on the surface of the electrode. Identifying the possible non-respiratory role of electrochemically active riboflavin within these cultures, a role that serves in the redox-like taxis behavior of riboflavin. Leading to biofilm formation. Other applied potentials (-0.45V, +0.10 V, and open circuit) did not lead to the formation of a biofilm on the surface.

These observations lead to the most significant contribution to the science of this field from this study, the hypothesis of biofilm formation by *S. oneidensis*: as the culture proliferates in a batch system (or low nutrient flux environment like sediments) and "consumes" oxygen, the culture drives itself into a micro-aerobic environment. This is happening simultaneously with carbon substrate oxidation leading to a transition metabolic state based on carbon and oxygen limitation. While in this state, the culture begins to release riboflavin, which may act in some redox cell-to-cell sensing (and adsorbing to electron accepting surface), leading to biofilm formation and a culture capable of sustaining metabolic activity on an insoluble electron acceptor as the surrounding transitions to a bulk anaerobic environment (**Figure 8.5, page 103**).

Based on the newly acquired knowledge for *S. oneidensis* biofilm formation, a novel anode was created based on the electrode, having an applied potential of -0.3 V, being

exposed to large density planktonic cultures of *S. oneidensis*. The subsequent biofilm exhibited spectacular catalytic activity when the CV was measured under turnover conditions. This CV being the first of it's kind for a *S. oneidensis* populated anode and being comparable to contemporary *G. sulfurreducens* CVs (measured and modeled). The electrode was also evaluated using the idea of expanded uncertainty; the first evaluation of it's kind for a microbial fuel cell. Using expanded uncertainty, the polarization curves were normalized to the electrochemical accessible surface area, yielding current densities that had reduced variability between duplicate experiments. This can now guide researchers to more reproducible results, overcoming major difficulties in system comparisons inherent to biological fuel cell research.

This dissertation describes an effort to not only elucidate the mechanisms of biofilm formation for *S. oneidensis* and associated extra-cellular electron transfer processes, but to also incorporate the methodology of biofilm formation into the design and characterization of an anode for a microbial fuel cell. While an industrial scale application will never likely be based on a single organism catalyzing the oxidation of a substrate on the anode; the discoveries herein will shed light on how multiple organisms may engage in symbiotic relationships in complicated environments to survive. For example, an organism like *S. oneidensis* may be a buffer organism between other dissimilatory metal reducing organisms in a mature multi-species biofilm. Where *S. oneidensis*, or another facultative anaerobe, may be the intermediate between aerobic (or micro-aerobic) regions of the biofilm and anaerobic regions, enabling a biofilm to be engaged in cross-species electron transfer. Future research in the possible symbiosis of

these organisms represents an exciting frontier for this field while the methodologies outlined within this study can be adapted as the MFC technology matures and reaches an industrial relevance.

References

(1) Lovley, D. R.; Ueki, T.; Zhang, T.; Malvankar, N. S.; Shrestha, P. M.; Flanagan, K. A.; Aklujkar, M.; Butler, J. E.; Giloteax, L.; Rotaru, A.-E.; Holmes, D. E.; Franks, A. E.; Orellana, R.; Risso, C.; Nevin, K. P. In *Advances in Microbial Physiology*; Poole, R. K., Ed.; Elsevier: 2011.

(2) Thormann, K.; Saville, R.; Shukla, S.; Pelletier, D.; Spormann, A. *Journal of Bacteriology* **2004**, *186*, 8096.

(3) Carmona-Martinez, A. A.; Harnisch, F.; Kuhlicke, U.; Neu, T. R.; Schröder, U. *Bioelectrochemistry* **2012**.

(4) Saravanan, R.; Kavanagh, P.; O'Flaherty, V.; Leech, D.; Katrui, K. P. *Langmuir* **2012**.

(5) Bullen, R. A.; Arnot, T. C.; Lakeman, J. B.; Walsh, F. C. *Biosensors and Bioelectronics* **2006**, *21*.

(6) Potter, M. C. *Proc. R. Soc. Lond. B. Biol. Sci.* **1911**, 260.

(7) *Bioelectrochemical Systems: from extracellular electron transfer to biotechnological application*; Rabaey, K.; Angenent, L.; Schroder, U.; Keller, J., Eds.; IWA Publishing Alliance House: London, 2010.

(8) Kim, H. J.; Hyun, M. S.; Chang, I. S.; Kim, B. H. *J Microbiol Biotechn* **1999**, *9*, 365.

(9) Chang, I. S.; Moon, H.; Bretschger, O.; Jang, J. K.; Park, H. I.; Nealson, K. H.; Kim, B. H. *J Microbiol Biotechn* **2006**, *16*, 163.

(10) Chaudhuri, S. K.; Lovley, D. R. *Nat Biotechnol* **2003**, *21*, 1229.

(11) Jang, J. K.; Pham, T. H.; Chang, I. S.; Kang, K. H.; Moon, H.; Cho, K. S.; Kim, B. H. *Process Biochem* **2004**, *39*, 1007.

(12) Rozendal, R. A. R.; Hamelers, H. V. M. H.; Rabaey, K. K.; Keller, J. J.; Buisman, C. J. N. C. *Trends in Biotechnology* **2008**, *26*, 450.

(13) Tender, L. M. L.; Reimers, C. E. C.; Stecher, H. A. H.; Holmes, D. E. D.; Bond, D. R. D.; Lowy, D. A. D.; Pilobello, K. K.; Fertig, S. J. S.; Lovley, D. R. D. *Nature Biotechnology* **2002**, *20*, 821.

(14) Rosenbaum, M.; Aulenta, F.; Villano, M.; Angenent, L. T. *Bioresource Technology* **2011**, *102*, 324.

(15) Shon, H. K.; Vigneswaran, S.; Snyder, S. A. *Critical Reviews in Environmental Science and Technology* **2006**, *36*, 327.

(16) Shi, L.; Squier, T. C.; Zachara, J. M.; Fredrickson, J. K. *Molecular Microbiology* **2007**, *65*, 12.

(17) Myers, C.; Nealson, K. *Science* **1988**, *240*, 1319.

(18) Bond, D.; Lovley, D. *Applied and Environmental Microbiology* **2003**, *69*, 1548.

(19) Leang, C.; Qian, X.; Mester, T.; Lovley, D. R. *Applied and Environmental Microbiology* **2010**, *76*, 4080.

(20) *The Prokaryotes*; Nealson, K. H. D., Martin; Scott, J. F., Stanley; Rosenberg, E.; Schleifer, K.-H.; Stackebrandt, E., Eds.; Springer New York, 2006.

(21) Scott, J.; Nealson, K. *Journal of Bacteriology* **1994**, *176*, 3408.

(22) Lovley, D. R.; Phillips, J. P.; Lonergan, D. J. *Applied Environmental Microbiology* **1989**, *55*, 700.

(23) Myers, C. R.; Myers, J. M. *Journal of Bacteriology* **1992**, *174*, 3429.

(24) Rabaey, K.; Boon, N.; Hofte, M.; Verstraete, W. *Environmental Science & Technology* **2005**, *39*, 3401.

(25) Rabaey, K.; Boon, N.; Siciliano, S. D.; Verhaege, M.; Verstraete, W. *Applied and Environmental Microbiology* **2004**, *70*, 5373.

(26) Marsili, E.; Baron, D. B.; Shikhare, I. D.; Coursolle, D.; Gralnick, J. A.; Bond, D. R. *Proceedings of the National Academy of Sciences of the United States of America* **2008**, *105*, 3968.

(27) Fredrickson, J. K.; Romine, M. F.; Beliaev, A. S.; Auchtung, J. M.; Driscoll, M. E.; Gardner, T. S.; Nealson, K. H.; Osterman, A. L.; Pinchuk, G.; Reed, J. L.; Rodionov, D. A.; Rodrigues, J. L. M.; Saffarini, D. A.; Serres, M. H.; Spormann, A. M.; Zhulin, I. B.; Tiedje, J. M. *Nat Rev Microbiol* **2008**, *6*, 592.

(28) Gorby, Y. A.; Yanina, S.; McLean, J. S.; Rosso, K. M.; Moyles, D.; Dohnalkova, A.; Beveridge, T. J.; Chang, I. S.; Kim, B. H.; Kim, K. S.; Culley, D. E.; Reed, S. B.; Romine, M. F.; Saffarini, D. A.; Hill, E. A.; Shi, L.; Elias, D. A.; Kennedy, D. W.; Pinchuk, G.; Watanabe, K.; Ishii, S.; Logan, B.; Nealson, K. H.; Fredrickson, J. K. *Proceedings of the National Academy of Sciences of the United States of America* **2006**, *103*, 11358.

(29) El-Naggar, M. Y.; Wanger, G.; Leung, K. M.; Yuzvinsky, T. D.; Southam, G.; Yang, J.; Lau, W. M.; Nealson, K. H.; Gorby, Y. A. *Proceedings of the National Academy of Sciences of the United States of America* **2010**, *107*, 18127.

(30) Myers, C.; Myers, J. *Journal of Bacteriology* **1992**, *174*, 3429.

(31) Myers, C. R.; Myers, J. M. *Letters in Applied Microbiology* **2003**, *37*, 254.

(32) Covington, E. D.; Gelbmann, C. B.; Kotloski, N. J.; Gralnick, J. A. *Molecular Microbiology* **2010**, *78*, 519.

(33) Pitts, K. E.; Dobbin, P. S.; Reyes-Ramirez, F.; Thomson, A. J.; Richardson, D. J.; Seward, H. E. *J. Biol Chem* **2003**, *278*.

(34) Beliaev, A. S.; Saffarini, D. A.; McLaughlin, J. L.; Hunnicutt, D. *Molecular Microbiology* **2001**, *39*, 722.

(35) Beliaev, A. S.; Saffarini, D. A. *Journal of Bacteriology* **1998**, *180*, 6292.

(36) Myers, C. R.; Myers, J. M. *Applied Environmental Microbiology* **2002**, *68*, 5585.

(37) Myers, C. R.; Myers, J. M. *Lett. Appl. Micriobiol.* **2004**, *39*, 466.

(38) Gorby, Y. A.; Yanina, S.; McLean, J. S.; Rosso, K. M.; Moyles, D.; Dohnalkova, A.; Beveridge, T. J.; Chang, I. S.; Kim, B. H.; Kim, K. S.; Culley, D. E.; Reed, S. B.; Romine, M. F.; Saffarini, D. A.; Hill, E. A.; Shi, L.; Elias, D. A.; Kennedy, D. W.; Pinchuk, G.; Watanabe, K.; Ishii, S. a. i.; Logan, B.; Nealson, K. H.; Fredrickson, J. K. *Proceedings of the National Academy of Sciences of the United States of America* **2006**, *103*, 11358.

(39) Bouhenni, R. A.; Vora, G. J.; Biffinger, J. C.; Shirodkar, S.; Brockman, K.; Ray, R.; Wu, P.; Johnson, B. J.; Biddle, E. M.; Marshall, M. J.; Fitzgerald, L. A.; Little, B. J.; Fredrickson, J. K.; Beliaev, A. S.; Ringeisen, B. R.; Saffarini, D. A. *Electroanalysis* **2010**, NA.

(40) Bretschger, O.; Obraztsova, A.; Sturm, C. A.; Chang, I. S.; Gorby, Y. A.; Reed, S. B.; Culley, D. E.; Reardon, C. L.; Barua, S.; Romine, M. F.; Zhou, J.; Beliaev, A. S.; Bouhenni, R.; Saffarini, D.; Mansfeld, F.; Kim, B. H.; Fredrickson, J. K.; Nealson, K. H. *Applied and Environmental Microbiology* **2007**, *73*, 7003.

(41) Malvankar, N. S.; Vargas, M.; NEvin, K. P.; Franks, A. E.; Leang, C.; Kim, B.-C.; Inoue, K.; Mester, T.; Covalla, S. F.; Johnson, J. P.; Rotello, V. M.; Tuominen, M. T.; Lovley, D. R. *nature nanotechnology* **2011**, *6*, 573.

(42) Strycharz-Glaven, S. M.; Snider, R. M.; Guiseppi-Elie, A.; Tender, L. M. *Energy & Environmental Science* **2011**, *4*, 4366.

(43) von Canstein, H.; Ogawa, J.; Shimizu, S.; Lloyd, J. R. *Applied and Environmental Microbiology* **2008**, *74*, 615.

(44) Foster, J. **1944**.

(45) Tsuneda, S.; Aikawa, H.; Hayashi, H.; Yuasa, A.; Hirata, A. *Fems Microbiol Lett* **2003**, *223*, 287.

(46) Reguera, G.; Nevin, K. P.; Nicoll, J. S.; Covalla, S. F.; Woodard, T. L.; Lovley, D. R. *Applied and Environmental Microbiology* **2006**, *72*, 7345.

(47) Thormann, K. M.; Saville, R. M.; Shukla, S.; Pelletier, D. A.; Spormann, A. M. *Journal of Bacteriology* **2004**, *186*, 8096.

(48) Thormann, K. M.; Saville, R. M.; Shukla, S.; Spormann, A. M. *Journal of Bacteriology* **2005**, *187*, 1014.

(49) Thormann, K. M.; Duttler, S.; Saville, R. M.; Hyodo, M.; Shukla, S.; Hayakawa, Y.; Spormann, A. M. *Journal of Bacteriology* **2006**, *188*, 2681.

(50) Nevin, K. P.; Richter, H.; Covalla, S. F.; Johnson, J. P.; Woodard, T. L.; Orloff, A. L.; Jia, H.; Zhang, M.; Lovley, D. R. *Environ Microbiol* **2008**, *10*, 2505.

(51) Carmona-Martinez, A. A.; Harnisch, F.; Fitzgerald, L. A.; Biffinger, J. C.; Ringeisen, B. R.; Schroder, U. *Bioelectrochemistry* **2011**.

(52) Cheng, S.; Liu, H.; Logan, B. E. *Environmental Science & Technology* **2006**, *40*, 2426.

(53) Thormann, K.; Duttler, S.; Saville, R.; Hyodo, M.; Shukla, S.; Hayakawa, Y.; Spormann, A. *Journal of Bacteriology* **2006**, *188*, 2681.

(54) Thormann, K.; Saville, R.; Shukla, S.; Spormann, A. *Journal of Bacteriology* **2005**, *187*, 1014.

(55) McLean, J. S.; Pinchuk, G. E.; Geydebrekht, O. V.; Bilskis, C. L.; Zakrajsek, B. A.; Hill, E. A.; Saffarini, D. A.; Romine, M. F.; Gorby, Y. A.; Fredrickson, J. K.; Beliaev, A. S. *Environmental Microbiology* **2008**, *10*, 1861.

(56) Torres, C. I.; Krajmalnik-Brown, R.; Parameswaran, P.; Marcus, A. K.; Wanger, G.; Gorby, Y. A.; Rittmann, B. E. *Environmental Science & Technology* **2009**, *43*, 9519.

(57) Bard, A.; Faulkner, L. **2001**, 833.

(58) Logan, B. E.; Hamelers, B.; Rozendal, R.; Schröder, U.; Keller, J.; Freguia, S.; Aelterman, P.; Verstraete, W.; Rabaey, K. *Environmental Science & Technology* **2006**, *40*, 5181.

(59) Zhao, F.; Slade, R. C. T.; Varcoe, J. R. *Chemical Society Reviews* **2009**, *38*, 1926.

(60) Cesar, A.; Maria, O.; Tanize, F.; Vitor, H.; Dulcineia, A. *Biosensors for Health, Environment and Biosecurity* **2011**.

(61) Torres, C. I.; Marcus, A. K.; Lee, H.-S.; Parameswaran, P.; Krajmalnik-Brown, R.; Rittmann, B. E. *FEMS Microbiology Reviews* **2010**, *34*, 3.

(62) Logan, B. E.; Aelterman, P.; Hamelers, B.; Rozendal, R.; Schroder, U.; Keller, J.; Freguiac, S.; Verstraete, W.; Rabaey, K. *Environmental Science & Technology* **2006**, *40*, 5181.

(63) Lovely, D. R. *Nature Reviews in Microbiology* **2006**, *4*, 497.

(64) Lies, D. P.; Hernandez, M. E.; Kappler, A.; Mielke, R. E.; Gralnick, J. A.; Newman, D. K. *Applied and Environmental Microbiology* **2005**, *71*, 4414.

(65) Biffinger, J. C.; Pietron, J.; Ray, R.; Little, B.; Ringeisen, B. R. *Biosens Bioelectron* **2007**, *22*, 1672.

(66) Biffinger, J. C.; Pietron, J.; Bretschger, O.; Nadeau, L. J.; Johnson, G. R.; Williams, C. C.; Nealson, K. H.; Ringeisen, B. R. *Biosens Bioelectron* **2008**, *24*, 906.

(67) Biffinger, J. C.; Ray, R.; Little, B. J.; Fitzgerald, L. A.; Ribbens, M.; Finkel, S. E.; Ringeisen, B. R. *Biotechnol Bioeng* **2009**, *103*, 524.

(68) McLean, J. S.; Majors, P. D.; Reardon, C. L.; Bilskis, C. L.; Reed, S. B.; Romine, M. F.; Fredrickson, J. K. *Journal of Microbiological Methods* **2008**, *74*, 47.

(69) Yi, H.; Nevin, K. P.; Kim, B.-C.; Franks, A. E.; Klimes, A.; Tender, L. M.; Lovley, D. R. *Biosensors and Bioelectronics* **2009**, *24*, 3498.

(70) Coiffier, A.; Coradin, T.; Roux, C.; Bouvet, O. M. M.; Livage, J. *Journal of Materials Chemistry* **2001**, *11*, 2039.

(71) Collinson, M. M.; Howells, A. R. *Analytical Chemistry* **2000**, *72*, 702A.

(72) Lev, O.; Wu, Z.; Bharathi, S.; Glezer, V.; Modestov, A.; Gun, J.; Rabinovich, L.; Sampath, S. *Chemistry of Materials* **1997**, *9*, 2354.

(73) Nassif, N.; Bouvet, O.; Noelle Rager, M.; Roux, C.; Coradin, T.; Livage, J. *Nature Materials* **2002**, *1*, 42.

(74) Gupta, G.; Lopez, G.; Atanassov, P.; STC.UNM, Albuquerque, NM: 2008; Vol. US 2008/0311391 A1.

(75) Gupta, G.; Rathod, S. B.; Staggs, K. W.; Ista, L. K.; Oucherif, K. A.; Atanassov, P. B.; Tartis, M. S.; Montano, G. A.; Lopez, G. P. *Langmuir* **2009**, *25*, 13322.

(76) Gorby, Y. A.; Yanina, S.; McLean, J. S.; Rosso, K. M.; Moyles, D.; Dohnalkova, A.; Beveridge, T. J.; Chang, I. S.; Kim, B. H.; Kim, K. S.; Culley, D. E.; Reed, S. B.; Romine, M. F.; Saffarini, D. A.; Hill, E. A.; Shi, L.; Elias, D. A.; Kennedy, D. W.; Pinchuk, G.; Watanabe, K.; Ishii, S.; Logan, B.; Nealson, K. H.; Fredrickson, J. K. *Proc Natl Acad Sci U S A* **2006**, *103*, 11358.

(77) Biffinger, J. C.; Byrd, J. N.; Dudley, B. L.; Ringeisen, B. R. *Biosens Bioelectron* **2008**, *23*, 820.

(78) Logan, B. E.; Hamelers, B.; Rozendal, R.; Schroder, U.; Keller, J.; Freguia, S.; Aelterman, P.; Verstraete, W.; Rabaey, K. *Environmental science & technology* **2006**, *40*, 5181.

(79) Luckarift, H. R.; Sizemore, S. R.; Roy, J.; Lau, C.; Gupta, G.; Atanassov, P.; Johnson, G. R. *Chem Commun (Camb)* **2010**, *46*, 6048.

(80) Scott, K.; Rimbu, G. A.; Katuri, K. P.; Prasad, K. K.; Head, I. M. *Trans IChemE, Part B, Process safety and environmental protection* **2007**, *85*, 481.

(81) Xie, X.; Hu, L.; Pasta, M.; Wells, G. F.; Kong, D.; Criddle, C. S.; Cui, Y. *Nano Letters* **2011**, *11*, 291.

(82) Lau, C.; Cooney, M. J.; Atanassov, P. *Langmuir* **2008**, *24*, 7004.

(83) Lau, C.; Martin, G.; Minteer, S. D.; Cooney, M. J. *Electroanalysis* **2010**, *22*, 793.

(84) Yoon, S. H.; Jin, H.-J.; Kook, M.-C.; Pyun, Y. R. *Biomacromolecules* **2006**, *7*, 1280.

(85) Logan, B. E.; Cheng, S.; Watson, V.; Estadt, G. *Environmental science & technology* **2007**, *41*, 3341.

(86) Anderson, A.; Dawes, E. *Microbiological Reviews* **1990**, *54*, 450.

(87) Grage, K.; Jahns, A. C.; Parlane, N.; Palanisamy, R.; Rasiah, I. A.; Atwood, J. A.; Rehm, H. A. *Biomacromolecules* **2009**, *10*, 660.

(88) Ahmed, T.; Marcal, H.; Lawless, M.; Wanandy, N. S.; Chiu, A.; Foster, L. J. R. *Biomacromolecules* **2010**, *11*, 2707.

(89) Misra, S. K.; Ansari, T.; Mohn, D.; Valappil, S. P.; Brunner, T. J.; Stark, W. J.; Roy, I.; Knowles, J. C.; Sibbons, P. D.; Jones, E. V.; Boccaccini, A. R.; Salih, V. *Journal of the Royal Society, Interface / the Royal Society*, *7*, 453.

(90) Misra, S. K.; Ansari, T. I.; Valappil, S. P.; Mohn, D.; Philip, S. E.; Stark, W. J.; Roy, I.; Knowles, J. C.; Salih, V.; Boccaccini, A. R. *Biomaterials* **2010**, *31*, 2806.

(91) Misra, S. K.; Mohn, D.; Brunner, T. J.; Stark, W. J.; Philip, S. E.; Roy, I.; Salih, V.; Knowles, J. C.; Boccaccini, A. R. *Biomaterials* **2008**, *29*, 1750.

(92) Misra, S. K.; Nazhat, S. N.; Valappil, S. P.; Moshrefi-Torbati, M.; Wood, R. J.; Roy, I.; Boccaccini, A. R. *Biomacromolecules* **2007**, *8*, 2112.

(93) Misra, S. K.; Ohashi, F.; Valappil, S. P.; Knowles, J. C.; Roy, I.; Silva, S. R.; Salih, V.; Boccaccini, A. R. *Acta biomaterialia*, *6*, 735.

(94) Misra, S. K.; Philip, S. E.; Chrzanowski, W.; Nazhat, S. N.; Roy, I.; Knowles, J. C.; Salih, V.; Boccaccini, A. R. *Journal of the Royal Society, Interface / the Royal Society* **2009**, *6*, 401.

(95) Misra, S. K.; Valappil, S. P.; Roy, I.; Boccaccini, A. R. *Biomacromolecules* **2006**, *7*, 2249.

(96) Sanchez-Garcia, M. D.; Lagaron, J. M.; Hoa, S. V. *Composites science and technology* **2010**, *70*, 1095.

(97) Bretschger, O.; Cheung, A. C. M.; Mansfeld, F.; Nealson, K. H. *Electroanalysis* **2010**, *22*, 883.

(98) Marsili, E.; baron, D. B.; Shikhare, I. D.; Coursolle, D.; Gralnick, J. A.; Bond, D. R. *Proceedings of the National Academy of Science* **2008**, *105*, 3968.

(99) Higgins, S. R.; Lau, C.; Atanassov, P. B.; Minteer, S. D.; Cooney, M. J. *ACS Catalysis* **2011**.

(100) Schaetzle, O.; Barrière, F.; Schröder, U. *Energy & Environmental Science* **2008**, *2*, 96.

(101) Beliaev, A. S.; Thompson, D. K.; Khare, T.; Lim, H.; Brandt, C. C.; Li, G.; Murray, A. E.; Heidelberg, J. F.; Giometti, C. S.; Yates, J.; Nealson, K. H.; Tiedje, J. M.; Zhoui, J. *Omics : a journal of integrative biology* **2002**, *6*, 39.

(102) Luckarift, H. R.; Sizemore, S. R.; Roy, J.; Lau, C.; Gupta, G.; Atanassov, P.; Johnson, G. R. *Chemical Communications* **2010**, *46*, 6048.

(103) Luckarift, H. R.; Sizemore, S. R.; Farrington, K. E.; Roy, J.; Lau, C.; Atanassov, P. B.; Johnson, G. R. *ACS applied materials & interfaces* **2012**.

(104) Wang, C.; Waje, M.; Wang, X.; Tang, J.; Haddon, R.; Yan, Y. *Nano Letters* **2004**, *4*, 345.

(105) Gupta, G.; Lau, C.; Rajendran, V.; Colon, F.; Branch, B.; Ivnitski, D.; Atanassov, P. *Electrochemistry Communications* **2011**.

(106) Rincón, R. A.; Lau, C.; Garcia, K. E.; Atanassov, P. *Electrochimica Acta* **2011**, *56*, 2503.

(107) Biffinger, J. C.; Pietron, J.; Bretschger, O.; Nadeau, L. J.; Johnson, G. R.; Williams, C. C.; Nealson, K. H.; Ringeisen, B. R. *Biosensors and Bioelectronics* **2008**, *24*, 900.

(108) Ray, R.; Lizewski, S.; Fitzgerald, L. A.; Little, B.; Ringeisen, B. R. *Journal of Microbiological Methods* **2010**, *82*, 187.

(109) Logan, B. E. *Nature Reviews Microbiology* **2009**, *7*, 375.

(110) Lovley, D. R. *Nature Reviews Microbiology* **2006**, *4*, 497.

(111) Watson, V. J.; Logan, B. E. *Biotechnology and Bioengineering* **2010**, *105*, 489.

(112) Lovley, D. R. *Current Opinion in Biotechnology* **2008**, *19*, 564.

(113) Logan, B. E.; Regan, J. M. *Trends in Microbiology* **2006**, *14*, 512.

(114) Gorby, Y.; Mclean, J.; Korenevsky, A.; Rosso, K.; El-Naggar, M.; Beveridge, T. *Geobiology* **2008**, *6*, 232.

(115) Dauner, M.; Sonderegger, M.; Hochuli, M.; Szyperski, T.; Wuthrich, K.; Hohmann, H.; Sauer, U.; Bailey, J. *Applied and Environmental Microbiology* **2002**, *68*, 1760.

(116) Berchmans, S.; Vijayavalli, R. *Langmuir* **1995**, *11*, 286.

(117) Coursolle, D.; Baron, D. B.; Bond, D. R.; Gralnick, J. A. *Journal of Bacteriology* **2009**, *192*, 467.

(118) Li, R.; Tiedje, J. M.; Chiu, C.; Worden, R. M. *Environmental Science & Technology* **2012**, *46*, 2813.

(119) Wang, H.; Hollywood, K.; Jarvis, R. M.; Lloyd, J. R.; Goodacre, R. *Applied and Environmental Microbiology* **2010**, *76*, 6266.

(120) Velasquez-Orta, S. B.; Head, I. M.; Curtis, T. P.; Scott, K.; Lloyd, J. R.; von Canstein, H. *Applied Microbiology and Biotechnology* **2010**, *85*, 1373.

(121) Walsh, C. *Accounts of Chemical Research* **1980**.

(122) Bonazzola, C.; Calvo, E. *Journal of Electroanalytical Chemistry* **1998**.

(123) Albert, A. *Proceedings of the Biochemical Society* **1950**, 27.

(124) Pereira, A.; Santos, A. d. S.; Kubota, L. T. *Journal of Colloid and Interface Science* **2003**, *265*, 351.

(125) Shi, L.; Richardson, D. J.; Wang, Z.; Kerisit, S. N.; Rosso, K. M.; Zachara, J. M.; Fredrickson, J. K. *Environmental Microbiology Reports* **2009**, *1*, 220.

(126) Baron, D.; LaBelle, E.; Coursolle, D.; Gralnick, J. A.; Bond, D. R. *Journal of Biological Chemistry* **2009**, *284*, 28865.

(127) Laviron, E. *Journal of Electroanalytical Chemistry* **1979**, *101*, 19.

(128) Nealson, K. H.; Scott, J. *The prokaryotes* **2006**, *6*, 1133.

(129) Marsili, E.; Rollefson, J. B.; Baron, D. B.; Hozalski, R. M.; Bond, D. R. *Applied and Environmental Microbiology* **2008**, *74*, 7329.

(130) Reguera, G.; McCarthy, K. D.; Mehta, T.; Nicoll, J. S.; Tuominen, M. T.; Lovley, D. R. *Nature* **2005**, *435*, 1098.

(131) McLean, J. S.; Wanger, G.; Gorby, Y. A.; Wainstein, M.; McQuaid, J.; Ishii, S. i.; Bretschger, O.; Beyenal, H.; Nealson, K. H. *Environmental Science & Technology* **2010**, *44*, 2721.

(132) Carmona-Martinez, A. A.; Harnisch, F.; Fitzgerald, L. A.; Biffinger, J. C.; Ringeisen, B. R.; Schröder, U. *Bioelectrochemistry* **2011**, 1.

(133) Ramasamy, R. P.; Gadhamshetty, V.; Nadeau, L. J.; Johnson, G. R. *Biotechnology and Bioengineering* **2009**, *104*, 882.

(134) Bibikov, S.; Biran, R.; Rudd, K.; Parkinson, J. *Journal of Bacteriology* **1997**, *179*, 4075.

(135) Bibikov, S. I.; Barnes, L. A.; Gitin, Y.; Parkinson, J. S. *Proceedings of the National Academy of Sciences* **2000**, *97*, 5830.

(136) Roy, J. N.; Luckarift, H. R.; Lau, C.; Falase, A.; Garcia, K. E.; Ista, L. K.; Chellamuthu, P.; Ramasamy, R. P.; Gadhamshetty, V.; Wanger, G.; Gorby, Y. A.; Nealson, K. H.; Bretschger, O.; Johnson, G. R.; Atanassov, P. *RSC Advances*.

(137) Reardon, C. L.; Dohnalkova, A. C.; Nachimuthu, P.; Kennedy, D. W.; Saffarini, D. A.; Arey, B. W.; Shi, L.; Wang, Z.; Moore, D.; McLean, J. S.; Moyles, D.; Marshall, M. J.; Zachara, J. M.; Fredrickson, J. K.; Beliaev, A. S. *Geobiology* **2010**, *8*, 56.

(138) Xie, X.; Hu, L.; Pasta, M.; Wells, G. F.; Kong, D.; Criddle, C. S.; Cui, Y. *Nano Letters* **2011**, *11*, 291.

(139) Pinto, R. P.; Tartakovsky, B.; Perrier, M.; Srinivasan, B. *Industrial & Engineering Chemistry Research* **2010**, *49*, 9222.

(140) Torres, C. I.; Kato Marcus, A.; Rittmann, B. E. *Applied Microbiology and Biotechnology* **2007**, *77*, 689.

(141) Babanova, S.; Hubenova, Y.; Mitov, M.; Mandjukov, P. *Fuel Cells* **2011**, *11*, 824.